UNIVERSITÉ CATHOLIQUE DE LOUVAIN & KATHOLIEKE UNIVERSITEIT LEUVEN

SECTEUR DES SCIENCES DE LA SANTÉ

INSTITUT DE RECHERCHE CLINIQUE ET EXPÉRIMENTALE (IREC)
POLE OF PNEUMOLOGY, ORL (AIRWAYS) AND DERMATOLOGY (SKIN) (LUNS)

DEPARTMENT OF MICROBIOLOGY, ALLERGY AND CLINICAL IMMUNOLOGY RESEARCH GROUP, IMMUNOLOGY AND TRANSPLANTATION, KULEUVEN

TRANSLATIONAL STUDY OF THE ROLE OF SECRETORY IGA IN CHRONIC RHINOSINUSITIS USING INNOVATIVE EXPERIMENTAL MODELS

Alba SÁNCHEZ MONTALVO, MSc

Promoteur : Valérie HOX, MD PhD

Co-promoteur : Dominique Bullens, MD PhD

Thèse présentée en vue de l'obtention du grade de Docteur en Sciences Médicales

Juin 2025

Members of the jury

Jury president

Professor Charles Pilette
Université catholique de Louvain (UCL)
Institute of Experimental & Clinical Research
Pole Of Pneumology, ORL (Airways) and Dermatology (Skin) (LUNS)
Avenue Hippocrate 54, B1.5.04
B-1200 Brussels, BELGIUM

Promotor

Professor Valérie Hox
Université catholique de Louvain (UCL)
Institute of Experimental & Clinical Research
Pole Of Pneumology, ORL (Airways) and Dermatology (Skin) (LUNS)
Avenue Hippocrate 54, B1.54.04
B-1200 Brussels, BELGIUM

Department of Otorhinolaryngology
Cliniques universitaires Saint-Luc
Avenue Hippocrate 10
B-1200 Brussels, BELGIUM

Co-promotor

Professor Dominique Bullens
Katholieke Universiteit Leuven (KULeuven)
Department of Microbiology, Allergy and Clinical Immunology Research Group,
Immunology and Transplantation, KU Leuven
Clinical Division of Paediatrics, UZ Leuven
UZ Herestraat 49 - bus 811, 3000
B-3000 Leuven, Belgium

Supervisory panel

Professor Laure Dumoutier
Université catholique de Louvain (UCL)
de Duve Institute
Médecine expérimentale
Avenue Hippocrate 75, B1.75.02
B-1200 Brussels, BELGIUM

Invited members

Professor Stijn VanHee
University of Ghent (UGhent)
Laboratory of Immunoregulation and Mucosal Immunology, VIB Center for Inflammation Research
Department of Internal Medicine and Pediatrics, Ghent University; Department of Head and Skin, Ghent University
B-9000 Ghent, Belgium

Professor Aurélie Crabbé
University of Ghent (UGhent)
Laboratory of Pharmaceutical Microbiology (LPM)
Ottergemsesteenweg 460,
B-9000 Gent, Belgium

Professor Peter Hellings
Katholieke Universiteit Leuven (KULeuven)
Allergy and Clinical Immunology Research group
Kapucijnenvoer 33 blok I - box 7001
B-3000 Leuven, Belgium

"We must never forget that what we do in our laboratory has an impact on people's real life."

William Kaelin Jr., private conversation at the 72nd Lindau Nobel Laureate Meeting
30/06/2023 Lindau, Germany

TABLE OF CONTENTS

ACKNOWLEDGEMENTS

During these 5 years, I have had the opportunity to work surrounded by many people, some of whom I have really got to admire and respect.

First and foremost, I would like to thank my supervisor, Valérie Hox, for your dedication and commitment in guiding me through this project. I admire your devotion to research and I have learned a lot from our experience working together. We have gone through hard moments in this project and it has not been easy, but we finally made it. Thank you for giving me this opportunity.

I would like to express my sincere gratitude to my co-supervisor, Dominique Bullens. Whenever I needed advice, guidance or just someone to talk to, you were always there. I deeply appreciate your kindness and your commitment to science, which has always been inspiring and helpful. Thank you very much for your guidance and for your optimism.

This project would not have been possible either without the valuable support of Charles Pilette. You have always put light on this project whenever needed, from the very global perspective to the smallest details. Thank you very much for your invaluable support through these years.

This journey would not have been possible without the support of all the PIs in the lab. Thank you for your time, suggestions and for helping me move this project forward. Thank you for the encouragement and support of my lab colleagues. Alessia, I have no doubts you will achieve anything you aim at, I'm really proud of you, keep It up! Aaron, my friend, who came as a master student, it was a pleasure working with you and sharing our time together. Agnès, Céline, Youri, and especially Charlotte, thank you for all our talks, laughs, fun… for understanding me, sharing emotions and for your support. I wish the best to you all. Ludovic, Thomas, François… thank you very much for these years, for being part of my pathway and for your valuable support. Thanks a lot, Marylène, as I always said, you are the motor of this lab. Thank you for your patience, for your help and for your implication.

To my KULeuven lab colleagues. I cannot tell how lucky I was by counting on having a second lab where I could feel at home. Tine, An-Sofie, Emma, Katleen, Brecht, Birgit, Janne, Inge, Toon, Willen, Paulien, Liselot, Nora, Daan, Cheyenne, Ellen, Lies, Jonathan… you have been my ray of sun in the cloudy days. Thank you for accompanying me through these years, for the gossips, the

laughs, the hard work… and specially for the ‘Friday, Cryday’. I would not have been able to get through this without your support.

To Caroline Bouzin and Aurélie Daumerie (IREC 2IP), for your invaluable help, for listening and for reminding me to fight for what I want every day.

To Davide Brusa for his help (IREC CytoFlux platform), his patience regarding IgA-bacterial sorting and the optimization of the binding assay and for always making some time to discuss whatever I needed or wanted to discuss.

Thank you, Ilke and Tim, from the University of Antwerp, for your valuable expertise and your patience in performing the sequencing and the bioinformatics for the IgA-SEQ section.

Scientific research would not be possible without the valuable support of institutions like the ‘Fonds National de Recherche Scientifique’ (FNRS), who granted me an Aspirant fellowship to conduct part of my research project, for which I am truly grateful.

Huge thanks to the organizing Council for the Lindau Nobel Laureate Meetings, for giving me the opportunity to be part of the #LINO23 in Chemistry and Medicine and Physiology. Meeting and living with so many inspiring minds was an incredibly unique and life changing experience. Thank you for the opportunity and for the learnings. Thanks to my Biosheets group, you were a huge part of the LINO experience and will always be thankful for the amazing time we had together, both working for the Sciathon and for the personal one.

Gracias a mi familia. Mamá, siempre has sido y serás mi mayor inspiración. No hay palabras suficientes para agradecerte todo lo que haces y has hecho por mí y por mi hermana durante toda nuestra vida. Fuerte, leal, valiente. La “insoportable” y verdadera doctora Montalvo. Ojalá algún día llegue a tener tu fuerza. Tata, siempre has sido y serás un pilar fundamental para mi. Estoy orgullosa de la persona que eres y de cada paso que das. Siempre estaré a tu lado para acompañarte en cada uno de ellos, aunque a veces seamos como el perro y el gato. Gracias, Ángel, por cuidar de la persona más importante de mi vida y por tu paciencia durante estos años. A mis tías, tíos, abuelo y abuela, primos, primas... Ha sido muy duro estar lejos de todos vosotros tanto tiempo, pero siempre me habéis apoyado y habéis celebrado mis logros como si fueran los vuestros. No sería la persona que soy sin la familia tan increíble que tengo. Gracias por estar a mi lado. En especial, gracias a la estrella más brillante del cielo, tita Ita, mi viaje en la investigación empezó por ti, y continuará por todas las personas que luchan día a día para hacer frente a una enfermedad.

Papá, Eva, gracias por apoyarme siempre, por escucharme y por hacer que la distancia nunca importara, a pesar de todo. Os quiero mucho.

A Marta y Paola, por seguir demostrando año tras año que juntas podemos con todo. Por seguir avanzando juntas, por apoyarnos en los peores momentos y por siempre celebrar los buenos. Gracias por ser parte de mi vida.

A Finoula. No sé qué habría sido de mi sin ti. Gracias por tanto compartido en estos años juntas; las comidas, las frustraciones, las alegrías, las noches de chicas serie tras serie, las meriendas, los fines de semana en el laboratorio, las carreras hasta el metro bajo la lluvia… Gracias por tu apoyo incondicional dentro y fuera del laboratorio. Jorge, gracias por ser como eres y por hacerla feliz, por lo que ambos significáis para mí. Estoy deseando que llegue septiembre para celebrar vuestro amor y el resto de vuestra vida juntos.

Justin, you were also a big part of this journey. I have learnt a lot from you and I cannot be prouder of you. Thank you for every moment together, inside and outside the lab. You are a wonderful person, and I wish you all the best.

A Claudia, por ser un gran apoyo estos últimos años, por acogerme las veces que hicieran falta (gracias también a Marta <3) y por todos los momentos compartidos que espero que sean muchos más, empezando por tremendo concierto que nos espera a finales de Junio !!!

A mis amigos de toda la vida: Guillem, Margui, Isa, Sergi, Alberto, … desde pequeños, desde las pistas de voleibol y baloncesto hasta que no nos soportemos más jajaja. Os quiero con todo mi corazón, gracias por estar siempre ahí a pesar de la distancia y apoyarme y escucharme siempre.

A Darío, gracias por haber formado parte de mí, durante los que empezaban a ser los peores años de mi vida. Te mereces y te deseo lo mejor.

A Miki, por hacer que el tiempo no signifique nada para nuestra amistad y por seguir con nuestros planes improvisados. Espero compartir muchos momentos más contigo.

A Álvaro, por compartir experiencias tan únicas como el LINO23 y por acompañarme en la recta final. Por nuestros ratitos de desahogo, de risas, nuestras llamadas, por tirar el uno del otro cuando hace falta. Espero que sigamos contando el uno con el otro muchos años más.

A Julia, mi psicóloga, por acompañarme y por ayudarme a no perder la cabeza este último año tan difícil. Haces un trabajo impecable y estoy muy feliz de haberte encontrado.

A Dirk y Mariola, por convertiros en amigos y demostrarme siempre vuestro apoyo incondicional.

A Juan, gracias por demostrar que la distancia no puede con la amistad. Por escucharme siempre que lo necesito, por las alegrías compartidas durante este tiempo y por formar parte de mi vida.

A mis compañeros divulgadores científicos, a las personas que forman Scenio, por acompañarme, por poder contar siempre con vosotros y por celebrar juntos las buenas noticias. Especialmente a mis chicas, Estefi y Patri, mis imprescindibles. Gracias por ser unas amigas increíbles y por vuestro apoyo. La divertiroom del próximo camp va a caerse cuando celebremos esto juntas.

A todos los que me han acompañado en esta experiencia a través de @inmunominuto, gracias por vuestro apoyo y por tener siempre palabras bonitas hacia mí.

To my Martian family. Romain, Imane, Loriane, Maxime, Louis, Hippolyte and Arnaud. M.A.R.S. UCLouvain was a once in a lifetime experience and I could not have had a better team to share such an adventure. Thank you for making those months memorable and for becoming friends. Spain will be waiting for you!

To my Belgian volleyball team. My dinos, DINO-BAM-BAM, thank you for letting me be myself, in my natural habitat which is a volleyball field. Thank you for the seasons together, for the celebrations, for enjoying together, for your support and for making me happy during my time in Belgium.

Last but not least, to you, Romain. I cannot thank you enough for your support during these last months. You always held my hand when I could not stand by myself. You did not hesitate to stay by my side when everything was too complicated, even if I have not been the easiest person to accompany lately. You made me smile in my darkest days. You will always be my soulmate.

LIST OF ABBREVIATIONS

AFRS	allergic fungal rhinosinusitis
AR	allergic rhinitis
ABSL	animal biosafety level
APC	antigen-presenting cell
APRIL	a proliferation-inducing ligand
BAFF	B-cell activating factor
BAL	bronchoalveolar lavage
BCRS	bacterial chronic rhinosinusitis
BSA	bovine serum albumin
CCAD	central compartment atopic disease
CDR	complementary determining regions
CFU	colony forming units
CLC	Charcot-Leyden crystals
COPD	chronic obstructive pulmonary disease
CRS	chronic rhinosinusitis
CRSsNP	chronic rhinosinusitis without nasal polyp
CRSwNP	chronic rhinosinusitis with nasal polyp
DC	dendritic cell
d-IgA	dimeric IgA
eCRS	eosinophilic chronic rhinosinusitis
eCRSwNP	eosinophilic chronic rhinosinusitis with nasal polyps
ELISA	enzyme-linked immunosorbent assay
ESS	endoscopic sinus surgery
FcαRI	immunoglobulin A Fc receptor
H&E	hematoxylin and eosin

IC	immune complexes
IFNγ	interferon gamma
IgA	immunoglobulin A
IgE	immunoglobulin E
IHC	immunohistochemistry
IL	interleukin
ILC2	type 2 innate lymphoid cells
ILC3	type 3 innate lymphoid cell
i.n.	intranasal
i.p.	intraperitoneal
IQR	interquartile range
LPS	lipopolysaccharide
Ly6G	lymphocyte antigen 6 family member G
MALT	mucosa-associated lymphoid tissue
ND	non-detectable
NL	nasal lavage
NP	nasal polyp
OVA	ovalbumin
pIgR	polymeric immunoglobulin receptor
PBS	phosphate-buffered saline
PRR	pathogen recognition receptor
RT	room temperature
SC	secretory component
SEB	*Staphylococcus aureus* enterotoxin B
S-IgA	secretory IgA
SIgAD	selective IgA deficiency
TACI	transmembrane activator and CAML interactor

TGFβ	transforming growth factor-β
TJ	tight juntions
Th	T helper
TLR	toll-like receptor
TNFα	tumor necrosis factor alpha
TSLP	thymic stromal lymphopoietin
T2	type 2

LIST OF FIGURES

LIST OF TABLES

Chapter I – Introduction and goals of the thesis

Adapted from

Sánchez Montalvo A[1,2], Gohy S[1,3,4], Rombaux P[5], Pilette C[1,2], Hox V[1,5]. The Role of IgA in Chronic Upper Airway Disease: Friend or Foe? Front Allergy. 2022 Mar 9;3:852546. doi: 10.3389/falgy.2022.852546.

[1] Pole of Pneumology, ORL (airways) and Dermatology (skin) (LUNS), Institute of Experimental and Clinical Research (IREC), Université Catholique de Louvain (UCLouvain), Brussels, Belgium
[2] Department of Microbiology, Allergy and Clinical Immunology Research Group, Immunology and Transplantation, KU Leuven, Leuven, Belgium
[3] Department of Pulmonology, Cliniques Universitaires Saint-Luc, Brussels, Belgium
[4] CF reference center, Cliniques Universitaires Saint-Luc, Brussels, Belgium
[5] Department of Otorhinolaryngology, Cliniques Universitaires Saint-Luc, Brussels, Belgium

Preface

Chronic rhinosinusitis (CRS) is a complex and heterogeneous inflammatory disease affecting the sinonasal mucosa, with a substantial burden on patients' quality of life and healthcare systems.

Understanding the immunopathological mechanisms underlying CRS is challenging due to the diversity of clinical presentations and immune endotypes, notably type 2 (T2) eosinophilic and non-type 2 (non-T2) neutrophilic forms.

Secretory immunoglobulin A (s-IgA), a key player in mucosal immunity, has emerged as a potentially critical regulator of host-microbiota interactions and chronic inflammation. Yet, its role in CRS remains insufficiently characterized.

This chapter provides a comprehensive overview of the clinical, immunological and microbiological aspects of CRS, establishing the scientific rationale and objectives that guided the experimental work presented throughout this dissertation.

1. Chronic rhinosinusitis

1.1. Definitions

The respiratory epithelium in the nose and sinuses serves as the body's first line of defense in the airways, continuously exposed to a variety of inhaled particles and agents with each breath [1]. The nasal mucosal lining, along with its immune system, must efficiently manage these challenges to prevent damage. Maintaining a proper epithelial barrier function is, therefore, crucial for upper airway health. When this mucosal barrier fails to sustain a balanced and tolerant immune response to environmental or microbiota-derived antigens, inflammation can arise [2].

Chronic inflammatory diseases of the upper airways are among the most prevalent long-term conditions, affecting approximately 25% of the population in Western countries [3,4]. Rhinitis is the most common upper airway disease, characterized by inflammation of the nasal mucosa, leading to symptoms such as nasal congestion, runny nose, sneezing, and itching [5]. When this inflammation extends to the mucosa of the paranasal sinuses, it results in rhinosinusitis, a condition that affects around 11% of the European population [6], although the estimated prevalence varies from country to country.

Rhinosinusitis is normally identified by the presence of at least two of the following symptoms: facial pain or pressure, nasal congestion, nasal cavity obstruction, rhinorrhea and (partial) loss of smell or anosmia. Additionally, objective evidence of mucosal changes in the paranasal sinuses or signs of sinonasal inflammation must be confirmed through computed tomography or rhinoscopic examination [7]. When symptoms last for more than 12 weeks, we talk about chronic rhinosinusitis (CRS). CRS significantly impacts patients' quality of life [8] and contributes to high healthcare costs and reduced work productivity [9].

1.2. Pathophysiology of CRS

Published guidelines describe chronic rhinosinusitis (CRS) as a complex multifactorial, inflammatory and heterogeneous condition affecting the lining of the nasal and paranasal mucosa. It can present with or without nasal polyps (CRSwNP or CRSsNP, respectively) which determines the phenotypical division of the disease.

Globally, CRSsNP remains the most prevalent phenotype worldwide, comprising 70–85% of all cases, although CRSwNP is relatively more frequent in Western cohorts [7,10,11].

However, as biotherapeutic treatments evolve, the most clinically relevant distinction for CRS is based on the inflammatory endotype, which can be broadly categorized into eosinophilic and non-eosinophilic forms [7,12]. Half of the patients with CRSsNP present with an eosinophilic endotype [13], while in the Western World, around 50-60% of patients with CRSwNP show an eosinophilic inflammation [7,10,14]. Eosinophilic inflammation involves T helper (Th) 2 cells and T2 innate lymphoid cells (ILC2), leading to the production of Interleukin (IL)-4, IL-5, and IL-13, which drive eosinophil accumulation and increased mucus production. In contrast, non-eosinophilic CRS, characterized primarily by neutrophilic or pauci-inflammatory infiltrates, are more commonly observed in CRSsNP where it is the predominant endotype in the other half of patients, although they also appear in a subset of CRSwNP cases [7,10,14]. This type of inflammation involves a mix of Th1, Th17, and Th22 cells, without IgE involvement [3] and is characterized by the production of IL-6, IL-8, tumor necrosis factor alpha (TNF-α), and interferon gamma (IFN-γ), leading to a neutrophilic infiltration [10].

The picture shifts considerably in East Asian populations, where the prevalence of eosinophilic inflammation is markedly lower, ranging between 30–40%, and neutrophilic inflammation dominates the immunopathological landscape, even among CRSwNP patients [7,11]. These regional differences underscore the influence of

genetic, environmental and possibly microbiome-related factors in shaping CRS pathogenesis.

An overview of the estimated prevalence by phenotype and endotype across regions is summarized in Table 1. The above mentioned epidemiological and immunological variability presents a major challenge for the development of targeted treatments and precision medicine strategies in CRS.

Table 1. Estimated distribution of CRS endotypes and phenotypes across Western and Eastern populations.

	By inflammatory endotype	
	Eosinophilic CRS	**Non-eosinophilic CRS**
Western countries	50–60% (mixed CRSsNP + CRSwNP)	40–50% (mainly CRSsNP)
Eastern countried	30–40% (mainly CRSsNP)	60–80% (mainly CRSwNP)
	By phenotype	
	CRSwNP (%)	**CRSsNP (%)**
Western countries	20–30%	70–80%
Eastern countried	10–20%	80–90%

Many patients with severe eosinophilic inflammation are colonized with *Staphylococcus aureus* and exhibit a polyclonal IgE response to its enterotoxins [10] and this reaction has been shown to correlate with severity of the disease [15–17]. Particularly, the interplay between epithelial barrier dysfunction and *Staphyloccal* presence has been suggested as a potential disease driver in eosinophilic CRS (eCRS) [18] . Despite these advancements in mechanistic studies, many aspects of the disease pathophysiology remain unclear.

On the other hand, non-eosinophilic CRS comprises a very heterogeneous patient population and therefore proper mechanistic studies are very scarce. The disease drivers for non-eosinophilic CRS are believed to be multifactorial such as irritant exposure, smoking and bacterial or viral infections. Also, it has been suggested that CRS results from dysfunctional interaction at the interface between the host (internal factors) and the environment (external factors) in the sinonasal mucosa, leading to sinonasal mucosal inflammation [7,13,19–21] but more studies will need to confirm this hypothesis.

The development and clinical expression of CRS are not only influenced by region but also gender and age. Epidemiological data consistently show that women are more likely to report CRS symptoms than men, with some population-based surveys indicating a nearly 1.5-fold higher prevalence in females [22]. Interestingly, while women tend to experience more severe symptom burden, particularly in terms of facial pain, pressure, and reduced quality of life, men more often report nasal obstruction as a predominant complaint [23]. Beyond physical symptoms, gender differences also extend to psychological outcomes as well. Female patients with CRS exhibit significantly higher rates of depression and anxiety than their male counterparts, suggesting a complex biopsychosocial interplay in disease perception and coping mechanisms [24]. Age is another key determinant in CRS development, becoming more prevalent with advancing age, peaking in individuals between 50 and 59 years old [22]. Interestingly, younger patients report a higher psychological burden, possibly due to the disruptive impact of chronic symptoms on social and professional functioning [25]. Taken together, these findings underscore the multifactorial nature of CRS and highlight the importance of considering demographic context when interpreting symptoms, planning interventions, or evaluating disease burden.

In patients with CRS, it is described in literature that a dysfunctional epithelial barrier, a critical defense mechanism against microbial invaders and environmental

irritants, exists [26]. This barrier consists of tightly connected cells supported by structures like tight junctions (TJ) and adherent junctions. Together with the mucociliary clearance system, they act as the first line of defense, trapping and expelling harmful particles [26]. One major factor compromising this system in CRS is the impairment of mucociliary clearance, driven by the destructive activities of some bacteria, notably *Pseudomonas aeruginosa* and *Staphylococcus aureus*, which release toxins that damage cilia. *P. aeruginosa*, with its robust biofilm-forming ability, not only resists antibiotics, but also secretes proteases that degrade TJ proteins, severely weakening the mucosal barrier [15,27]. Meanwhile, *S. aureus* produces enterotoxins that induce oxidative stress and disrupt epithelial integrity [15,27]. This degradation increases the permeability of the epithelium, allowing allergens, irritants, and pathogens to penetrate deeper tissues. Additionally, the interaction of *S. aureus* enterotoxins with TLR2 receptors triggers an inflammatory cascade, releasing cytokines like IL-6 and IL-8. These inflammatory molecules further weaken the barrier and perpetuate tissue damage [16,18,28].

As the epithelial layer weakens, its role may shift from a protective barrier to an active participant in inflammation. Damaged epithelial cells release bioactive substances to recruit immune cells, fueling the inflammatory response and, over time, this chronic inflammation drives tissue remodeling, a hallmark of CRS. The nasal tissues thicken, fibrosis develops, and in some cases, NP can form. This remodeling is exacerbated by oxidative stress and endoplasmic reticulum stress induced by bacterial toxins, creating a loop of damage and repair [26,29]. Therefore, in the context of CRS, the failure of the epithelial barrier might not be merely a consequence but a driving force in disease progression.

1.3. Microbial dysbiosis in CRS

The human microbiota consists of a community of microorganisms, primarily diverse bacterial species, along with archaea (primitive single-celled organisms), eukaryotes, and viruses that inhabit the mucosal surfaces of the gut, skin, respiratory tract, and genital tract [30]. The nose and paranasal sinuses are home to a diverse microbiome, consisting of both commensal and pathogenic bacteria [31–33].

The interaction between host and microbial communities is essential for developing and maintaining several key functions, including immune system regulation and pathogen defense [34–36]. However, factors like genetic susceptibility, environmental influences, infections, and changes in antibiotic use, diet, or lifestyle can disrupt this host–microbiota symbiosis. Such disturbances, leading to dysbiosis, are linked to the pathogenesis of various inflammatory and autoimmune diseases, including CRS [37–39].

Recent studies also suggest that the immunopathogenesis of CRS may partially result from disruptions in the host microbiota, including reduced bacterial diversity, an increase in inflammatory-inducing pathogenic bacteria (e.g., *Staphylococcus aureus* or *Pseudomonas aeruginosa*), and a loss of beneficial bacteria with potential immune-protective roles (such as *Lactobacillus*, *Dolosigranulum*, and *Citrobacter* species) [40–42].

In a healthy state, the bacterial strains commonly identified in the upper airways are *Firmicutes* (which are mainly *Staphylococci*), *Actinobacteria* (mainly *Corynebacterium*, *Bifidobacterium* and *Propionibacterium* species) and *Proteobacteria* (mainly *Moraxella*, *Pseudomonas*, *Enterobacte*r and *Aggregatibacter*) [38,40]. The total bacterial load present in healthy and diseased sinuses appears to be very similar between individuals, with a large inter-individual variation in the microbiome. In some patients, the nasopharynx has shown a more divergent bacterial profile, being enriched in *Haemophilus*, *Streptococcus* and *Prevotella* [41].

De Boeck et al. have shown that the bacterial diversity was reduced in patients with CRSsNP compared with healthy patients, however, this was not the case for patients with CRSwNP [42]. They have also proven that *Dolosigranulum pigrum* was clearly associated with healthy subjects, while *Corynebacterium tuberculostearicum, Haemophilus influenzae/H. aegyptius, and Staphylococcus* taxa were found to be potential pathobionts in patientis with CRS [42].

Many opportunistic pathogens are present in low amounts in healthy sinuses and therefore have a low potential to induce a disease after acute alteration of the stable basal microbial community [43]. Furthermore, an increased amount and variety of members from the phylum *Actinobacteria* and genus *Propionibacterium* distinct healthy sinuses from chronically inflamed sinuses. The absence of *Burkholderia* and *Propionibacterium* phylotypes from healthy patients is associated with an increased network decentralization, which can lead us to conclude that these two strains may act as protectors by their occupancy playing a powerful role in providing a stable sinonasal bacterial community [38,44].

The disruption of the stable microbiota characterized by a loss of beneficial commensal bacteria that act as gatekeepers against the overgrowth of opportunistic pathogenic bacteria may contribute to the exacerbation of chronic inflammatory disease in the absence of acute infection [38–45]. CRS has been associated with shifts in the resident microbiota from a healthy to a diseased state. This disruption, called dysbiosis, can lead to microbial communities becoming pro-inflammatory or invasive and/or allowing pathogens to overgrow.

The study of dysbiosis in human CRS is especially challenging but relevant since antibiotic therapies are frequently used in CRS treatment and are likely to affect resident bacterial communities [38,42,43]. Analysis of the normal state of the microbiome in the sinus cavities is crucial, as commensals play an obvious role in the exclusion of pathogens and in modulating the healthy immune response between the host and

the microbes [43]. The deep nasal cavities and the sinuses present unique local microenvironments and immune properties of the host. Studies comparing the microbiota in healthy subjects versus those with CRS have been carried out by researchers and it appears that *C. tuberculostearicum*, *C. accolens* and *S. aureus* seem to be significantly enriched in the sinuses or the middle meatus (the nasal passage nasal cavity, located between the turbinate of the middle meatus and the lateral nasal wall) of patients with CRS [46]. The increased relative abundance and diversity of other members belonging to a loss of bacterial diversity in the microbiome of patients with CRSsNP compared to controls can be noted, however this is not the case in CRSwNP. This suggests a probable role of the microbiome in disease development or advancement mainly in CRSsNP [38,42]. Other data suggest that colonizing bacteria can contribute to the pathogenesis of CRS by the formation of biofilms. The latter are composed of multiple layers of living bacteria surrounded by a matrix of protein and nucleic acid. These biofilms on mucosal surfaces may grant the infectious pathogens the ability to develop antimicrobial resistance and consequently avoid the host defenses [45–50].

1.4. Management of CRS

Managing CRS involves addressing symptoms, underlying inflammation and microbial imbalance through different therapeutic strategies. Currently, patients with CRS are often treated with corticosteroids, antibiotics, or more recently, biological therapies [7].

A cornerstone of CRS treatment is the use of corticosteroids. Intranasal corticosteroids, such as budesonide and mometasone, are widely used for symptom relief. These therapies reduce inflammation and progressively enhance microbial diversity in the sinonasal cavity, although long-term effects remain uncertain. In severe cases, oral corticosteroids are utilized for their potent anti-inflammatory properties, though their impact on the microbiome is inconsistent and typically limited to short-term use uncertain [7,38,51].

Antibiotics also play a significant role in managing CRS, although with mixed outcomes. Systemic antibiotics, normally delivered orally or intravenously, reach the sinonasal mucosa through systemic circulation. Penicillins (eg. Amoxicillin-clavulanate) act inhibiting bacteria cell wall synthesis, especially for gram-positive bacteria but also for some gram-negative ones. On the other hand, macrolides (eg. Azithromycin, clarithromycin) function blocking bacterial protein synthesis and have anti-inflammatory effects. Fluoroquinolones (eg. Levofloxacin, mixofloxacin), which can inhibit bacterial DNA replication, are especially effective against gram-negative bacteria. Last, tetracyclines (eg. Doxycycline) are bacteriostactic and inhibit bacterial protein synthesis with additional anti-inflammatory benefits [7,38]. Systemic antibiotics show moderate effectiveness for CRS, with better effects for acute cases, and display a broad-espectrum activity against multiple pathogens. However, their main limitations are antibiotic resistance with overuse, side effects especially in the gastrointestinal tract and limited efficacy in penetrating biofilms, which are commonly found in CRS [52]. They are commonly prescribed, but some

studies suggest they offer minimal symptom improvement while potentially reducing microbial diversity [7,52].

Topical antibiotics are applied directly to the sinonasal mucosa, delivered via high-volume irrigations, nasal sprays or nebulizers. Some commonly used are mupirocin, which is effective against *S. aureus* infections; tobramycin, against *P. aeruginosa*; gentamicin with a broad-spectrum activity and especially used for gram-negative infections; and neomycin-polymyxin B which combines broad-spectrum coverage for gram-positive and -negative bacteria. Their main advantages are minimal systemic absorption and therefore, less risk of side effects; direct delivery to the site of infection, ensuring high local concentrations of antibiotic which improves efficacy against biofilm-forming bacteria; and less risk of systemic antibiotic resistance. However, topical antibiotics show limited penetration into unoperated sinuses, risk of local resistance with prolonged use and they require proper delivery methods [7,38,52]. In general, topical antibiotics have shown greater effectiveness in targeting localized infections like *Staphylococcus aureus* biofilms [38]. These targeted therapies could address specific pathogens without significantly altering the broader microbiome, though their effects remain unpredictable.

For patients with persistent symptoms despite medical therapy, endoscopic sinus surgery (ESS) is often the next step. ESS aims to restore normal sinus function and alleviate obstruction, leading to improved symptoms [7]. Interestingly, surgery can increase microbial richness, but it may also destabilize the delicate balance of the sinonasal microbiome. Outcomes tend to be better in patients with higher pre-surgical levels of protective bacteria, such as *Corynebacterium*, which inhibits the growth of pathogenic strains like *Staphylococcus aureus* [38,53].

Emerging biotherapies also offer exciting new options for CRS management. Probiotics, including *Lactobacillus sakei* and *Corynebacterium accolens*, have shown promise in restoring microbial balance and reducing inflammation [54–57]. These

therapies can suppress harmful bacteria and promote a healthier sinonasal environment. Similarly, bacteriophages (viruses that specifically target bacteria) are being explored as a novel way to disrupt biofilms and reduce infections caused by resistant strains like *Staphylococcus aureus* [58]. Bacteriophage therapy has demonstrated efficacy in preclinical studies, reducing biofilm formation and eliminating bacterial pathogens in animal models of sinusitis. Currently, the field is progressing toward clinical applications, with early phase clinical trials evaluating the safety and efficacy of phage therapy for various infections, including those relevant to CRS [58–62]. These trials aim to address critical questions regarding optimal delivery methods, dosing regimens, and the development of personalized phage cocktails adapted to individual microbial profiles. Despite these advances, significant challenges remain, such as regulatory approval processes and ensuring phage stability in clinical formulations. Nevertheless, bacteriophage therapy holds substantial potential as a targeted, adjunctive treatment for CRS, particularly in cases involving multidrug-resistant bacteria [38].

Despite these treatments, a significant portion of patients remains inadequately controlled [63]. Greater understanding of the underlying disease mechanisms is needed to develop new therapeutic options with fewer side effects and to refine these therapies to confirm their clinical applicability.

2. Mouse models to study CRS pathophysiology

Studying the pathophysiology of human disease is often limited due to the heterogeneity of patient population. Therefore, animal models are used to study and to understand health problems that affect both humans and animals. Animal models of inflammatory respiratory disease have contributed to our knowledge about the pathogenesis and pathophysiologic process of these diseases in humans. However, the search for an adequate CRS animal model that mimics the human situation has been shown to be more difficult than e.g. rhinitis or asthma.

The development of a model of CRS is only possible in mammals due to their relatively comparable anatomy and physiology to humans. Different sorts of animals have been tested for this purpose and initially, rabbits were mostly used due to their anatomical sinus resemblance to humans and the possibility to perform relatively easy surgical interventions [64–68].

In recent years, murine models have emerged as a potential alternative. Although many differences exist between humans and mice, they have been proven to be a powerful tool to study immunological pathways in respiratory diseases and the organization and immunological responses of the upper airway are comparable to humans (Figure 1) [69,70]. The wide availability of murine-directed antibodies as well as transgenic strains makes mice a very attractive animal model to study pathophysiological pathways of CRS.

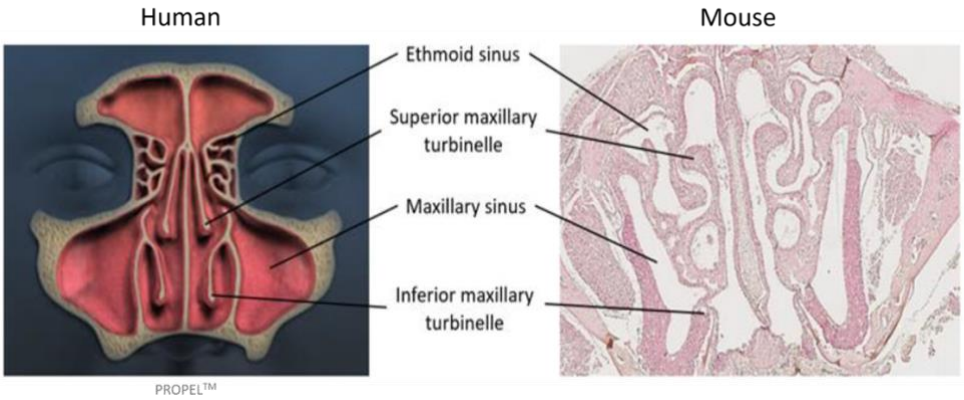

Figure 1. The similarity of the human and mouse paranasal mucosal cavities.
Representation of the paranasal cavities in humans (left) and in mice (right).

Researchers have focused their attention on the development of murine models that reflect what is described in human CRS. Regarding the T2 inflammatory profile, a mouse model that shows eosinophilic infiltration, goblet cells hyperplasia, epithelial thickness and nasal polyp (NP)-like lesions is becoming more and more used and accepted within upper airway research groups. It is based on an intra-peritoneal sensitization of the mouse with the experimental allergen ovalbumin (OVA), followed by nasal challenges with OVA to induce an allergic inflammation. At a later stage, nasal instillations with *Staphylococcus aureus* Enterotoxin B (SEB) are introduced to induce NP-like formations [71]. However, the major drawback of this model was the lack of development of macroscopic NPs, as seen in humans [72]. Despite that, this mouse model has been widely accepted and used in a growing number of publications investigating the mechanisms of human eCRSwNP [73].

Compared to T2 CRS inflammation, there is a huge science gap concerning the non-T2 CRS disease pathways. This is probably because this endotype comprises a very heterogenous patient group which hinders mechanistic research within this field. To unravel the non-T2 mechanisms playing in CRSsNP, it would be an enormous added

value to have a reliable mouse model mimicking this type of sinus inflammation at hand.

So far, no validated mouse model mimicking the non-T2 CRS exists, and only 2 models have been described in literature. One is based on long-term nasal instillations of lipopolysaccharide (LPS) [74], and the second one is based on a model of bacterial CRS (BCRS) [75]. The LPS model, which was not reproducible in our hands, describes a neutrophilic inflammation of the sinuses with the formation of polyp-like lesions. The BCRS model is based on the introduction of a bacterium into the nasal cavity in combination with an obstruction of the sinonasal outflow tract. This is accomplished by surgically introducing a nasal tampon inoculated with bacteria, *Bacteroides fragilis*, in one of the nasal fossae. This model was first described by Jacob et al. and they evaluated the characteristic histologic changes in BCRS [75].

Wang et al. repeated this experiment, comparing it with T2 CRS mouse models. However, they used a different bacterium, *Streptococcus pneumoniae*, and sacrificed mice at different time points that seemed more relevant for modelling CRS. He performed immunological analysis and measured specific cytokines belonging to the non-T2 inflammatory endotype. Interestingly, he found that 2 weeks after surgery, the causal bacteria could still be cultured from the nasal lavage (NL), however at 4 weeks after surgery, no increased presence of the microbe could be detected, indicating that the persisting rhinosinusitis was no longer caused by an acute bacterial infection, but rather due to a persistent post-infectious inflammation [76]. This finding makes this mouse model very attractive, since it corresponds with what is frequently detected in human CRS. Later, another research group reported on the use of this model to prove that bacterial-induced CRS causes tissue inflammation by altering multiple genes relevant to cytokine-cytokine receptor interaction, chemokine signaling, cell adhesion molecules, and the complement and coagulation cascade pathway [77].

Apart from these publications to our knowledge, no other studies using this model have been published. Although it looked quite promising, the publications lacked essential information on the technique and results were little substantiated by figures or pictures, making it difficult to reproduce. Thus, the field of respiratory research still lacks a validated model to study non-eosinophilic or neutrophilic CRS (nCRS) pathogenesis.

3. The role of IgA in respiratory mucosal immunity

3.1. General IgA biology

Immunoglobulin A (IgA), first described in 1953, is the most abundant immunoglobulin produced in external body fluids [78]. Composed of two heavy and two light chains, human IgA exists in two isotype forms, IgA1 and IgA2. Serum IgA, primarily made of monomeric IgA1 (80%), is produced in the bone marrow, while secretory IgA (s-IgA) has a higher proportion of IgA2, which is relatively more resistant to enzymatic degradation [79].

In humans, serum IgA predominantly exists as a monomer and can bind to various receptors expressed by granulocytes, monocytes, macrophages, dendritic cells (DCs), and eosinophils. These receptors include the myeloid-specific type I Fc receptor for IgA (FcαRI or CD89), the Fcα/Fcμ receptor, the asialoglycoprotein receptor, and the transferrin receptor [80]. The effector functions of these receptors are not yet fully understood, encompassing both pro-inflammatory and anti-inflammatory pathways. Anti-inflammatory signals are generated when monomeric IgA binds to FcαRI, while IgA immune complexes trigger pro-inflammatory responses through FcαRI [81].

Although IgA is present in the serum, its primary functions are at the mucosal level, where it exists as s-IgA, produced almost exclusively by local plasma cells. The luminal epithelium, continuously exposed to external antigens, allows these antigens to be taken up by subepithelial antigen-presenting cells (APCs). These APCs process the antigens and initiate mucosal immune responses within mucosa-associated lymphoid tissue (MALT), a structure in which local immune responses are generated. In the upper respiratory tract, MALT is concentrated in the nasopharynx,

across the nasal epithelium, and in structures like the tonsils and adenoids, collectively referred to as nasal-associated lymphoid tissue (NALT) [82].

Within MALT, naïve B-cells are activated by T-cells that respond to APC-processed antigens. This interaction triggers B-cells in the follicles to undergo somatic hypermutation, leading to the development of memory cells and antigen-specific antibodies, including IgA. The production of IgA is primarily driven by transforming growth factor-β1 (TGFβ1), which activates promoters for IgA class switching, making TGFβ1 crucial for T-cell-dependent IgA class switching.

Besides TGFβ1, IgA class switching may also be induced through B-cell activation combined with cytokines like interleukin-2 (IL-2), IL-4, IL-5, IL-6, and IL-10 [82–88].

The MALT environment uniquely fosters the development of IgA-producing B-cells [89]. When primed B-cells in MALT encounter their specific antigen, they mature into conventional B2 cells that produce antigen-specific IgA [90,91]. These cells then migrate to the sinonasal epithelium, where they differentiate into IgA-secreting plasma cells, providing targeted defense against harmful antigens.

Alternatively, to provide a rapid IgA response to inhaled antigens, B-cells can be directed to produce non-specific, polyreactive IgA through a T-cell-independent pathway. Certain T-cell-independent antigens directly activate B-cells, such as lipopolysaccharide (LPS) via Toll-like receptors (TLRs) [92] or polysaccharides through the B-cell receptor (BCR) [93]. Additionally, retinoic acid has been shown to selectively induce an IgA class switch in B-cells [94]. Other T-cell-independent antigens promote IgA production indirectly by stimulating DCs to release B-cell activating factor (BAFF) and a proliferation-inducing ligand (APRIL), which drive IgA1 and IgA2 production in B-cells, respectively [95,96].

Epithelial and local stromal cells can also enhance T-cell-independent IgA production by secreting thymic stromal lymphopoietin (TSLP), IL-6, IL-10, BAFF, and APRIL [97]. TACI (transmembrane activator and CAML interactor), a

transmembrane receptor on B-cells, binds BAFF and APRIL, playing a central role in IgA class switching. B-cells activated through this T-cell-independent pathway are typically of an innate-like type (B1 cells), known to produce unmutated, "natural" IgA, especially in the gut. This natural IgA exhibits spontaneous antigenic specificity for common surface epitopes on erythrocytes, thymocytes, and microorganisms such as phosphorylcholine or LPS [97]. These polyreactive antibodies recognize multiple antigens with low affinity, offering broad, though limited, protection against a range of pathogens [98–100].

Figure 2 summarizes the most important pathways of the IgA/pIgR system at the mucosal barrier.

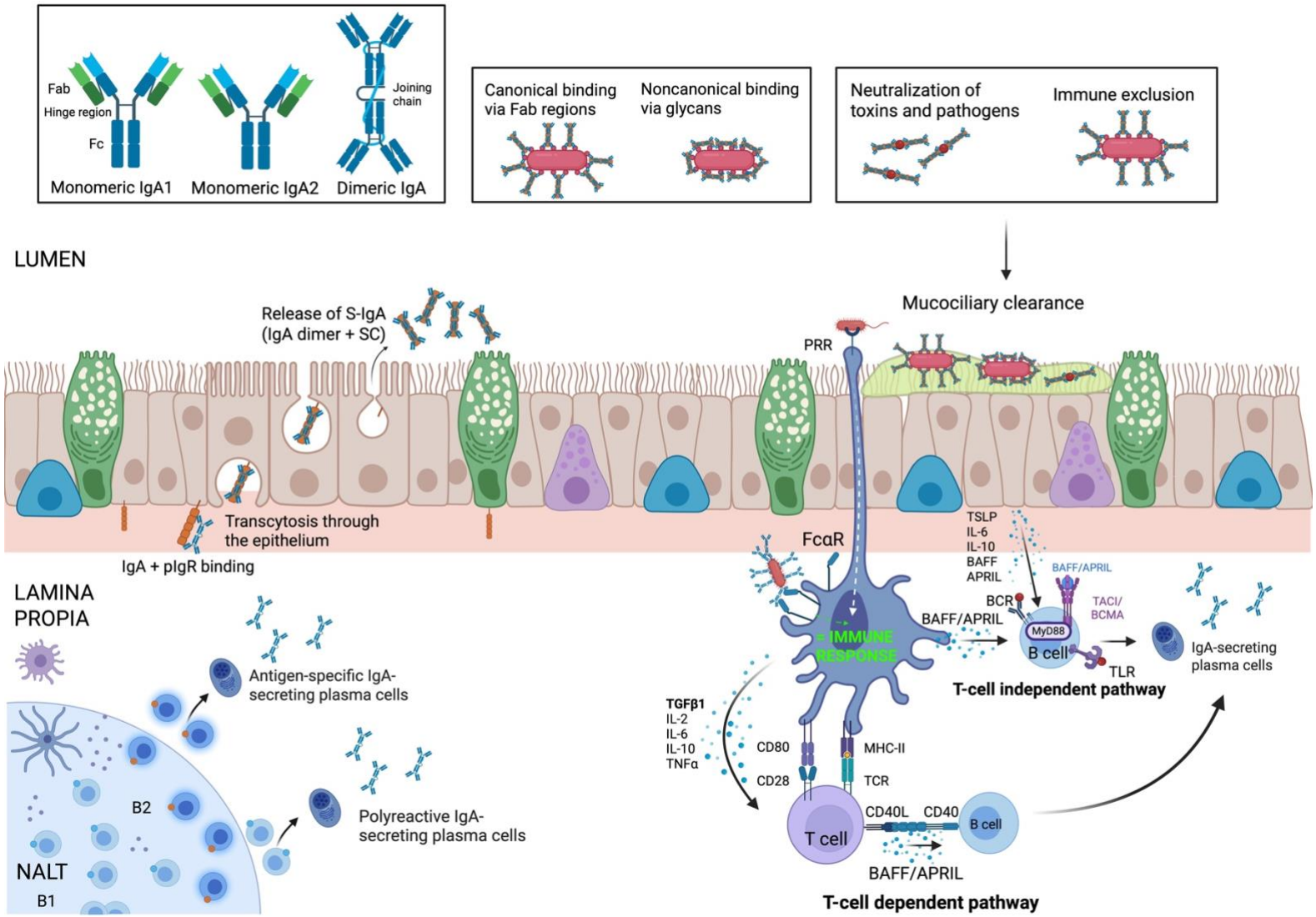
Fab
Hinge region
Fc
Joining chain
Monomeric IgA1
Monomeric IgA2
Dimeric IgA
Canonical binding via Fab regions
Noncanonical binding via glycans
Neutralization of toxins and pathogens
Immune exclusion
LUMEN
Mucociliary clearance
Release of S-IgA (IgA dimer + SC)
PRR
Transcytosis through the epithelium
IgA + pIgR binding
FcαR
TSLP
IL-6
IL-10
BAFF
APRIL
BAFF/APRIL
BCR
TACI/ BCMA
MyD88
B cell
TLR
IgA-secreting plasma cells
T-cell independent pathway
BAFF/APRIL
= IMMUNE RESPONSE
LAMINA PROPIA
Antigen-specific IgA-secreting plasma cells
Polyreactive IgA-secreting plasma cells
B2
NALT
B1
TGFβ1
IL-2
IL-6
IL-10
TNFα
CD80
CD28
MHC-II
TCR
T cell
CD40L
CD40
B cell
BAFF/APRIL
T-cell dependent pathway

Figure 2. IgA biology at the nasal mucosa surface.
Isoforms of IgA are illustrated in upper-left square. In the NALT, antigen-specific and polyreactive IgA is produced by B2 and B1 cells respectively and secreted in the lamina propria by plasma cells as dIgA. The pIgR is responsible for its transepithelial transport towards the lumen, where dIgA is released bound to the SC. The complex IgA/SC is what we know as s-IgA. In the lumen, S-IgA binds toxins and allergens in either a canonical and/or non-canonical way to perform its main roles: neutralization and immune exclusion, preventing bacterial colonization by invasive species (panel inserts). Antigen-activated T-cells induce an IgA class switch in B-cells, typically in the presence of TGF-β, or other mediators secreted by dendritic cells (DC) or epithelium. T-cell independent IgA class switch occurs either via direct antigenic activation of B-cells or via production of B-cell activating factor (BAFF) and/or a proliferation-inducing ligand (APRIL) by DCs. TSLP: thymic stromal lymphopoietin. PRR: pattern-recognition receptor. TLR: toll like receptor. TACI: transmembrane activator and calcium modulating cyclophilin ligand interactor. Created with BioRender.com. Figure from Sánchez-Montalvo et al. 2022 [144].

3.2. The different roles of IgA at the mucosal barrier

3.2.1. Induction of mucosal tolerance against harmless antigens

Beyond its role as a neutralizing antibody that blocks antigens, s-IgA also contributes to antigen sampling by selectively transporting antigens from the lumen to the MALT [101]. Not all antigens encountered threaten the host, and it is crucial that not all trigger immune activation, as this could result in inappropriate inflammatory responses. Ideally, when a harmless antigen is inhaled, immune effector cell responses are suppressed or downregulated, a process known as mucosal tolerance, which helps prevent unnecessary immune reactions.

S-IgA is essential for maintaining mucosal tolerance, largely due to its inability to provoke an inflammatory response when binding its specific receptor, the FcαRI, on its own. FcαRI, expressed by myeloid cells, requires cooperation with other receptors to either amplify or inhibit cytokine production. When IgA binds to its antigen, it forms immune complexes (ICs). Whether these ICs induce tolerance or inflammation via FcαRI depends on the presence or absence of a secondary signal. Without additional signals, the recognition of ICs by FcαRI leads to antigen uptake, resulting in only partial activation of dendritic cells (DCs) without triggering proinflammatory responses [102] (Figure 3). This mechanism is crucial for inducing mucosal tolerance, particularly to inhaled allergens, where s-IgA is thought to play a role, although much about its mechanisms remains unknown.

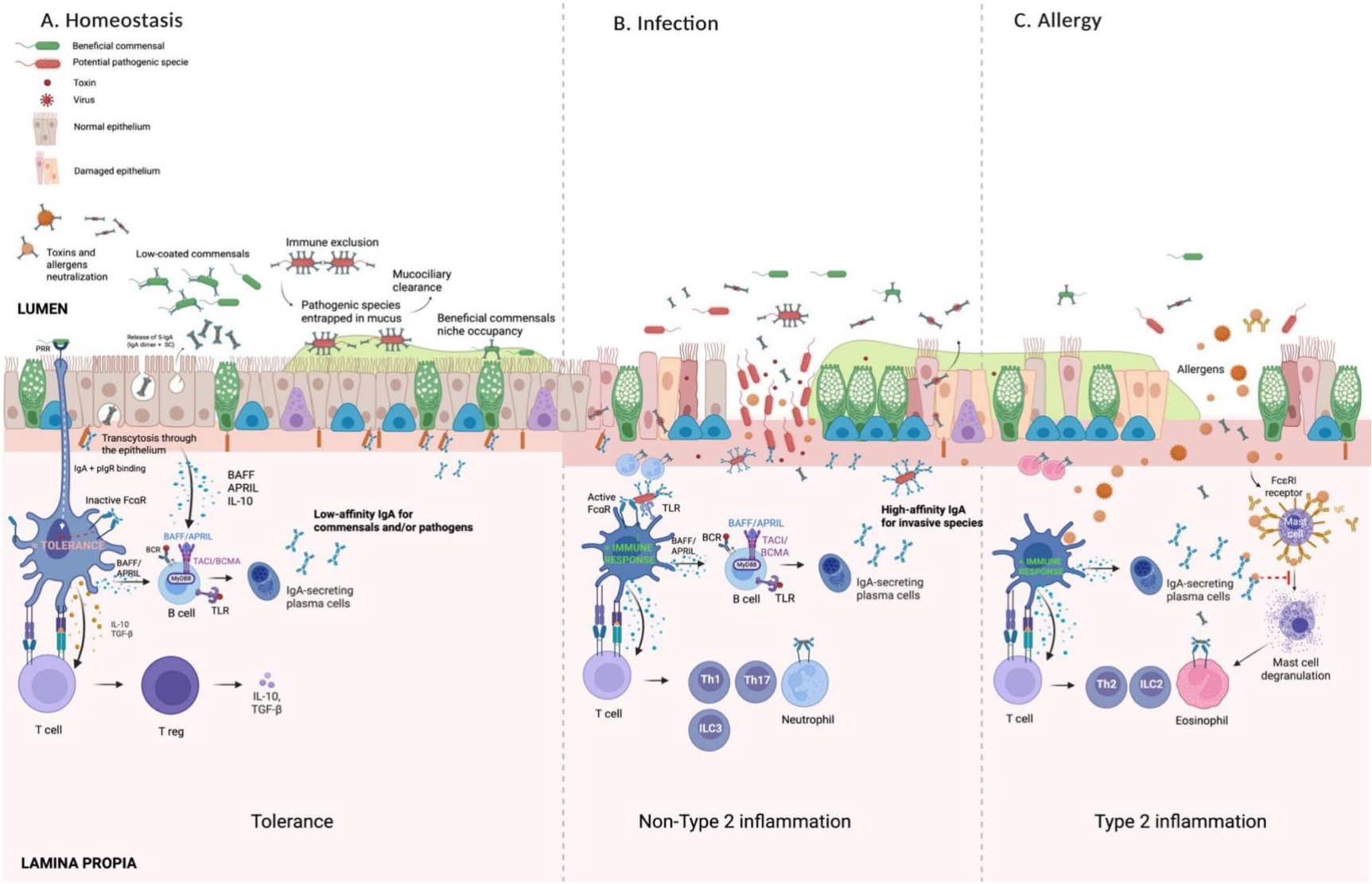
A. Homeostasis
B. Infection
C. Allergy
Beneficial commensal
Potential pathogenic specie
Toxin
Virus
Normal epithelium
Damaged epithelium
Toxins and allergens neutralization
Low-coated commensals
Immune exclusion
Mucociliary clearance
Pathogenic species entrapped in mucus
Beneficial commensals niche occupancy
LUMEN
PRR
Release of S-IgA (IgA dimer + SC)
Transcytosis through the epithelium
IgA + pIgR binding
Inactive FcαR
TOLERANCE
BAFF/APRIL
IL-10
BAFF/APRIL
BCR
TACI/BCMA
MyD88
B cell
TLR
IgA-secreting plasma cells
Low-affinity IgA for commensals and/or pathogens
IL-10
TGF-β
T cell
T reg
IL-10, TGF-β
Active FcαR
TLR
IMMUNE RESPONSE
BAFF/APRIL
BCR
TACI/BCMA
MyD88
B cell
TLR
High-affinity IgA for invasive species
IgA-secreting plasma cells
T cell
Th1
Th17
ILC3
Neutrophil
Allergens
FcεRI receptor
IgE
Mast cell
IMMUNE RESPONSE
IgA-secreting plasma cells
Mast cell degranulation
T cell
Th2
ILC2
Eosinophil
Tolerance
Non-Type 2 inflammation
Type 2 inflammation
LAMINA PROPIA

Figure 3. Suggested roles of IgA in homeostasis and disease.
(A) Homeostasis panel: commensal bacteria colonize mucosal surfaces of the respiratory tract. IgA-secreting plasma cells produce IgA that binds microbes with low affinity, preventing exclusion of coated bacteria. In this way, IgA coating controls the composition of the microbiome by promoting growth of beneficial commensals. Isolated activation of FcαR on DCs induces tolerance via the activation of T regulatory cells. (B) Infection panel: Pathogens that penetrate the epithelial layer will be opsonized by local d-IgA present in the subepithelial space. These antibody-opsonized pathogens will activate DC by a double stimulation of both FcαRI and PRR, such as TLRs. This co-stimulation turns tolerogenic DCs into pro-inflammatory cells which induce an active adaptive immune response by activating Th1, Th17 and type 3 ILCs. (C) Allergy panel: in atopic individuals, the uptake of allergens by DC results in an induction of a type 2 inflammatory environment with the induction of Th2 cells and activation of ILC2 with an influx of eosinophils and production of antigen-specific IgE. In these sensitized individuals, re-exposure to allergens causes a cross-linking of mast-cell bound IgE on mast cells, leading to their degranulation. Secretory IgA (S-IgA) is known to bind and activate eosinophils and might promote this Th2 response. However, antigen-specific IgA is believed to act as a scavenger for allergens, preventing binding to its specific IgE. In the pre-sensitization phase, antigen-specific S-IgA is believed to play an important role in inducing allergenic tolerance. BAFF: B cell activation factor. APRIL: A proliferation inducing ligand. TSLP: Thymic stromal lymphopoietin. PRR: pattern-recognition receptor. IgA-IC: IgA-immune complexes. Created with BioRender.com. Figure from Sánchez-Montalvo et al. 2022 [144]

3.2.2. Protection against pathogenic infections

In addition to maintaining mucosal tolerance, s-IgA plays a vital role in the first-line immune defense against harmful inhaled agents, such as pathogenic microbes. It achieves this protective role through multiple mechanisms across various mucosal sites. S-IgA can bind to microbes in both canonical and non-canonical ways [103]. Canonical binding involves the Fab region of the antibody binding directly to the microbial antigen, while non-canonical binding involves alternative binding modes that do not rely on the complementarity determining regions (CDR) at the ends of the Fab arms. One of the primary roles attributed to s-IgA is immune exclusion, a process that includes several steps such as agglutination, mucus entrapment, and airway clearance [104]. S-IgA prevents first prevents the adhesion of toxins and bacterial surface antigens, like adhesins or pili, which facilitate epithelial invasion, by directly recognizing receptor-binding domains [105]. This is followed by agglutination, where IgA crosslinks with microbial antigens, forming macroscopic clumps of pathogens. Studies in both the gut and airways have shown that these clumped pathogens become trapped in the epithelial mucus layer and are subsequently cleared from the airways [106,107]. This entrapment is largely facilitated by the oligosaccharide side chains of the secretory component (SC), highlighting the advantage of s-IgA over monomeric IgA in secretions [108].

Despite IgA's relatively limited ability to activate complement compared to IgG and IgM, subepithelial d-IgA can still initiate an adaptive immune response. When pathogens breach the epithelial layer, they are opsonized by local d-IgA in the subepithelial space. Under normal conditions, IgA-opsonized pathogens are rare in the lamina propria, but during infection, their presence increases significantly due to microbial invasion. These antibody-opsonized pathogens not only engage FcαRI but also activate pathogen-sensing receptors like Toll-like receptors (TLRs), providing a secondary signal to immune cells. The combination of these signals can co-activate otherwise tolerogenic DCs into pro-inflammatory cells, which then induce an active

adaptive immune response by activating Th17 cells and type 3 innate lymphoid cell (ILC3) responses [109] (Figure 3).

Moreover, the significance of IgA in the protective anti-bacterial immune response is evident, as bacteria have evolved mechanisms to produce anti-IgA or anti-FcαRI bacterial proteins. These proteins interfere with IgA-FcαRI interactions, helping bacteria evade phagocytosis by FcαRI-expressing immune cells [110].

3.2.3. IgA and nasal microbiome homeostasis

The nose and paranasal sinuses are home to a diverse microbiome, consisting of both commensal and pathogenic bacteria [31,32]. In healthy individuals, commensal microbes form a symbiotic relationship with the host and can even help strengthen the mucosal barrier against invading external pathogens. Since both commensals and invading pathogens often share similar antigens, the detection of microbial structures by pathogen recognition receptors (PRRs), like TLRs, alone cannot fully explain how the mucosal immune system differentiates between harmless commensals and harmful bacteria [109]. Given the immunomodulatory properties of IgA, it is believed that this antibody plays a critical role in distinguishing between these microbes, a concept largely explored in the gut. Research suggests that IgA may be responsible for maintaining the balance of indigenous bacteria, rather than eliminating them, to preserve microbial diversity in the gut [111].

At the intestinal mucosal level, it has been observed that IgA binds to the surface of certain members of the intestinal microbiota (up to 74% of gut bacteria are estimated to be coated with s-IgA) yet, in most cases, this binding does not result in their removal from the system [112]. Recent studies have uncovered new aspects of IgA coating, particularly its role in regulating host tolerance towards specific commensals [113]. The question of why some microbes are coated with IgA while others are not remains unanswered. One theory suggests that IgA can directly or indirectly influence microbial gene expression [114,115], leading to varied host cell

responses depending on whether the bacteria are coated with IgA [114]. Another hypothesis is that IgA coating may be linked to the pathogenic potential of the microbe; research by Palm and colleagues found that IgA coating of microbiota could determine the "colitogenic" potential of bacteria, linking it to the development of chronic inflammatory bowel disease [116].

Further evidence supporting this theory comes from patients with selective IgA deficiency (SIgAD), who tend to exhibit gut dysbiosis, marked by an overabundance of certain pathogenic species and a concurrent reduction in beneficial commensals [116–119]. Additionally, it has been demonstrated that s-IgA coating of microorganisms can promote the formation of biofilms, which support the growth of slow-growing commensals while suppressing the growth of pathogenic microbes [120].
Compared to the gut, hardly anything is known about the role of s-IgA in relation to the microbiome of other mucosal surfaces such as the airways.

3.3. IgA in the airways

At the level of the respiratory mucosal epithelium, plasma cells from the lamina propria secrete IgA in the form of dimers, comprising two IgA monomers that are covalently linked to a polypeptide known as J-chain [121]. The J-chain of the dimeric IgA (d-IgA) can bind to the polymeric immunoglobulin receptor (pIgR) at the basolateral site of the nasal epithelium and the complex d-IgA/pIgR is transported, through the epithelial layer, toward the mucosal lumen. In the apical site of the epithelium and after proteolytic cleavage, d-IgA is released bound to the extracellular component of the pIgR, called SC. SC is crucial for further antibody stabilization and for enabling IgA to bind effectively with pathogenic proteins [108].
The complex d-IgA/SC conforms what is known as s-IgA [122]. In the lumen, s-IgA is believed to primarily act through physical mechanisms such as coating, cross-linking, agglutination and promoting the interconnected growth of mucosal antigens. These functions produce a range of effects that generally do not trigger inflammation and contribute to defense of the nasal mucosa in a non-specific way [103] (Figure 2).
Unlike most antibodies, IgA possesses both immunosuppressive and pro-inflammatory properties. This dual role makes IgA crucial for maintaining homeostasis at the mucosal barrier, which is constantly exposed to a wide range of antigens, both harmful and benign (or even beneficial). In the gut, IgA contributes to mucosal balance in three key ways: (1) by neutralizing potentially harmful microbes, (2) by preventing inappropriate inflammatory responses to microbial and food antigens and (3) by shaping the composition of the commensal microbiota. While data on these specific IgA functions in the airways is more limited, similar mechanisms are likely to support respiratory mucosal homeostasis. Figure 3 illustrates the primary pathways through which IgA may contribute to both homeostasis and inflammation triggered by bacteria or allergens in the airways.

4. IgA research in CRS

When studying pathophysiology of CRS, and specifically the role of the humoral immune system, immunoglobulin E (IgE) has received significant attention due to its established role in allergic rhinitis (AR) [5] and CRS with nasal polyps (CRSwNP) [16]. However, the potential contributions of other immunoglobulins in rhinitis and rhinosinusitis have been less explored. Since IgA is the most abundant immunoglobulin in nasal secretions and is regarded to play a crucial role in the first-line immune defense [109,123], surprisingly few research papers have been dedicated to study its role in CRS.

Most of the knowledge on the role of IgA and its receptors in upper airways derives from studies of individuals presenting with SIgAD. SIgAD is characterized by significantly reduced or absent levels of IgA in the serum (typically < 7mg/dl), while IgG and IgM levels remain normal. It is the most common immune deficiency worldwide, affecting approximately 0.7% of the Caucasian population [6]. It has been reported that 16.7 % of patients with CRS have low levels of IgA with 6.2 % matching the definition of SIgAD [124]. Conversely, SIgAD is present more frequently with CRS (up to 78%) compared to individuals with normal antibody levels [125]. In addition to low serum levels, it has been shown that these patients also exhibit absent or very low IgA production in their upper airways [126]. Despite the seemingly critical roles of s-IgA, most patients diagnosed with SIgAD are asymptomatic. This might be explained by either inadequate diagnostic testing or compensation mechanisms by other immunoglobulins. Nevertheless, these patients seem to present with more frequent respiratory infections, allergies, and auto-immune diseases compared to patients with normal IgA levels [127,128].

Initially, the role of IgA in the upper airways was thought to be passive, given that these individuals do not typically present with obvious infectious or inflammatory symptoms. However, recent research indicates that IgA plays a more active role in

immunity [129], and disturbances in IgA biology have been linked to the pathophysiology of rhinitis [130,131]and chronic rhinosinusitis [132].

Several studies have studied the production of IgA in patients with CRS (Table 1). At the serum level, all studies seem to agree that no significant differences are detected between CRS patients and controls [133,134].

The study by Lal et al. reported significantly increased specific IgA production in response to microbial proteins compared to healthy controls in serum. IgA reactivity was particularly higher for several bacterial and viral species, including *Staphylococcus aureus*, human metapneumovirus, human herpesvirus 5, and human herpesvirus 4 [135]. At the level of local IgA production, differences are detected between patients with CRS and healthy controls. Four studies found higher levels of IgA (total and/or IgA1) in sinus tissue from patients with CRSwNP [132,136–138] and three of them showed increased numbers of IgA+ plasma cells [136–138 135-137]. Two studies also reported an overexpression of BAFF, an important inducer of local IgA class switching, in CRSwNP patients [138,139]. These findings indicate an increase in the local IgA production by T2 inflamed polyp tissue (as is the case for IgE) and most of the plasma cells detected in NP tissue are of the IgA producing type [140]. One recent paper suggests the possibility of local conversion of bacterial antigen-specific IgA to IgE that might occur in a Th2 environment [141], but more insight is needed to confirm its relevance.

With regards to s-IgA levels in nasal secretions, results are a bit less straightforward; while a large study performed by Tsybikov and colleagues found increased S-IgA levels in 54 patients with CRSwNP compared to 40 healthy controls [142], this increase was not in keeping with the – smaller – study by Hupin and colleagues [132]. Although they confirmed the previously described increase in tissue IgA in CRSwNP patients, this was not translated into higher S-IgA levels in the nasal secretions, but rather due to an accumulation of IgA in the subepithelial tissue. This could be explained by the

fact that CRSwNP patients showed significantly lower expression levels of pIgR on their epithelium, leading to a reduced transepithelial transport of the immunoglobulin. Although no significant differences in S-IgA were detected, they did demonstrate reduced antigen-specific IgA levels directed towards SEB [132], a powerful superantigen linked to the severity of Th2 inflammation. Most of the other studies looking at IgA levels in CRS did not characterize the specificity of IgA in patients. However, another study found elevated mucosal levels of autoreactive IgA to nuclear antigens, including double stranded DNA and basement membrane components that might contribute to the disease mechanism [143].

Table 2. Human studies investigating the role of IgA in CRS.
Table adapted from Sánchez-Montalvo 2022 [144].

Reference	Populations	IgA expression (tissue)	IgA in serum	IgA in secretions	pIgR expression (tissue)
Lal et al., 2023	39 CRS, 79 healthy controls	Not investigated	- Significantly elevated levels of IgA in response to microbial proteins	Not investigated	Not investigated
Aazami et al., 2020	36 CRSwNP, 12 CRSsNP, 22 healthy controls.	- Increase of total IgA+ cells in the lamina propia of both CRS groups - Increase of total IgA+ cells in the epithelium of patients with CRSwNP - Increase of total IgA and IgA1 in patients with CRSwNP (protein level)	Not investigated	Not investigated	Not investigated
Takeda et al., 2019	46 CRSwNP, 15 healthy controls	- No significant differences in patients with CRSwNP - IgE class switching from IgA-producing B cells	Not investigated	Not investigated	Not investigated

Aazami et al., 2018	10 CRSwNP, 10 CRSsNP, 10 healthy controls.	Not investigated	- No significant differences in total IgA levels and subclasses (IgA1, IgA2) in serum among groups	Not investigated	Not investigated
Dilidaer et al., 2017	25 CRSwNP, 12 CRSsNP, 10 healthy controls	- Increase of BAFF in patients with CRSwNP	Not investigated	Not investigated	Not investigated
Sokoya et al., 2017	6 CRSwNP, 6 CRSsNP, 6 healthy controls.	- Increase of IgA+ cells in patients with CRSwNP - Increase of IgA expression in patients with CRSwNP	Not investigated	Not investigated	Not investigated
Zhang et al., 2017	36 CRSwNP	- Increase of IgA in CRSwNP	Not investigated	Not investigated	- Decrease of pIgR in CRSwNP
Tsybikov et al., 2015	54 CRSwNP, 46 CRSsNP, 40 healthy controls.	Not investigated	Not investigated	- Increased sIgA in both CRS groups, being more pronounced in CRSwNP	Not investigated

Hupin et al., 2013	10 CRSwNP, 13 CRSsNP, 20 healthy controls.	- Decrease of IgA expression in CRSwNP, submucosal accumulation	Not investigated	- No significant differences among groups - Decrease of specific IgA vs *S. aureus* enterotoxin B in CRSwNP	- Decrease of pIgR in CRSwNP - Decrease of SC concentration in CRSwNP (in nasal secretions)
Tan et al., 2011	44 CRSwNP, 25 CRSsNP, 22 healthy controls	- Increase of total IgA levels in patients with CRSwNP	Not investigated	Not investigated	Not investigated
Kato et al., 2008	60 CRSwNP, 39 CRSsNP, 30 healthy controls	- Significant increase of IgA in patients with CRSwNP. - Significant increase of BAFF in patients with CRSwNP. - Significant increase of BAFF in patients with CRSwNP.	Not investigated	- Significant increase of BAFF in patients with CRSwNP.	Not investigated
Van Zele et al., 2007	15 CRSwNP, 15 CRSsNP, 10 healthy controls	- Increase of IgA levels in patients with CRSwNP	- No significant differences in IgA levels among groups	Not investigated	Not investigated
Chee et al., 2001	78 patients with refractory sinusitis	Not investigated	- Below-normal range IgA levels in 13 of 78 patients	Not investigated	Not investigated
Sánchez-Segura et al., 2000	19 CRSwNP, patients' peripheral blood as control	- Increase of IgA-producing cells in nasal polyp tissue	Not investigated	Not investigated	Not investigated

Very little additional information can be retrieved from animal models, mostly due to the lack of well-established models of CRS. Only one paper reported on increased s-IgA levels in nasal secretions of mice with experimentally induced CRS [71].

5. Hypothesis and objectives of the thesis

CRS currently constitutes a major global health burden, with an important impact on the quality of life of patients and important health-care costs [7]. Today, still a lot of question marks remain around its pathogenesis. This is partially linked to the fact that proper mouse models of CRS are lacking. Because of the increased prevalence of CRS in SIgAD patients and the fact that IgA seems to be implicated in chronic inflammatory diseases of the lower airways and the gut, we wanted to dig deeper into the role this immunoglobulin might play in CRS.

Our working hypothesis is that patients with CRS show an aberrant mucosal IgA response, at a quantitative level (via reduced IgA production or reduced receptor-mediated epithelial transport) and/or at a functional level. These abnormalities might lead to a dysregulation of sinonasal microbiome homeostasis and contribute to CRS development.

Thus, the current project aimed at addressing this hypothesis through three main work-packages, through which we aim at addressing the following objectives:

- Objective 1: to establish and/or develop reliable mouse models of eosinophilic and non-eosinophilic CRS to be able to study IgA biology in CRS *in vivo.*

- Objective 2: to evaluate whether the absence of IgA and/or pIgR leads to more severe sinus inflammation *in vivo* using the established mouse models of CRS.

- Objective 3: to study the levels of sinonasal IgA and its receptor (pIgR) in our cohort of patients with CRS and compare them to healthy controls.

- Objective 4: to investigate whether patients with CRS exhibit altered mucosal IgA responses towards their nasal microbiota compared to healthy controls.

To address the complexity of CRS and investigate the role of mucosal immunity, particularly secretory IgA, we structured the thesis in a progressive and logical workflow.

First, we established and characterized a murine model of eosinophilic CRS, mimicking T2 or eosinophilic inflammation, as described in Chapter II. This model served as the foundation to study immune responses associated with eosinophilic forms of CRS.

Recognizing that CRS is a heterogeneous disease with distinct inflammatory endotypes, we then developed and characterized a complementary murine model of neutrophilic CRS, reflecting non-T2 or non-eosinophilic inflammation, as detailed in Chapter III. This bacterial-induced model aimed to better reproduce the infectious and dysbiotic components often implicated in non-T2 CRS pathogenesis.

In Chapter IV, we aimed to bridge experimental models with clinical reality by integrating human samples and pioneering mucosal immunology techniques. First, we characterized nasal mucosal biopsies from CRS patients to validate key immune and inflammatory features. Then, we expanded the use of our established mouse models described in Chapter II and Chapter III by using genetically modified mice lacking s-IgA (pIgR knockout mice), allowing us to assess the impact of s-IgA deficiency on disease development and inflammatory responses. A major innovation of this chapter was the application of the IgA-SEQ technology in bacteria obtained from our patients' cohort, which enabled the identification of bacteria specifically targeted by mucosal IgA. To our knowledge, this was the first time IgA-SEQ was applied in the context of CRS, providing novel insights into host-microbiota interactions at the sinonasal surface. However, we also recognize some limitations of the IgA-SEQ approach in this setting, particularly related to the low biomass nature of sinonasal samples, which may affect detection sensitivity and the interpretation of coating patterns.

Through this combined approach, using human biopsies, established murine model and the use of IgA-SEQ technology, we sought to provide a more comprehensive and translational understanding of the role of mucosal IgA in CRS pathogenesis.

6. References

1. Johnston, S. L., Goldblatt, D. L., Evans, S. E., Tuvim, M. J. & Dickey, B. F. Airway Epithelial Innate Immunity. Front Physiol 12, (2021).
2. Zhang, R. et al. Epithelial Barrier in the Nasal Mucosa, Related Risk Factors and Diseases. Int Arch Allergy Immunol 184, 481–501 (2023).
3. Bachert, C. et al. Adult chronic rhinosinusitis. Nat Rev Dis Primers 6, 86 (2020).
4. Bousquet, J. et al. Allergic rhinitis. Nat Rev Dis Primers 6, 95 (2020).
5. Greiner, A. N., Hellings, P. W., Rotiroti, G. & Scadding, G. K. Allergic rhinitis. The Lancet 378, 2112–2122 (2011).
6. Momtazmanesh, S. et al. Global burden of chronic respiratory diseases and risk factors, 1990–2019: an update from the Global Burden of Disease Study 2019. EClinicalMedicine 59, 101936 (2023).
7. Fokkens, W. J. et al. European Position Paper on Rhinosinusitis and Nasal Polyps 2020. Rhinology journal 0, 1–464 (2020).
8. Khan, A. et al. The GALEN rhinosinusitis cohort: chronic rhinosinusitis with nasal polyps affects health-related quality of life. Rhinology journal 0, 0–0 (2019).
9. Rudmik, L. Economics of Chronic Rhinosinusitis. Current Allergy and Asthma Reports vol. 17 Preprint at https://doi.org/10.1007/s11882-017-0690-5 (2017).
10. Tomassen, P. et al. Inflammatory endotypes of chronic rhinosinusitis based on cluster analysis of biomarkers. Journal of Allergy and Clinical Immunology 137, 1449-1456.e4 (2016).
11. Zhang, N. et al. Different types of T-effector cells orchestrate mucosal inflammation in chronic sinus disease. Journal of Allergy and Clinical Immunology 122, 961–968 (2008).
12. De Greve, G. et al. Endotype-driven treatment in chronic upper airway diseases. Clin Transl Allergy 7, 22 (2017).
13. Delemarre, T. et al. Type 2 inflammation in chronic rhinosinusitis without nasal polyps: Another relevant endotype. Journal of Allergy and Clinical Immunology 146, 337-343.e6 (2020).
14. Bachert, C. et al. Adult chronic rhinosinusitis. Nat Rev Dis Primers 6, (2020).
15. Chegini, Z. et al. The role of Staphylococcus aureus enterotoxin B in chronic rhinosinusitis with nasal polyposis. Cell Communication and Signaling 20, 29 (2022).
16. Delemarre, T., De Ruyck, N., Holtappels, G., Bachert, C. & Gevaert, E. Unravelling the expression of interleukin-9 in chronic rhinosinusitis: A possible role for Staphylococcus aureus. Clin Transl Allergy 10, 41 (2020).
17. Van Zele, T. et al. Staphylococcus aureus colonization and IgE antibody formation to enterotoxins is increased in nasal polyposis [6]. Journal of Allergy and Clinical Immunology vol. 114 981–983 Preprint at https://doi.org/10.1016/j.jaci.2004.07.013 (2004).
18. Tuli, J. F. et al. Association between mucosal barrier disruption by Pseudomonas aeruginosa exoproteins and asthma in patients with chronic rhinosinusitis. Allergy 76, 3459–3469 (2021).
19. Hammad, H. & Lambrecht, B. N. The basic immunology of asthma. Cell 184, 1469–1485 (2021).
20. Cao, P.-P., Wang, Z.-C., Schleimer, R. P. & Liu, Z. Pathophysiologic mechanisms of chronic rhinosinusitis and their roles in emerging disease endotypes. Annals of Allergy, Asthma & Immunology 122, 33–40 (2019).
21. Lam, K., Schleimer, R. & Kern, R. C. The Etiology and Pathogenesis of Chronic Rhinosinusitis: a Review of Current Hypotheses. Curr Allergy Asthma Rep 15, 41 (2015).
22. Ference, E. H. et al. Commentary on Gender Differences in Prevalence, Treatment, and Quality of Life of Patients with Chronic Rhinosinusitis. Allergy & Rhinology 6, (2015).

23. Bartosik, T. J. et al. Differences in men and women suffering from CRSwNP and AERD in quality of life. European Archives of Oto-Rhino-Laryngology 278, 1419–1427 (2021).
24. Fan, H. et al. Prevalence and predictors of depression and anxiety in patients with chronic rhinosinusitis: a systematic review and meta-analysis. BMJ Open 14, e079273 (2024).
25. Fan, H. et al. Prevalence and predictors of depression and anxiety in patients with chronic rhinosinusitis: a systematic review and meta-analysis. BMJ Open 14, e079273 (2024).
26. Jiao, J., Wang, C. & Zhang, L. Epithelial physical barrier defects in chronic rhinosinusitis. Expert Rev Clin Immunol 15, 679–688 (2019).
27. Shaghayegh, G. et al. Chronic Rhinosinusitis, S. aureus Biofilm and Secreted Products, Inflammatory Responses, and Disease Severity. Biomedicines 10, 1362 (2022).
28. Martens, K. et al. Staphylococcus aureus enterotoxin B disrupts nasal epithelial barrier integrity. Clinical & Experimental Allergy 51, 87–98 (2021).
29. Chegini, Z., Noei, M., Hemmati, J., Arabestani, M. R. & Shariati, A. The destruction of mucosal barriers, epithelial remodeling, and impaired mucociliary clearance: possible pathogenic mechanisms of Pseudomonas aeruginosa and Staphylococcus aureus in chronic rhinosinusitis. Cell Communication and Signaling 21, 306 (2023).
30. Hou, K. et al. Microbiota in health and diseases. Signal Transduct Target Ther 7, 135 (2022).
31. Ramakrishnan, V. R. et al. The Microbiome of the Middle Meatus in Healthy Adults. PLoS One 8, e85507 (2013).
32. Mahdavinia, M., Keshavarzian, A., Tobin, M. C., Landay, A. L. & Schleimer, R. P. A comprehensive review of the nasal microbiome in chronic rhinosinusitis (CRS). Clinical & Experimental Allergy 46, 21–41 (2016).
33. Escapa, I. F. et al. New Insights into Human Nostril Microbiome from the Expanded Human Oral Microbiome Database (eHOMD): a Resource for the Microbiome of the Human Aerodigestive Tract. mSystems 3, (2018).
34. Hillman, E. T., Lu, H., Yao, T. & Nakatsu, C. H. Microbial Ecology along the Gastrointestinal Tract. Microbes Environ 32, 300–313 (2017).
35. Riccio, P. & Rossano, R. The human gut microbiota is neither an organ nor a commensal. FEBS Lett 594, 3262–3271 (2020).
36. Khaledi, M. et al. The role of gut microbiota in human metabolism and inflammatory diseases: a focus on elderly individuals. Ann Microbiol 74, 1 (2024).
37. Zheng, D., Liwinski, T. & Elinav, E. Interaction between microbiota and immunity in health and disease. Cell Res 30, 492–506 (2020).
38. Fischer, J. L. & Lee, J. T. Update on the Role of the Microbiome in Chronic Rhinosinusitis. Curr Treat Options Allergy 11, 17–33 (2024).
39. van Dalen, R. et al. Secretory IgA impacts the microbiota density in the human nose. Microbiome 11, 233 (2023).
40. Lee, K., Pletcher, S. D., Lynch, S. V., Goldberg, A. N. & Cope, E. K. Heterogeneity of Microbiota Dysbiosis in Chronic Rhinosinusitis: Potential Clinical Implications and Microbial Community Mechanisms Contributing to Sinonasal Inflammation. Front Cell Infect Microbiol 8, (2018).
41. Gan, W. et al. The influence of nasal microbiome diversity and inflammatory patterns on the prognosis of nasal polyps. Sci Rep 11, 6364 (2021).
42. De Boeck, I. et al. Anterior Nares Diversity and Pathobionts Represent Sinus Microbiome in Chronic Rhinosinusitis. mSphere 4, (2019).
43. Cho, D.-Y., Hunter, R. C. & Ramakrishnan, V. R. The Microbiome and Chronic Rhinosinusitis. Immunol Allergy Clin North Am 40, 251–263 (2020).
44. Lee, J. T., Kim, C. M. & Ramakrishnan, V. Microbiome and disease in the upper airway. Curr Opin Allergy Clin Immunol 19, 1–6 (2019).

45. Kumpitsch, C., Koskinen, K., Schöpf, V. & Moissl-Eichinger, C. The microbiome of the upper respiratory tract in health and disease. BMC Biol 17, 87 (2019).
46. Lal, D. et al. Mapping and comparing bacterial microbiota in the sinonasal cavity of healthy, allergic rhinitis, and chronic rhinosinusitis subjects. Int Forum Allergy Rhinol 7, 561–569 (2017).
47. Palmer, J. Bacterial Biofilms in Chronic Rhinosinusitis. Annals of Otology, Rhinology & Laryngology 115, 35–39 (2006).
48. Hekiert, A. M. et al. Biofilms correlate with TH1 inflammation in the sinonasal tissue of patients with chronic rhinosinusitis. Otolaryngol Head Neck Surg 141, 448–53 (2009).
49. Foreman, A. et al. Adaptive immune responses in Staphylococcus aureus biofilm-associated chronic rhinosinusitis. Allergy: European Journal of Allergy and Clinical Immunology 66, 1449–1456 (2011).
50. Costerton, J. W., Stewart, P. S. & Greenberg, E. P. Bacterial Biofilms: A Common Cause of Persistent Infections. Science (1979) 284, 1318–1322 (1999).
51. Chong, L. Y. et al. Different types of intranasal steroids for chronic rhinosinusitis. Cochrane Database Syst Rev 4, CD011993 (2016).
52. Smith, S. S., Kim, R. & Douglas, R. Is there a role for antibiotics in the treatment of chronic rhinosinusitis? Journal of Allergy and Clinical Immunology 149, 1504–1512 (2022).
53. Wang, J. C., Moore, C. A., Epperson, M. V. & Sedaghat, A. R. Association of the sinonasal bacterial microbiome with clinical outcomes in chronic rhinosinusitis: a systematic review. Int Forum Allergy Rhinol 10, 433–443 (2020).
54. Psaltis, A. J., Mackenzie, B. W., Cope, E. K. & Ramakrishnan, V. R. Unraveling the role of the microbiome in chronic rhinosinusitis. Journal of Allergy and Clinical Immunology 149, 1513–1521 (2022).
55. Bianco, M. R. et al. The Role of Probiotics in Chronic Rhinosinusitis Treatment: An Update of the Current Literature. Healthcare 9, 1715 (2021).
56. Menberu, M. A. et al. In vitro and in vivo evaluation of probiotic properties of Corynebacterium accolens isolated from the human nasal cavity. Microbiol Res 255, 126927 (2022).
57. Menberu, M. A. et al. Corynebacterium accolens Has Antimicrobial Activity against Staphylococcus aureus and Methicillin-Resistant S. aureus Pathogens Isolated from the Sinonasal Niche of Chronic Rhinosinusitis Patients. Pathogens 10, 207 (2021).
58. Uyttebroek, S. et al. The Potential Role of Bacteriophages in the Treatment of Recalcitrant Chronic Rhinosinusitis. Antibiotics 10, 675 (2021).
59. Penziner, S., Schooley, R. T. & Pride, D. T. Animal Models of Phage Therapy. Front Microbiol 12, (2021).
60. Fong, S. A. et al. Safety and efficacy of a bacteriophage cocktail in an in vivo model of Pseudomonas aeruginosa sinusitis. Translational Research 206, 41–56 (2019).
61. Liu, S., Lu, H., Zhang, S., Shi, Y. & Chen, Q. Phages against Pathogenic Bacterial Biofilms and Biofilm-Based Infections: A Review. Pharmaceutics 14, 427 (2022).
62. Cui, L. et al. A Comprehensive Review on Phage Therapy and Phage-Based Drug Development. Antibiotics 13, 870 (2024).
63. van der Veen, J. et al. Real-life study showing uncontrolled rhinosinusitis after sinus surgery in a tertiary referral centre. Allergy 72, 282–290 (2017).
64. Marks, S. C. Acute Sinusitis in the Rabbit: A New Rhinogenic Model. Laryngoscope 107, 1579–1585 (1997).
65. Maeyama, T. A Study of Experimental Sinusitis in Rabbits. Auris Nasus Larynx 8, 87–98 (1981).
66. Johansson, P., Kumlien, J., Carlsöö, B., Drettner, B. & Nord, C. E. Experimental Acute Sinusitis in Rabbits: A Bacteriological and Histological Study. Acta Otolaryngol 105, 357–365 (1988).
67. Min, Y. G., Lee, Y. M., Lee, B. J., Jung, H. W. & Chang, S. O. The effect of ostial opening on experimental maxillary sinusitis in rabbits. Rhinology 31, 101–5 (1993).

68. Westrin, K. M., Norlander, T., Stierna, P., Carlsöö, B. & Nord, C. E. Experimental Maxillary Sinusitis Induced by Bacteroides fragilis A Bacteriological and Histological Study in Rabbits. Acta Otolaryngol 112, 107–114 (1992).
69. Chamanza, R. & Wright, J. A. A Review of the Comparative Anatomy, Histology, Physiology and Pathology of the Nasal Cavity of Rats, Mice, Dogs and Non-human Primates. Relevance to Inhalation Toxicology and Human Health Risk Assessment. Journal of Comparative Pathology vol. 153 287–314 Preprint at https://doi.org/10.1016/j.jcpa.2015.08.009 (2015).
70. Al-Sayed, A. A., Agu, R. U. & Massoud, E. Models for the study of nasal and sinus physiology in health and disease: A review of the literature. Laryngoscope Investig Otolaryngol 2, 398–409 (2017).
71. Kim, D.-Y. et al. A Recently Established Murine Model of Nasal Polyps Demonstrates Activation of B Cells, as Occurs in Human Nasal Polyps. Am J Respir Cell Mol Biol 55, 170–5 (2016).
72. Sánchez-Montalvo, A. et al. Validation and shortcomings of the most common mouse model of chronic rhinosinusitis with nasal polyps. Rhinology Journal 0, 0–0 (2024).
73. Leite-Santos, F., Tamashiro, E., de Andrade Batista Murashima, A., Anselmo-Lima, W. T. & Valera, F. C. P. Which are the best murine models to study Eosinophilic Chronic Rhinosinusitis? A contemporary review. Braz J Otorhinolaryngol 89, 101328 (2023).
74. Wang, S. et al. Establishment of a mouse model of lipopolysaccharide induced neutrophilic nasal polyps. Exp Ther Med (2017) doi:10.3892/etm.2017.5208.
75. Jacob, A., Faddis, B. T. & Chole, R. A. Chronic bacterial rhinosinusitis: description of a mouse model. Arch Otolaryngol Head Neck Surg 127, 657–64 (2001).
76. Wang, H. et al. Histological and Immunological Observations of Bacterial and Allergic Chronic Rhinosinusitis in the Mouse. Am J Rhinol 22, 343–348 (2008).
77. Geng, L., Wang, S., Zhao, Y. & Hu, H. Gene expression profile in mouse bacterial chronic rhinosinusitis. Exp Ther Med (2019) doi:10.3892/etm.2019.7366.
78. KERR, M. A., MAZENGERA, R. L. & STEWART, W. W. Structure and function of immunoglobulin A receptors on phagocytic cells. Biochem Soc Trans 18, 215–217 (1990).
79. Kerr, M. A., Loomes, L. M., Bonner, B. C., Hutchings, A. B. & Senior, B. W. Purification and Characterization of Human Serum and Secretory IgAl and lgA2 Using Jacalin. in Lectin Methods and Protocols 265–278 (Humana Press, New Jersey). doi:10.1385/0-89603-396-1:265.
80. Mkaddem, S. Ben et al. IgA, IgA Receptors, and Their Anti-inflammatory Properties. in 221–235 (2014). doi:10.1007/978-3-319-07911-0_10.
81. Bakema, J. E. & van Egmond, M. The human immunoglobulin A Fc receptor FcαRI: a multifaceted regulator of mucosal immunity. Mucosal Immunol 4, 612–624 (2011).
82. Brandtzaeg, P. Immunology of tonsils and adenoids: everything the ENT surgeon needs to know. Int J Pediatr Otorhinolaryngol 67, S69–S76 (2003).
83. Muramatsu, M., Nagaoka, H., Shinkura, R., Begum, N. A. & Honjo, T. Discovery of Activation-Induced Cytidine Deaminase, the Engraver of Antibody Memory. in 1–36 (2007). doi:10.1016/S0065-2776(06)94001-2.
84. Cerutti, A. et al. CD40 ligand and appropriate cytokines induce switching to IgG, IgA, and IgE and coordinated germinal center and plasmacytoid phenotypic differentiation in a human monoclonal IgM+IgD+ B cell line. J Immunol 160, 2145–57 (1998).
85. Zan, H., Cerutti, A., Dramitinos, P., Schaffer, A. & Casali, P. CD40 engagement triggers switching to IgA1 and IgA2 in human B cells through induction of endogenous TGF-beta: evidence for TGF-beta but not IL-10-dependent direct S mu-->S alpha and sequential S mu-->S gamma, S gamma-->S alpha DNA recombination. J Immunol 161, 5217–25 (1998).
86. Snapper, C. M. et al. B cells from p50/NF-kappa B knockout mice have selective defects in proliferation, differentiation, germ-line CH transcription, and Ig class switching. J Immunol 156, 183–91 (1996).

87. Zhang, K., Mills, F. C. & Saxon, A. Switch circles from IL-4-directed epsilon class switching from human B lymphocytes. Evidence for direct, sequential, and multiple step sequential switch from mu to epsilon Ig heavy chain gene. J Immunol 152, 3427–35 (1994).
88. Fagarasan, S. & Honjo, T. T-Independent Immune Response: New Aspects of B Cell Biology. Science (1979) 290, 89–92 (2000).
89. Craig, S. W. & Cebra, J. J. PEYER'S PATCHES: AN ENRICHED SOURCE OF PRECURSORS FOR I <scp>G</scp> A-PRODUCING IMMUNOCYTES IN THE RABBIT. J Exp Med 134, 188–200 (1971).
90. Stashenko, P., Nadler, L. M., Hardy, R. & Schlossman, S. F. Characterization of a human B lymphocyte-specific antigen. J Immunol 125, 1678–85 (1980).
91. Bhan, A. K., Nadler, L. M., Stashenko, P., McCluskey, R. T. & Schlossman, S. F. Stages of B cell differentiation in human lymphoid tissue. J Exp Med 154, 737–749 (1981).
92. Peng, S. L. Signaling in B cells via Toll-like receptors. Curr Opin Immunol 17, 230–236 (2005).
93. Mond, J. T cell independent antigens. Curr Opin Immunol 7, 349–354 (1995).
94. Seo, G.-Y. et al. Retinoic acid acts as a selective human IgA switch factor. Hum Immunol 75, 923–929 (2014).
95. He, B. et al. Intestinal Bacteria Trigger T Cell-Independent Immunoglobulin A2 Class Switching by Inducing Epithelial-Cell Secretion of the Cytokine APRIL. Immunity 26, 812–826 (2007).
96. Hardenberg, G., van Bostelen, L., Hahne, M. & Medema, J. P. Thymus-independent class switch recombination is affected by APRIL. Immunol Cell Biol 86, 530–534 (2008).
97. Berland, R. & Wortis, H. H. Origins and Functions of B-1 Cells with Notes on the Role of CD5. Annu Rev Immunol 20, 253–300 (2002).
98. Franco, M. A. & Greenberg, H. B. Immunity to Rotavirus in T Cell Deficient Mice. Virology 238, 169–179 (1997).
99. Macpherson, A. J. & Uhr, T. Induction of Protective IgA by Intestinal Dendritic Cells Carrying Commensal Bacteria. Science (1979) 303, 1662–1665 (2004).
100. Wijburg, O. L. C. et al. Innate secretory antibodies protect against natural Salmonella typhimurium infection. J Exp Med 203, 21–26 (2006).
101. Corthésy, B. Roundtrip Ticket for Secretory IgA: Role in Mucosal Homeostasis? The Journal of Immunology 178, 27–32 (2007).
102. Golebski, K. et al. FcγRIII stimulation breaks the tolerance of human nasal epithelial cells to bacteria through cross-talk with TLR4. Mucosal Immunol 12, 425–433 (2019).
103. Pabst, O. & Slack, E. IgA and the intestinal microbiota: the importance of being specific. Mucosal Immunol 13, 12–21 (2020).
104. Mantis, N. J. & Forbes, S. J. Secretory IgA: Arresting Microbial Pathogens at Epithelial Borders. Immunol Invest 39, 383–406 (2010).
105. Williams, R. C. & Gibbons, R. J. Inhibition of Bacterial Adherence by Secretory Immunoglobulin A: A Mechanism of Antigen Disposal. Science (1979) 177, 697–699 (1972).
106. Boullier, S. et al. Secretory IgA-Mediated Neutralization of Shigella flexneri Prevents Intestinal Tissue Destruction by Down-Regulating Inflammatory Circuits. The Journal of Immunology 183, 5879–5885 (2009).
107. Michetti, P., Mahan, M. J., Slauch, J. M., Mekalanos, J. J. & Neutra, M. R. Monoclonal secretory immunoglobulin A protects mice against oral challenge with the invasive pathogen Salmonella typhimurium. Infect Immun 60, 1786–1792 (1992).
108. Phalipon, A. et al. Secretory Component. Immunity 17, 107–115 (2002).
109. Hoepel, W., Golebski, K., van Drunen, C. M. & den Dunnen, J. Active control of mucosal tolerance and inflammation by human IgA and IgG antibodies. Journal of Allergy and Clinical Immunology 146, 273–275 (2020).

110. Aleyd, E., Heineke, M. H. & van Egmond, M. The era of the immunoglobulin A Fc receptor Fcα <scp>RI</scp>; its function and potential as target in disease. Immunol Rev 268, 123–138 (2015).
111. Holmgren, J. et al. Mucosal adjuvants and anti-infection and anti-immunopathology vaccines based on cholera toxin, cholera toxin B subunit and CpG DNA. Immunol Lett 97, 181–188 (2005).
112. Sterlin, D. et al. Human IgA binds a diverse array of commensal bacteria. Journal of Experimental Medicine 217, (2020).
113. Bunker, J. J. & Bendelac, A. IgA Responses to Microbiota. Immunity 49, 211–224 (2018).
114. Peterson, D. A. et al. Characterizing the Interactions between a Naturally Primed Immunoglobulin A and Its Conserved Bacteroides thetaiotaomicron Species-specific Epitope in Gnotobiotic Mice. Journal of Biological Chemistry 290, 12630–12649 (2015).
115. Peterson, D. A., McNulty, N. P., Guruge, J. L. & Gordon, J. I. IgA Response to Symbiotic Bacteria as a Mediator of Gut Homeostasis. Cell Host Microbe 2, 328–339 (2007).
116. Palm, N. W. et al. Immunoglobulin A Coating Identifies Colitogenic Bacteria in Inflammatory Bowel Disease. Cell 158, 1000–1010 (2014).
117. Catanzaro, J. R. et al. IgA-deficient humans exhibit gut microbiota dysbiosis despite secretion of compensatory IgM. Sci Rep 9, 13574 (2019).
118. Fadlallah, J. et al. Microbial ecology perturbation in human IgA deficiency. Sci Transl Med 10, (2018).
119. Jørgensen, S. F. et al. Selective IgA deficiency in humans is associated with reduced gut microbial diversity. Journal of Allergy and Clinical Immunology 143, 1969-1971.e11 (2019).
120. Bollinger, R. R. et al. Secretory IgA and mucin-mediated biofilm formation by environmental strains of Escherichia coli: role of type 1 pili. Mol Immunol 43, 378–387 (2006).
121. Woof, J. M. & Russell, M. W. Structure and function relationships in IgA. Mucosal Immunol 4, 590–597 (2011).
122. Stadtmueller, B. M. et al. The structure and dynamics of secretory component and its interactions with polymeric immunoglobulins. Elife 5, (2016).
123. Mestecky, J. The common mucosal immune system and current strategies for induction of immune responses in external secretions. J Clin Immunol 7, 265–276 (1987).
124. Chee, L., Graham, S. M., Carothers, D. G. & Ballas, Z. K. Immune Dysfunction in Refractory Sinusitis in a Tertiary Care Setting. (2001).
125. Aghamohammadi, A. et al. IgA Deficiency: Correlation Between Clinical and Immunological Phenotypes. J Clin Immunol 29, 130–136 (2009).
126. Brandtzaeg, P. et al. The clinical condition of IgA-deficient patients is related to the proportion of IgD- and IgM-producing cells in their nasal mucosa. Clin Exp Immunol 67, 626–36 (1987).
127. Aytekin, C., Tuygun, N., Gokce, S., Dogu, F. & Ikinciogullari, A. Selective IgA Deficiency: Clinical and Laboratory Features of 118 Children in Turkey. J Clin Immunol 32, 961–966 (2012).
128. Yel, L. Selective IgA Deficiency. J Clin Immunol 30, 10–16 (2010).
129. Hansen, I. S., Baeten, D. L. P. & den Dunnen, J. The inflammatory function of human IgA. Cellular and Molecular Life Sciences 76, 1041–1055 (2019).
130. Stokes, C. R., Taylor, B. & Turner, M. W. ASSOCIATION OF HOUSE-DUST AND GRASS-POLLEN ALLERGIES WITH SPECIFIC IgA ANTIBODY DEFICIENCY. The Lancet 304, 485–488 (1974).
131. Bahceciler, N. N. et al. Impact of Sublingual Immunotherapy on Specific Antibody Levels in Asthmatic Children Allergic to House Dust Mites. Int Arch Allergy Immunol 136, 287–294 (2005).

132. Hupin, C. et al. Downregulation of polymeric immunoglobulin receptor and secretory IgA antibodies in eosinophilic upper airway diseases. Allergy: European Journal of Allergy and Clinical Immunology 68, 1589–1597 (2013).
133. Aazami, H. et al. Levels of total IgA and IgA subclasses in the serum of chronic rhinosinusitis patients. Med J Islam Repub Iran 32, 1–4 (2018).
134. Van Zele, T., Gevaert, P., Holtappels, G., Van Cauwenberge, P. & Bachert, C. Local immunoglobulin production in nasal polyposis is modulated by superantigens. Clinical and Experimental Allergy 37, 1840–1847 (2007).
135. Lal, D. et al. Antibody responses to the host microbiome in chronic rhinosinusitis. Int Forum Allergy Rhinol 13, 1503–1510 (2023).
136. Aazami, H. et al. Local eosinophils are associated with increased IgA subclass levels in the sinonasal mucosa of chronic rhinosinusitis with polyp patients. Allergy, Asthma and Clinical Immunology 16, (2020).
137. Sokoya, M. et al. Expression of immunoglobulin D is increased in chronic rhinosinusitis. Annals of Allergy, Asthma and Immunology 119, 317-323.e1 (2017).
138. Kato, A. et al. Evidence of a role for B cell-activating factor of the TNF family in the pathogenesis of chronic rhinosinusitis with nasal polyps. Journal of Allergy and Clinical Immunology 121, (2008).
139. Dilidaer et al. Increased BAFF expression in nasal polyps is associated with local IgE production, Th2 response and concomitant asthma. European Archives of Oto-Rhino-Laryngology 274, 1883–1890 (2017).
140. Sánchez-Segura, A., Brieva, J. A. & Rodríguez, C. Regulation of immunoglobulin secretion by plasma cells infiltrating nasal polyps. Laryngoscope 110, 1183–1188 (2000).
141. Takeda, K. et al. Allergic conversion of protective mucosal immunity against nasal bacteria in patients with chronic rhinosinusitis with nasal polyposis. Journal of Allergy and Clinical Immunology 143, 1163-1175.e15 (2019).
142. Tsybikov, N. N., Egorova, E. V., Kuznik, B. I., Fefelova, E. V. & Magen, E. Anticytokine autoantibodies in chronic rhinosinusitis. Allergy Asthma Proc 36, 473–480 (2015).
143. Tan, B. K. et al. Evidence for intranasal antinuclear autoantibodies in patients with chronic rhinosinusitis with nasal polyps. Journal of Allergy and Clinical Immunology 128, (2011).
144. Sánchez Montalvo, A., Gohy, S., Rombaux, P., Pilette, C. & Hox, V. The Role of IgA in Chronic Upper Airway Disease: Friend or Foe? Frontiers in Allergy 3, (2022).

Chapter II – Establishment and characterization of an experimental murine model of eosinophilic CRS

Adapted from

Sanchez-Montalvo A[1,2], Lecocq M[1], Bouillet E[1], Steelant B[1,2], Gohy S[1,3,4], Froidure A[1,3], Bullens D[2,5], Pilette C[1,3], Hox V[1,6]. Validation and shortcomings of the most common mouse model of chronic rhinosinusitis with nasal polyps. Rhinology. 2024 Aug 1;62(4):446-456. doi: 10.4193/Rhin23.331.

[1] Department of Pneumology, ENT and Dermatology, Institute of Experimental and Clinical Research (IREC), Université Catholique de Louvain (UCLouvain), 1200 Brussels, Belgium
[2] Department of Microbiology, Immunology and Transplantation; Allergy, and Clinical Immunology Research Group, KULeuven, 3000 Leuven, Belgium
[3] Department of Pneumology, Cliniques Universitaires Saint-Luc, 1200 Brussels, Belgium
[4] Cystic Fibrosis Reference Centre, Cliniques Universitaires Saint-Luc, 1200 Brussels, Belgium.
[5] Clinical Division of Paediatrics, UZ Leuven, 3000 Leuven, Belgium.
[6] Department of Otorhinolaryngology, Cliniques Universitaires Saint-Luc, 1200 Brussels, Belgium.

Preface

CRS is a heterogeneous disease characterized by distinct inflammatory endotypes, including T2 or eosinophilic and non-T2 or non-eosinophilic forms. Understanding the immunological mechanisms underlying these subtypes is essential for improving therapeutic strategies.

To explore these mechanisms underlying eosinophilic CRS experimentally, we first established and characterized a murine model reproducing key features of type 2 inflammation.

Chapter II presents the establishment and characterization of a murine model mimicking eosinophilic CRS, providing the basis for subsequent investigations into mucosal immune responses.

1. Abstract

Background: Chronic rhinosinusitis (CRS) is a highly prevalent airway disease worldwide. Whereas eosinophilic CRS with nasal polyps (eCRSwNP) represents its most severe phenotype, pathogenic mechanisms remain poorly understood despite a wide spectrum of *in vitro* and *in vivo* experimental models. A mouse model of experimental ovalbumin (OVA)-induced airway allergy with coadministration of *Staphylococcus aureus* enterotoxin B (SEB) has been widely used to study eosinophilic eCRSwNP. This study revisits the features of this model and its suitability for studying eCRS.

Methodology: We implemented the most used eCRSwNP mouse model based on OVA+SEB intranasal challenges. Readouts including inflammatory features by (immuno)histology of the sinonasal epithelium (NP formation, eosinophils, epithelial and basement membrane thickness, fibrosis, goblet cells, Charcot-Leyden crystals (CLC)-like, tight junctions) and IgE production by enzyme-linked immunosorbent assay (ELISA), were compared to features of the corresponding human disease.

Results: The OVA+SEB model induced eosinophilic inflammation of upper and lower airways, with epithelial and basement membrane thickening, goblet cell hyperplasia and subepithelial fibrosis in the sinuses, along increased IgE production. Except local IgE in nasal lavage (NL), which was only increased in OVA+SEB group, all other features did not differ between OVA and OVA+SEB groups. Macro- or microscopic NP were not detected.

Conclusions: With the notable exception of local IgE production, the addition of SEB did not induce additional inflammatory or structural changes in the sinuses from mice exposed to and challenged with OVA. This model, although it is a good tool to study eosinophilic inflammation, might represent a model for severe upper airway allergy rather than a specific model of human eCRSwNP.

2. Introduction

Chronic rhinosinusitis (CRS) is one of the most common upper airway inflammatory diseases in the Western world, with a prevalence of 11% [1]. CRS may severely impair patients' quality of life, leading to a significant socio-economic burden [2]. In the most recent guidelines, CRS is classified according to its inflammatory subtype: T2 inflammation, characterized by the canonical T helper (h) 2 inflammatory pathways; and non-T2 inflammation, a more heterogeneous group characterized by the presence of Th1/Th17/Th22 cytokines [3]. In the Western world, patients with a T2 profile often present with the formation of nasal NP arising from the paranasal sinuses and protruding into the nasal cavities [4]. Patients suffering from eCRS with NP (eCRSwNP) suffer from more severe symptoms and experience increased recurrence after surgery compared to non-T2 patients [3]. Moreover, it has been described that around 22-40% of patients with eCRS present with asthma, fitting the united airways hypothesis [5].

Although many scientific advancements have helped unraveling disease mechanisms of T2 eCRS in recent years [6-9], its exact pathophysiology and driving triggers for NP formation remain elusive. One of the best-studied disease-modifying factors is increased sinonasal colonization with *Staphylococcus aureus* and the link between its enterotoxins and CRSwNP. Especially, SEB plays a role as a superantigen but can also elicit several direct harmful effects on the respiratory mucosa [10-14]. Another feature that has arisen as a key driver for CRSwNP is the loss of the epithelial barrier function formed by e.g. junctional complexes [15,16], which can also be affected by SEB [17].

Because of the IgE-mediated eosinophilic T2 inflammation seen in most CRSwNP patients, it was initially thought that IgE-mediated allergy was the inciting factor for this disease. Therefore, the link with allergic rhinitis (AR) has been extensively studied [18]. However, it has become clear that not all patients with CRSwNP suffer

from allergy and, to date, there's no conclusive evidence linking allergy to CRS. Some specific phenotypes of CRSwNP such as allergic fungal rhinosinusitis (AFRS) and the more recently described central compartment atopic disease (CCAD) seem to be more related to allergy. However, in other CRS phenotypes the prevalence of AR does not appear to be higher than in the general population [19]. Additionally, AR is a very prevalent disease that shows a significant overlap in symptomatology and histopathology with CRS [3].

Studying the pathophysiology of human disease is often limited due to the heterogeneity of patient population, which could be partially solved by the availability of a suitable animal model. In the past decades, murine models have emerged as useful tools to study immunological pathways in respiratory diseases such as asthma and AR [20,21]. Despite the differences between humans and mice, their airway organization and immunological responses are comparable [22]. In 2011, a mouse model of eCRS was described by Kim [23]. This model was based on the induction of experimental airway allergy followed by nasal exposure to SEB [23]. As a result, mice developed an eosinophilic influx at the sinus epithelium, characterized by general features of T2 inflammation. However, the major drawback of this model was the lack of development of macroscopic NPs, as seen in humans. Despite that, this mouse model has been widely used in a growing number of publications investigating the mechanisms of human eCRSwNP [24]. In general, while this model does not intend to fully replicate the heterogeneity of human CRS, it provides a valuable platform to investigate fundamental mechanisms relevant to disease development under standardized conditions.

In this chapter, we aimed to establish this common mouse model to study eCRS for further research and to evaluate the classical inflammatory features of this mouse model in a critical way. We searched whether the addition of SEB truly added value to the classical AR mouse and compared its features to those of human eCRSwNP. This section describes our experience with this widely used eCRS model. We discuss the different issues related to it and from which researchers in this field may benefit when interpreting results. Also, although it is a good tool to study eosinophilic sinonasal inflammation, we point out the gaps for the establishment of a more adequate mouse model for eCRSwNP.

3. Methodology

3.1. Experimental procedure to induce experimental eosinophilic CRS in mice

3.1.1. Animal model

7-8 weeks old C57BL/6NRJ female mice (weighting 20-25g) were purchased from the Janvier Labs (Centre d'élevage Roger Janvier) facility. Mice were housed in an animal facility with agreement reference LA1230292, maintained at 22-25 °C and 50-60% relative humidity. A summary of the experimental protocol is shown in Figure 4. Mice were randomly divided into four different groups with n = 4 to 10/group: control, SEB, OVA, and OVA+SEB. Briefly, based on Kim et al. 2011, OVA was used to sensitize mice with an intraperitoneal (i.p.) injection of a total volume of 200 µl containing 25 µg of OVA in 2 mg of aluminum hydroxide gel on days 0 and 7. Control mice were injected with 200 µl of Phosphate-Buffered Saline (PBS). This was followed by daily intranasal (i.n.) challenges from day 14 to 20 with 6% OVA diluted in 20 µl of PBS. Mice in the control and SEB groups received i.n. challenges with PBS instead. These i.n. challenges were continued at a rate of three times a week for 8 consecutive weeks. Mice that were planned to develop an eCRS, received, in addition to these i.n. OVA-challenges, a second i.n. challenge with 10 ng of SEB diluted in 20 µl of PBS, also three times a week for eight weeks. For i.n. installations, mice were slightly sedated by using isoflurane inhalation (Isoflutek 1,000 mg/g, Karizoo Laboratories). After i.n. installations, each mouse was closely followed until completely awakened. All animal experiments were performed in compliance with the ethical committee guidelines and approved under the reference code 2018/UCL/MD/42.

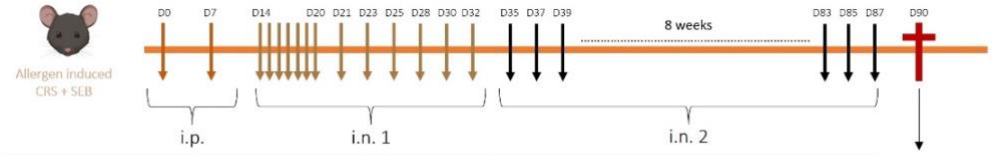

Group	i.p. injection (200 µl)	i.n. instillation 1 (20 µl)	i.n. instillation 2 (20 µl)
Control	PBS	PBS	PBS
SEB	PBS	PBS	SEB 10ng
OVA	OVA 25µg + Alum 2mg	OVA 6%	OVA 6%
OVA + SEB	OVA 25µg + Alum 2mg	OVA 6%	OVA 6% followed by SEB 10 ng

Figure 4. Experimental protocol for the induction of eCRS based on the original model.
OVA: ovalbumin; SEB: Staphylococcus aureus enterotoxin B; Alum: aluminum.

3.1.2. Sacrifice and sampling

Three days after the final i.n. challenge, mice were euthanized by administering an i.p injection of pentobarbital (200mg/kg). First, blood was drawn from the inferior cava vein and centrifuged at 650g for 20 minutes at room temperature (RT) and serum was collected and stored at -20ºC for further processing. NL fluid was collected and recovered via the nostrils by softly flushing 1ml of saline solution (NaCl 0.9%) by inserting a 22G cannula (VersatusTM I.V Catheter) through a tracheotomy. Then, the NL was centrifuged at 450g for 5 minutes at 4ºC to collect the cell pellet, which was used for performing cytospins, and the supernatant was stored at -20ºC for further processing. Bronchoalveolar Lavage (BAL) was collected by inserting a second catheter via the created tracheotomy, through which 1mL of saline solution was gently flushed and recovered from the bronchioles. Like the NL, the BAL was centrifuged at 450g for 5 minutes at 4ºC to collect the cell pellet, which was used for performing cytospins, and the supernatant was stored at -20ºC for further processing. Then, an intracardiac perfusion was performed with 5 ml of saline

solution to rinse the lung blood vessels and then the lungs were fixed in formaldehyde 4% for further histology analysis. Skulls were harvested and skin and soft tissues, as well as the inferior mandibula, were removed. They were fixed in formaldehyde 4% and decalcified in 20 ml of OsteoralTM (RAL Diagnostics) for 5 days. After decalcification, the snout and brain were removed to keep the skull region of interest containing the paranasal sinuses. The decalcified skull and lungs were dehydrated and treated according to standard paraffin-embedding procedures. Paraffinized Skulls and lungs were cut into 4 µm sections by using a semi-automated microtome (ThermoFisher Scientific).

3.2. Cytospins for inflammatory cell count

NL and BAL were collected as described and centrifuged at 450g for 5 minutes at 4ºC to separate the cell pellet. The supernatant was stored, and cells were counted by using a TC20^{TM} Automated Cell Counter (Bio-Rad). Cells were loaded into a Thermo Shandon Cytospin Centrifuge (Thermo Shandon) following the manufacturer's instructions and centrifuged at 500 revolutions per minute (rpm) for 5 min. Cytospins were stained by using the Kwik-Diff^{TM} kit (Thermo Fisher Scientific). In brief, sections are fixed in the 'Kwik-Diff' fixative solution I. Then the slides are stained with the 'Kwik-diff' eosin solution II and followed by a counterstaining with the 'Kwik-diff' methylene blue solution III. Last, slides are rinsed in distilled water to remove excess stain, coverslipped, and scanned by using a Pannoramic scan II (3DHistech).

3.3. Histopathologic analysis of the paranasal sinus epithelium

To analyze the below-mentioned parameters among the different mice groups, we decided to focus on the three fixed areas of both the right and the left maxillary sinus (two areas on the lateral side and one area on the medial side) were taken to evaluate histological features (Figure 5). After being stained by the respective staining protocols, all slides were coverslipped and scanned by using a Pannoramic scan II (3DHistech).

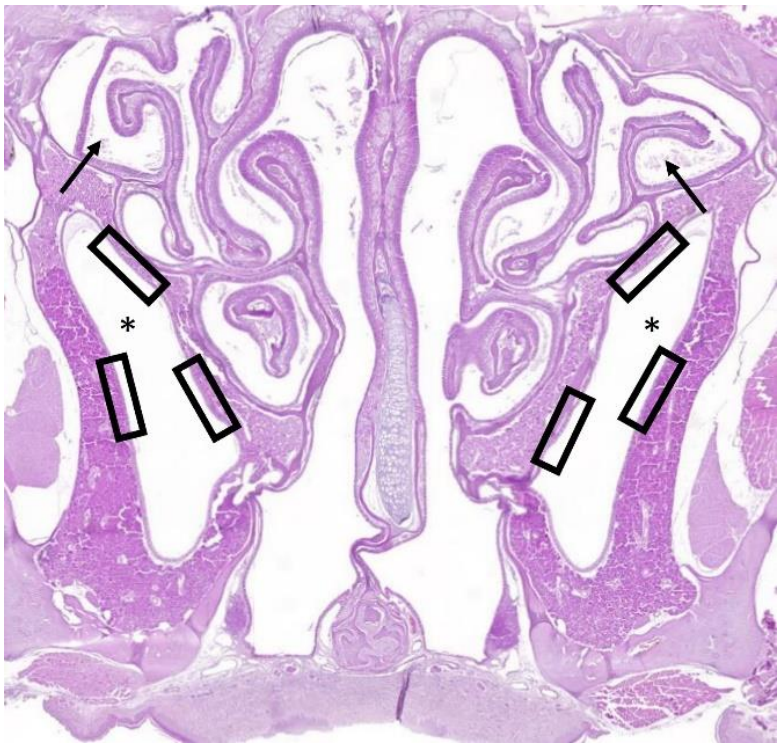

Figure 5. Coronal section of the sinonasal complex of mice showing the maxillary (*) and ethmoidal sinuses (arrow), H&E staining.
Rectangles indicate the regions of the maxillary sinuses that were selected in each mouse to evaluate different histological features in a systematic way.

To study the epithelial integrity, formation of NP-like lesions and epithelial thickness, H&E staining was performed. Briefly, paraffinized 4 µm sections the sections underwent deparaffination and rehydration by putting them into toluene and methanol for 3 times 5 minutes for each solvent and then, in tap water and distilled water for 5 minutes each. Next, the slides were incubated into hematoxylin for 5 minutes and after that, they were rinsed in tap and distilled water for 5 minutes each. Further, the slides were incubated with eosin for 10 minutes, followed by a double wash in methanol and a final incubation in xylene for 3 times 5 minutes each. Finally, the slides were coverslipped and scanned by using a Pannoramic scan II (3DHistech). To count NP-like lesions per mouse, consecutive sections at three consecutive levels of the skull were evaluated, similar to the initial model published by Kim [23]. NP-like lesions were defined as a projection from the lining of the epithelium to the lumen, with a tear-drop shape and filled with eosinophils. NP-like lesions were only considered when found in three consecutive sections at three different levels in the skull to account for artefacts.

To evaluate epithelial thickness, the cellular space between the basolateral to the apical pole of the epithelial cell layer was manually measured by using Cytomine [25].

To evaluate basement membrane thickness, the space between the basolateral pole of the epithelial layer and the first layer of submucosal glands was manually measured by using Cytomine [25].

Giemsa staining was performed to evaluate goblet cell hyperplasia and eosinophilic infiltration. Quantification was performed by using QuPath [26] and expressed as a percentage of positive area. Giemsa staining was performed to evaluate goblet cell hyperplasia and eosinophilic infiltration. Briefly, paraffinized 4 µm sections underwent deparaffination and rehydration by putting them into toluene and methanol for 3 times 5 minutes for each solvent and then, in tap water and distilled water for 5 minutes each. Next, the slides were incubated with Giemsa solution

(Merck) 2% for 20 minutes. Then, they were differentiated with absolute ethanol, coverslipped and scanned by using a Pannoramic scan II (3DHistech).

Sirius red (SR) staining was performed to evaluate collagen deposition. Briefly, paraffinized 4 µm sections underwent deparaffination and rehydration by putting them into toluene and methanol for 3 times 5 minutes for each solvent and then, in tap water and distilled water for 5 minutes each. Next, the slides were permeabilized by incubating them with phosphomolybdic acid for 2 minutes and then were rinsed in tap and distilled water for 5 minutes each. Further, the slides were incubated with Picrosirius Red for 2 hours at RT in a humid chamber. After that, the slides were incubated in hydrochloric acid for 2 minutes in light agitation, followed by a wash in distilled water and dehydration in absolute ethanol and a final incubation in xylene for 3 times 5 minutes each. Finally, the slides were coverslipped and scanned by using a Pannoramic scan II (3DHistech). Quantification was performed by using ImageJ, as described by Courtoy et al. [27], and expressed as a percentage of positive stained area following the formula:

$$\%\ positive\ staining = \frac{Positive\ area}{Total\ area}\ x\ 100.$$

3.4. Immunohistochemical expression of tight junctions in the sinus epithelium

Paraffinized 4 µm sections were deparaffinized in toluene and rehydrated through graded series from methanol to distilled water. Sections underwent antigen retrieval treatment using an antigen retriever (2100 antigen retriever, Aptum Biologics). Endogenous peroxidase and non-specific protein binding sites were inactivated by incubation in Bloxall (Vector Laboratories, Inc., USA) for 15 min and with 0.3% hydrogen peroxide in tris-buffered saline (TBS) 5% goat serum (Abcam) for 30 min. As primary antibodies, rabbit anti-mouse Claudin 3 (Invitrogen, 34-1700), mouse anti-mouse Claudin 4 (Invitrogen, 32-9400), rabbit anti-mouse occludin (Invitrogen,

71-1500) and mouse anti-ZO1 (Invitrogen, 33-9100) were respectively incubated overnight at 4ºC. After washing with TBS 0.1% Tween 20 (TBS-T), sections were incubated with either goat anti-rabbit poly HRP (B40962, ThermoFisher) or goat anti-mouse poly HRP (B40961, ThermoFisher) as secondary antibody for 40 minutes. Revelation was performed by using a DAB Plus Substrate Kit (D4168, Sigma-Aldrich) according to the manufacturer's instructions. Sections were counterstained with Hematoxylin (Sigma-Aldrich) and coverslipped. Slides were scanned using a Pannoramic scan II (3DHistech). Quantification was performed by using QuPath [26] and expressed as percentage of positive area. To compare the above-mentioned parameters between the different mice groups, three areas of both the right and the left maxillary sinus (two areas on the lateral side and one area on the medial side) were taken to evaluate histological features (Figure 5). The quantification strategy for tight junction' expression is shown in Figure 6.

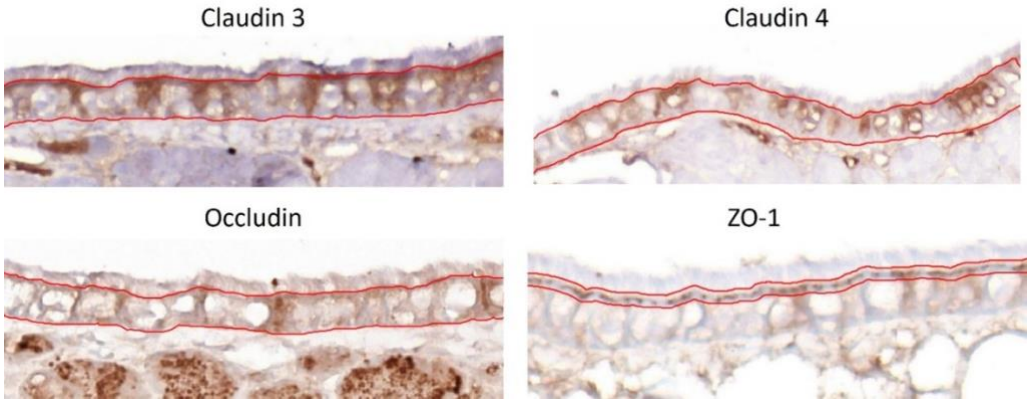

Figure 6. Validation and quantification strategy for TJ staining.
In red, the region of interest considered for the quantification of TJ staining (brown). Quantification was performed by using QuPath [26].

3.5. Total IgE and cytokine measurements

Serum and NL levels of total IgE were determined by sandwich ELISA. Briefly, a 96-well microplate (Greiner Bio-one) was coated with purified mouse IgE (BD Pharmingen 553413) as capture antibody and was incubated overnight at 4ºC. Next, the plates were blocked with bovine serum albumin (BSA) 1% and incubated for 1h at 37ºC and washed with PBS + 0.05% Tween 20. Standards (BD Pharmingen, 557079) and samples were added to the plates and incubated for 2h at 37ºC. After washing, the detection was performed with biotinylated anti-mouse IgE (BD Pharmingen, 553419) for 1h at 37ºC, followed by Streptavidin-HRP amplification for 30 min at RT. Revelation was performed using 1-Step™ Ultra TMB (Thermo Fisher Scientific) and sulfuric acid was added to stop the reaction. The absorbance was measured at 405 nm on a microplate reader (iMarkTM Microplate Absorbance Reader, Bio-Rad Laboratories, Inc). The lower limit of detection was 2.87 ng/ml. Serum samples were diluted 1:25 in PBS and NL samples were used undiluted.

The same protocol was performed to determine levels of IL-4 and IL-5 using the commercial DuoSet® ELISA kits from R&D systems following manufacturer instructions. The lower detection limit was 62,5 pg/ml for IL-4 and 125 pg/ml for IL-5. NL samples were used undiluted.

3.6. Histopathologic analysis of the bronchial epithelium

Giemsa staining was also performed in paraffinized 4 μm sections of the fixed left lung lobe as described above to evaluate the general state of the lung epithelium and to evaluate eosinophilic infiltration. Slides were coverslipped and scanned by using a Pannoramic scan II (3DHistech).

3.7. Statistical analysis

Analysis was performed with GraphPad Prism version 8.0.0 (GraphPad Software, San Diego, CA, USA). Results are presented as median from each group ± interquartile range (IQR). Statistical differences between experimental groups were evaluated with the Kruskal-Wallis test, with Dunn's post-hoc control test for comparing multiple groups. A value of $p<0.05$ was considered significant.

4. Results

4.1. Mice treated with OVA show an eosinophilic inflammation of the nose and sinuses

In NL, eosinophils were increased in mice treated with OVA without or with SEB compared to mice receiving PBS ($p<0.05$ and $p<0.01$, respectively) (Figure 7 A). Neutrophil counts were not different among groups (Figure 7 B). At tissue level, sub- and intraepithelial eosinophilic infiltration was increased in mice receiving OVA alone and OVA+SEB compared to those receiving PBS ($p<0.05$ and $p<0.001$, respectively) and in mice receiving OVA+SEB compared to SEB alone group ($p<0.05$) (Figure 7 C-D). CLC-like were detected in the sinuses and nasal fossae of all mice treated with OVA, in similar quantities between the OVA and OVA+SEB groups compare to mice treated with PBS and SEB alone (both $p<0.001$ and both $p<0.05$ respectively) (Figure 7 E-F). No differences were found between OVA and OVA+SEB groups for the above-mentioned parameters.

4.2. Mice treated with OVA show increased systemic IgE production. The addition of SEB to OVA induces the production of local IgE production

Total serum IgE levels were higher in mice receiving OVA and OVA+SEB compared to mice receiving PBS (both $p<0.05$). No difference in serum IgE levels was found between the OVA and OVA+SEB groups (Figure 7 G). Three of nine mice treated with OVA+SEB showed detectable IgE levels in their NL; all other values were below the detection limit (Figure 7 H). IL-4 and IL-5 in the NL were below detection level in the NL of all mice (data not shown).

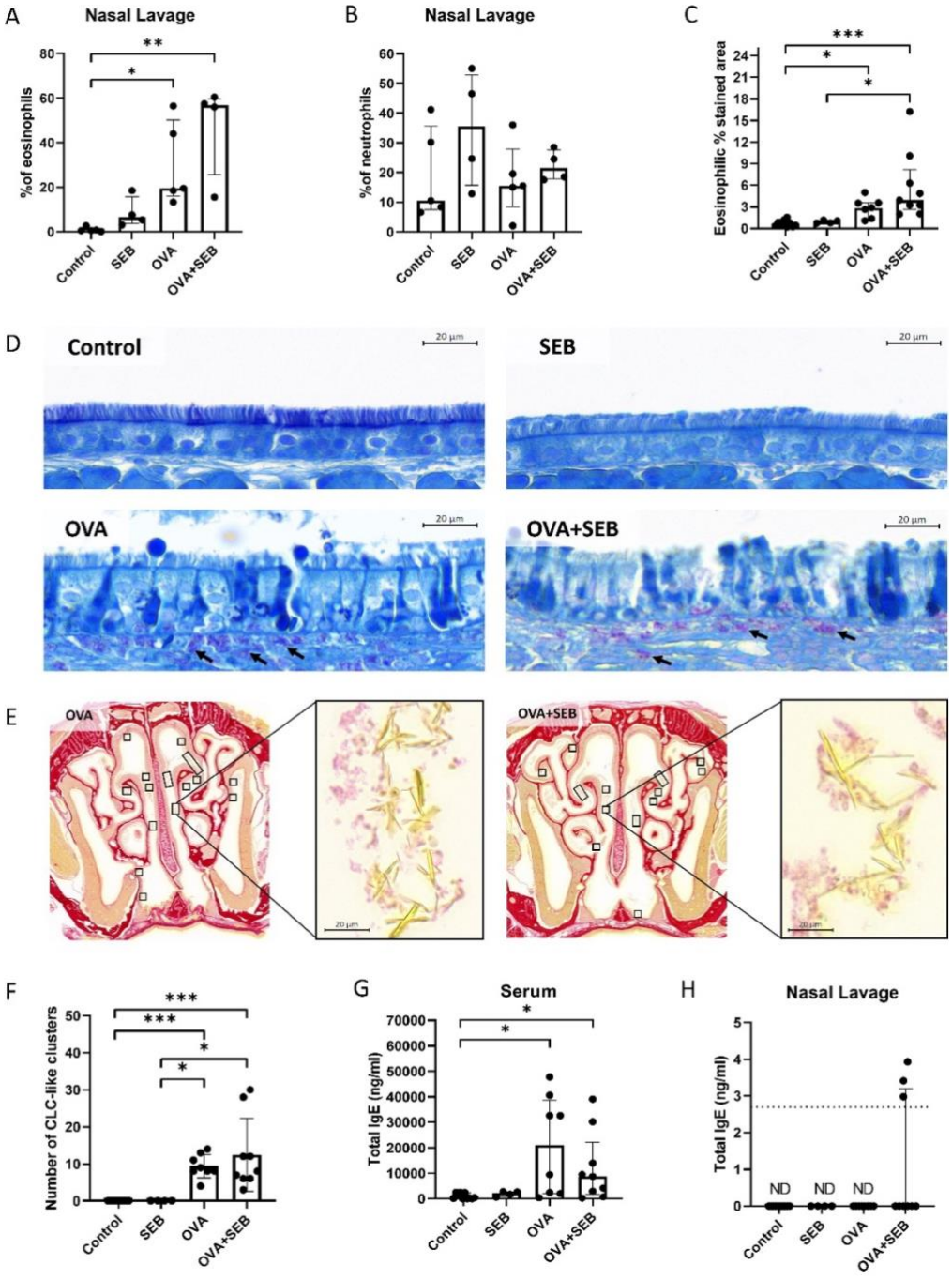
A
Nasal Lavage
%of eosinophils
Control
SEB
OVA
OVA+SEB
B
Nasal Lavage
%of neutrophils
C
Eosinophilic % stained area
D
Control
SEB
OVA
OVA+SEB
20 µm
E
OVA
OVA+SEB
F
Number of CLC-like clusters
G
Serum
Total IgE (ng/ml)
H
Nasal Lavage
Total IgE (ng/ml)
ND

Figure 7. T2 inflammatory markers in an experimental mouse model of eCRS.
(A) Eosinophils percentage of total inflammatory cells recovered from the NL. (B) Neutrophils percentage of total inflammatory cells recovered from the NL. Graph depicts median (±IQR). (C) Eosinophilic infiltration quantification. Every dot depicts the median (±IQR) of 6 measurements per mouse at the different levels of the maxillary sinus. Quantification was performed by using QuPath [26]. (D) representative Giemsa-stained sections of the epithelial layer from maxillary sinuses. Eosinophils infiltrating the subepithelial space are stained pink-purple (arrow). (E) representative CLC-like structures found in OVA (left) and OVA+SEB (right) groups, Sirius Red staining. (F) counting of the number of clusters of CLC-like structures Graph depicts median (±IQR). (G) total IgE levels in serum. Graph depicts median (±IQR). H: total IgE levels in NL. Graph depicts median (±IQR). ELISA detection limit was 2.87 ng/ml. Kruskal-Wallis test: *$p<0.05$; **$p<0.01$; ***$p<0.001$. ND: non-detectable. Scale bar= 20 µm.

4.3. Mice treated with OVA and OVA+SEB show similar epithelial abnormalities and remodelling at the levels of the sinuses

On H&E-stained skulls, the epithelial cell layer of the maxillary sinus was thicker in mice challenged with OVA alone and OVA+SEB compared with mice receiving PBS ($p<0.01$ and $p<0.001$, respectively) (Figure 8 A-B). Goblet cells were more abundant in mice treated with OVA and OVA+SEB than in mice treated with PBS ($p<0.05$ and $p<0.001$) (Figure 8, C-D). Also, basement membrane thickening was more pronounced in mice treated with OVA and OVA+SEB compared with mice receiving PBS ($p<0.05$ and $p<0.001$, respectively) (Figure 8, E-G). Subepithelial fibrosis was higher in the OVA and OVA+SEB groups compared with mice challenged with PBS ($p<0.01$ and $p<0.001$, respectively) (Figure 8 F-G). At the level of tight junction expression, no differences were seen among the treated groups (Figure 8 H; Figure 9). No changes were found between OVA and OVA+SEB groups for the above-mentioned epithelial changes.

In our hands, no NP-like lesions were detected in the maxillary, nasal fossae, or ethmoidal sinuses of mice treated with OVA+SEB, nor in any of the other groups.

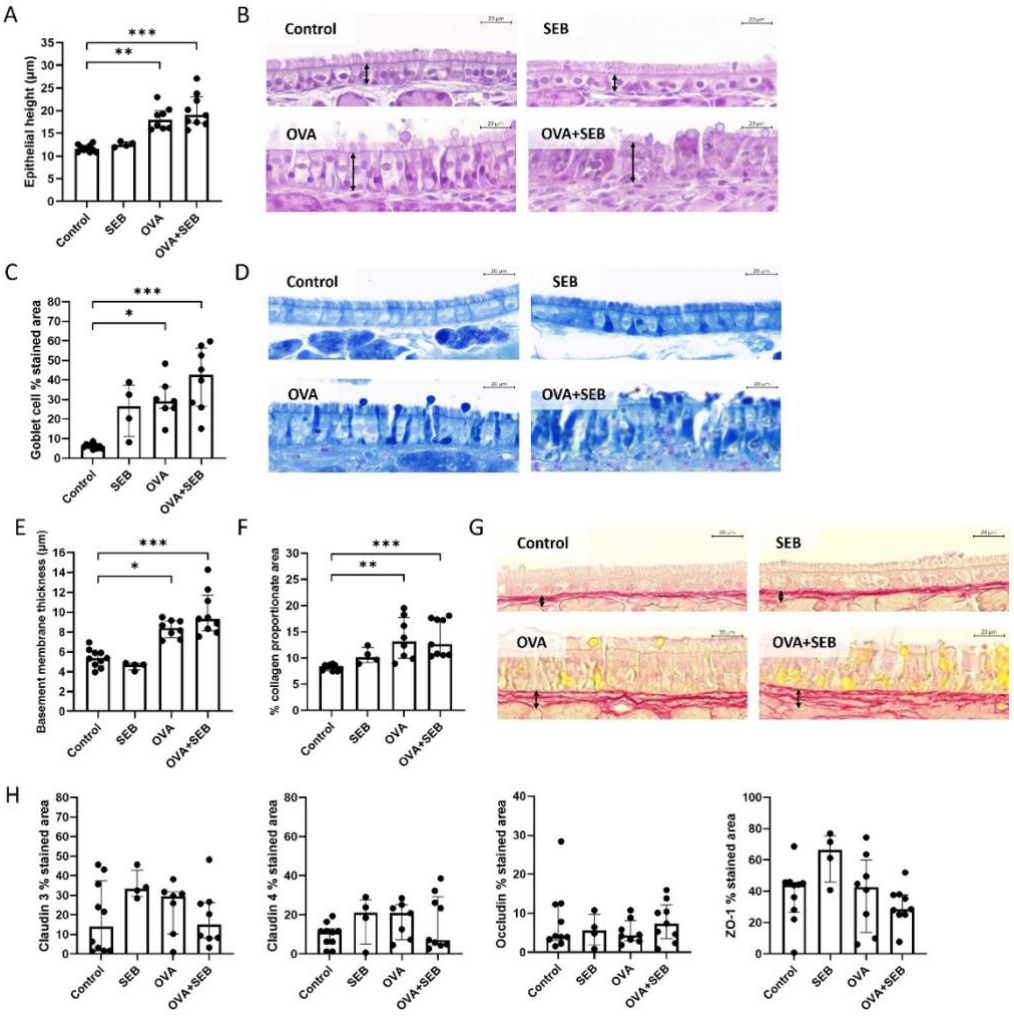
A
Epithelial height (µm)
Control
SEB
OVA
OVA+SEB
B
Control
SEB
OVA
OVA+SEB
C
Goblet cell % stained area
D
E
Basement membrane thickness (µm)
F
% collagen proportionate area
G
H
Claudin 3 % stained area
Claudin 4 % stained area
Occludin % stained area
ZO-1 % stained area

Figure 8. Airway epithelial remodeling in experimental eCRS.
(A) Epithelial thickness measurements quantification. Graph depicts median (±IQR) of 24 measurements per mouse performed by using Cytomine [25]. (B) Representative H&E-stained sections of the epithelial layer from maxillary sinuses. Arrows indicate how epithelial height was measured. (C) Goblet cell quantification. Graphs depict median (±IQR) of 6 measurements per mouse. Quantification was performed by using QuPath [26]. (D) Representative Giemsa-stained sections of the epithelial layer from maxillary sinuses. Goblet cells are stained in dark blue. (E) Basement membrane thickness measurements quantification. Graphs depict median (±IQR) of 24 measurements per mouse performed by using Cytomine [25]. (F) Collagen deposition quantification. Graphs depict median (±IQR) of 6 measurements per mouse. Quantification was performed by using ImageJ, as described by Courtoy et al. [27]. (G) Representative SR-stained sections of the epithelial layer from maxillary sinuses. Arrows indicate how basement membrane measurement was performed. (H) TJ expression and quantification. Graphs depict median (±IQR) of 6 measurements per mouse. Quantification was performed by using QuPath [26]. Kruskal-Wallis test: *p<0.05; **p<0.01; ***p<0.001. ND: non-detectable. Scale bar= 10 µm.

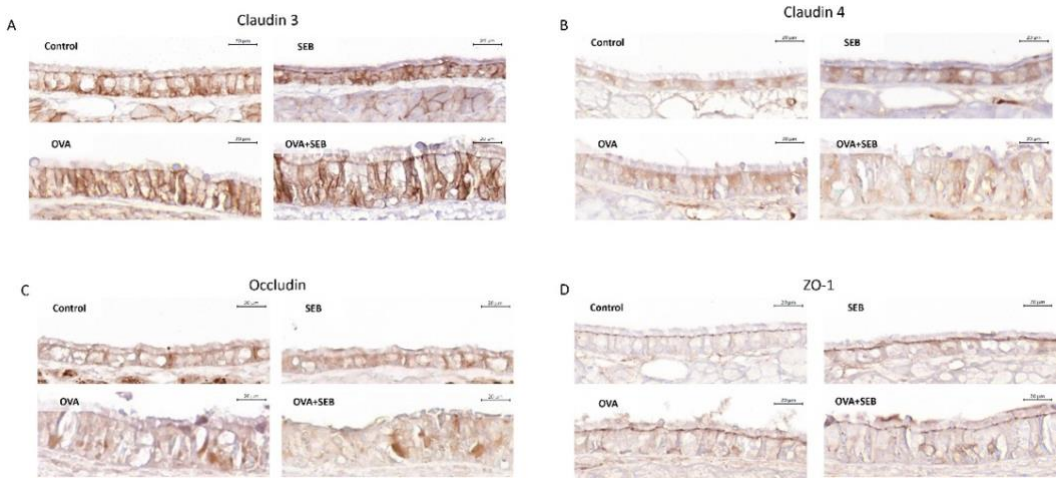

Figure 9. TJ' expression in experimental eCRS.
Representative sections of the epithelial layer from maxillary sinuses in each group. (A) Claudin 3 staining. (B) Claudin 4 staining. (C) Occludin staining. (D) ZO-1 staining. Scale bar= 20 µm. Quantification was performed by using QuPath [26].

4.4. Mice treated with OVA and OVA+SEB develop eosinophilic lower airway inflammation

Total inflammatory cell count was higher in the BAL of mice receiving OVA+SEB compared with mice treated with PBS ($p<0.01$) (Figure 10 A). BAL eosinophils were increased in the OVA alone and OVA+SEB groups compared with mice receiving PBS (both $p<0.05$) (Figure 10 B). Neutrophils were higher in mice receiving OVA+SEB group ($p<0.05$) (Figure 10 C). These findings were confirmed by histology, showing general edema, increased basement membrane thickening and peri-bronchial eosinophilic infiltration in the lungs of mice treated with OVA and OVA+SEB (Figure 10 D). Moreover, both OVA and OVA+SEB groups showed local production of IgE in the BAL compared with mice challenged with PBS (both $p<0.05$) (Figure 10 E). There was no difference between OVA and OVA+SEB groups for any of the above-mentioned parameters.

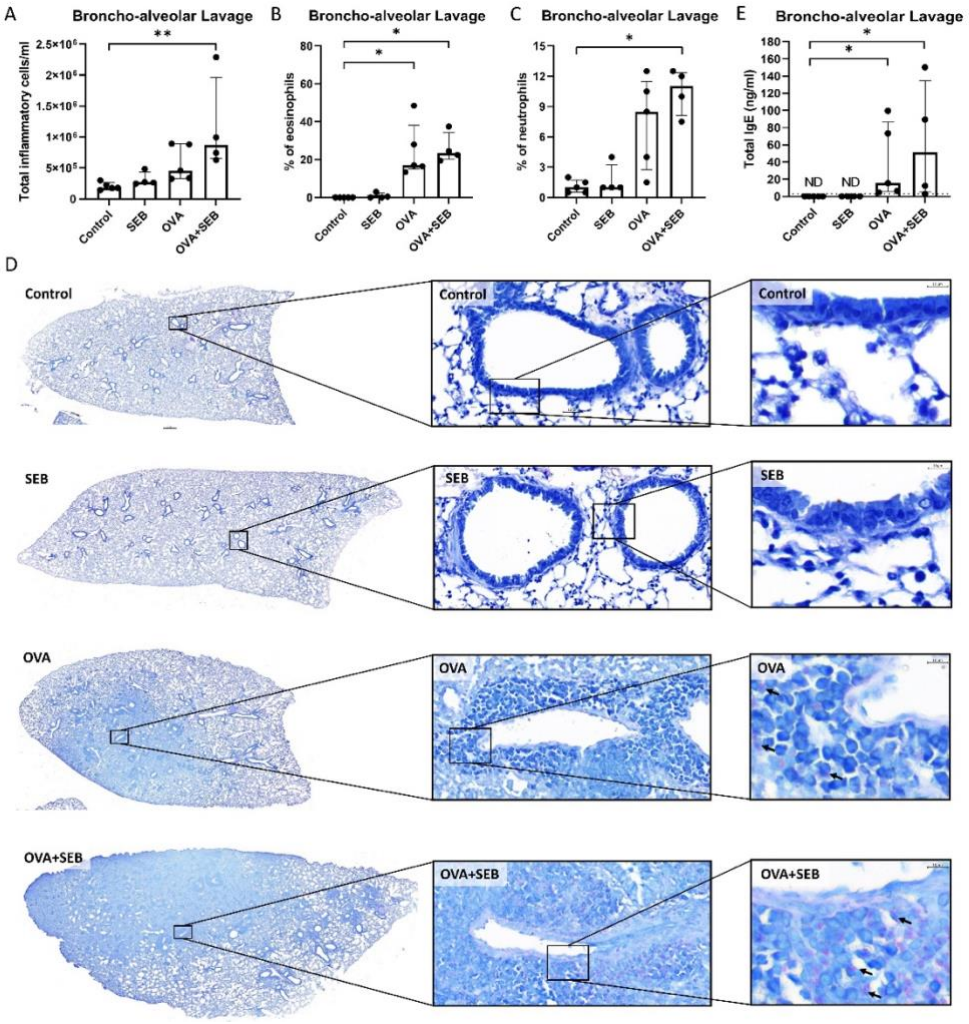

Figure 10. Inflammatory features in the lower airways in experimental eCRS.
(A)-(C) Inflammatory cell count in BAL: (A) total inflammatory cells, (B) eosinophils, (C) neutrophils. Graphs depict median (±IQR). (D) Overview of Giemsa-stained stained lung lobes in a mouse model of experimental eosinophilic CRS. Eosinophils infiltrating the subepithelial space are stained pink (arrow). (E) Total IgE levels in BAL. ELISA detection limit was 2.87 ng/ml. Kruskal-Wallis test: *p<0.05; **p<0.01. Scale bar, 10 µm. BAL: bronchoalveolar lavage. ND: non-detectable.

5. Discussion

In this study, we aimed at establishing and critically evaluating one of the most used mouse models to study eCRSwNP disease mechanisms. The model is based on the addition of the superantigen SEB to a mouse model of experimental respiratory allergy, in this case, induced by OVA. In our hands, C57/Bl6 mice treated with OVA alone and OVA+SEB showed similar histological sinonasal changes at the maxillary sinuses, such as eosinophilic infiltration, increased epithelial and basement membrane thickening, goblet cell hyperplasia, subepithelial fibrosis and the presence of CLC-like elements. We also detected increased systemic IgE production and inflammatory changes in lower airways. The only difference between mice receiving OVA and OVA+SEB, in our hands, was the induction of local nasal IgE in OVA+ SEB mice. No NP or NP-like lesions were detected in sinuses of OVA+SEB mice in our model.

Eosinophilic infiltration and IgE production are typical features of T2 diseases such as AR and eCRSwNP. B-cells are triggered to produce IgE antibodies in a T2 environment that is induced by exposure to allergens or other microbial/environmental antigens [28]. Increased levels of serum IgE are found in all AR patients, and some eCRSwNP patients. eCRSwNP patients typically show increased levels of local, polyclonal IgE in their NP tissue, which is believed to be the result of the superantigen effect of *Staphylococcal aureus* enterotoxins on the local B-cells [28]. Eosinophils are attracted and activated by the T2 cytokine IL-5, which is elevated in both AR and eCRSwNP patients [29]. The action of these cells is then responsible for causing a chronic inflammatory state in the sinonasal mucosa, leading to general inflammatory characteristics such as goblet cell hyperplasia, basement membrane thickening and fibrosis being features of chronic inflammation.

Why CRSwNP patients develop a more severe disease at the level of the sinus mucosa with the formation of large NPs that can protrude to the nasal cavities, is still not well understood.

For decades, researchers have been trying to elucidate the trigger for NP formation in CRSwNP, which included the search for a relevant mouse model. Most of these mouse models have been based on a respiratory allergy model to induce the required T2 response and allergens used range from the food allergen OVA to house dust mite and fungal allergens [30,31]. Because of the belief that the local polyclonal IgE production upon exposure to SEB could contribute to NP formation, a South Korean group decided to expose OVA-allergic mice to SEB to develop an eCRSwNP mouse model [23]. Unfortunately, this model did not lead to the formation of macroscopical NP, as seen in human CRSwNP. However, they do describe the presence of a few microscopic 'NP-like lesions', defined as eosinophilic protrusions of the epithelium involving micro cysts, being limited to one to four lesions per mouse. Most of these lesions were found at the level of the nasal passage (septum and turbinates) rather than in the paranasal sinuses [23]. Later, only a few papers addressed these microscopic NP-like structures in a reliable way. Graphs showing the number of NP-like lesions are often not accompanied by histological pictures of the lesions and if they are, they are mostly located outside the paranasal sinuses (septum and nasal floor) and can easily be confused with artefacts [24].

In our study, we were not able to detect any of these NP-like lesions in either of the experiments at the level of the maxillary and ethmoidal sinuses, olfactory cleft or nasal cavity lining. It is important to mention that we used the modified version of Kim's initial protocol (using 10ng of SEB and a slightly shorter challenge phase). However, this is the protocol that has been used in most of the articles reporting on this mouse model [24]. The absence of NP-like lesions in our hands could be explained by the use of C57BL/6 mice, which are genetically less prone to develop severe T2 disease. However, we observed a severe eosinophilic tissue inflammation with the

presence of Charcot-Leyden-type crystals. It does raise the question whether these NP-like structures are really similar to what is seen in human eCRS.

One of the explanations for the above-mentioned limitation might be that mice may not be able to develop NP due to anatomical differences between humans and mice or differences in the local mucosal immune system [22]. Another explanation could be that the current experimental protocol is not ideal for developing severe sinus inflammation with NP formation. One of the issues is that mouse models are limited in time and chronicity levels, since the ones observed in human eCRS cannot be reached in mice. There is also the possibility that allergic inflammation and SEB are not the (only) required mediators to develop CRSwNP or that the local inflammation induced might not be sufficiently severe to disrupt the epithelium in a way prompting NP formation. An old paper from Karolinska showed in a rabbit model of surgically induced infectious maxillary sinusitis that larger edematous NPs were formed in areas of severe epithelial desquamation, subepithelial edema and inflammatory cell influx. They showed that epithelial dedifferentiation and cell migration led to the formation of subepithelial microcavities and the formation of polyp stalks evolving to larger NPs [32]. Interestingly, in our study, we did not show a loss of tight junctions in the sinus epithelium of mice treated with OVA+SEB. This suggests a lack of mucosal barrier defect in contrast to what is seen in human CRSwNP [33], being one of the potential key triggers of NP formation.

Our study has several limitations, such as the fact that we stuck to a single mouse strain and allergen. However, we followed a consequent and reproducible methodology, which we feel is often lacking in other papers describing this model. The quantification of inflammatory tissue changes was performed in a consistent way sticking to 6 well-defined areas in the maxillary sinus. We avoided looking at ethmoidal sinuses because of their density in mice, leading to artifacts in histological staining. Unlike most other studies, we decided to not consider the septum and lateral nasal wall, since we were evaluating sinus disease and not rhinitis. Additionally, in

contrast to other papers, we included all experimental groups, including mice treated with OVA and SEB alone.

This led us to one of the pivotal observations of this study – the absence of differences between mice treated with OVA alone and OVA+SEB. Interestingly, apart from nasal IgE levels, we did not find significant differences in inflammatory features between mice treated with OVA alone (corresponding to a chronic AR mouse model) and those additionally receiving SEB. Most of the studies using this mouse model to study disease mechanisms of eCRSwNP only compared the OVA+SEB group with a control group. The initial publication by Kim showed an OVA alone group with a significant increase in local eosinophils, IL-5 and eotaxin levels between OVA and OVA+SEB groups [23], which we could not detect (eotaxin not measured). Their observed differences, however, can be attributed to SEB having an adjuvant effect on allergic sensitization, as has been shown previously in a mouse model of OVA-induced AR [34]. Furthermore, their use of BALB/c mice, instead of C57BL/6NRJ mice in our protocol, could explain differences detected in their study [35-37].

Although this is a good mouse model of eCRS, we question whether it is a suitable model to study eCRSwNP. All inflammatory findings described are features of both human eCRS and AR, and the most robust histopathological difference between the two diseases is the formation of large polyps in the sinus, lacking in our mouse model (Table 3). In humans, up to date, there are no other histopathological features distinguishing AR from eCRS and diagnosis of eCRS is based on symptoms and radiology which are currently not measurable in mice in a reliable way.

Table 3. Inflammatory features of the OVA/SEB mouse model in comparison to human eCRS and AR.

Inflammatory features	Murine model of eCRS	Human AR	Human eCRSwNP
Eosinophilic infiltration	√	√	√
IgE production	√	√	√
Epithelial disruption and thickening	√	√	√
Goblet cell hyperplasia	√	√	√
Basement membrane thickening	√	√	√
Type 2 cytokine production	√	√	√
Decreased tight junction expression	×	√	√
Edema with NP formation	×	×	√
United airway disease	√	√	√

Although biopsy studies are lacking, there is evidence that patients with AR also show T2 inflammation in their sinuses [38] and around 40% of eCRSwNP also suffer from AR [18]. Yet, despite overlap in symptomatology and T2 inflammatory profile, AR and eCRSwNP are two different disease entities requiring different treatment strategies [8]. Also, studies investigating the role of allergy as a contributing factor to eCRSwNP show contradictory results [19] and differences exist between the two diseases such as eosinophil activation levels, local remodeling leading to NP formation and presence of neutrophils [39]. There is growing recognition that even T2

CRSwNP population consists of a heterogeneous patient group where different disease mechanisms are playing. Notably, it has been suggested that the recently described CRS endotype 'CCAD' might be more related to IgE-mediated allergic phenomena than other types of T2 eCRSwNP, such as seen in severe asthma or Samter's triad [40]. In our hands, we did not observe the development of nasal polyp-like structures and even though only a small number of studies report such findings, the model does consistently induce an eosinophilic inflammation, which makes it a valuable tool for studying the eosinophilic inflammatory endotype of CRS, but not the CRSwNP phenotype. Therefore, this model might be a proper tool to study disease mechanisms of CCAD, but less those of other eCRSwNP endotypes. The spatial distribution of the NP-like lesions shown in mice by other authors, mostly found in the nasal fossa rather than in the sinuses [23,41-46], supports the theory of a more CCAD-like phenotype of the mouse model [3].

Finally, we want to highlight that we detected T2-related inflammatory changes in the lower airways of mice treated with OVA and OVA+SEB, resembling features associated with allergic asthma. These findings manifested even though the nasal installation volumes were too small to reach the lower airways [47,48]. Although we did not perform any functional bronchial testing, this emphasizes the importance of the robust connection between upper and lower airways, mirroring the observed interplay in human AR and eCRS [49].

6. References

1. Momtazmanesh, S. *et al.* Global burden of chronic respiratory diseases and risk factors, 1990–2019: an update from the Global Burden of Disease Study 2019. *EClinicalMedicine* **59**, 101936 (2023).

2. Rudmik, L. Economics of Chronic Rhinosinusitis. *Current Allergy and Asthma Reports* vol. 17 Preprint at https://doi.org/10.1007/s11882-017-0690-5 (2017).

3. Fokkens, W. J. *et al.* European Position Paper on Rhinosinusitis and Nasal Polyps 2020. *Rhinology journal* **0**, 1–464 (2020).

4. Newton, J. A review of nasal polyposis. *Ther Clin Risk Manag* **Volume 4**, 507–512 (2008).

5. Massoth, L., Anderson, C. & McKinney, K. A. Asthma and Chronic Rhinosinusitis: Diagnosis and Medical Management. *Medical Sciences* **7**, 53 (2019).

6. Gohy, S., Hupin, C., Ladjemi, M. Z., Hox, V. & Pilette, C. Key role of the epithelium in chronic upper airways diseases. *Clinical and Experimental Allergy* vol. 50 135–146 Preprint at https://doi.org/10.1111/cea.13539 (2020).

7. Fujieda, S. *et al.* Eosinophilic chronic rhinosinusitis. *Allergology International* **68**, 403–412 (2019).

8. Vlaminck, S., Acke, F., Scadding, G. K., Lambrecht, B. N. & Gevaert, P. Pathophysiological and Clinical Aspects of Chronic Rhinosinusitis: Current Concepts. *Frontiers in Allergy* **2**, (2021).

9. Shin, S.-H., Ye, M.-K., Park, J. & Geum, S.-Y. Immunopathologic Role of Eosinophils in Eosinophilic Chronic Rhinosinusitis. *Int J Mol Sci* **23**, 13313 (2022).

10. Van Zele, T. *et al.* Staphylococcus aureus colonization and IgE antibody formation to enterotoxins is increased in nasal polyposis [6]. *Journal of Allergy and Clinical Immunology* vol. 114 981–983 Preprint at https://doi.org/10.1016/j.jaci.2004.07.013 (2004).

11. Vickery, T. W., Ramakrishnan, V. R. & Suh, J. D. The Role of Staphylococcus aureus in Patients with Chronic Sinusitis and Nasal Polyposis. *Current Allergy and Asthma Reports* vol. 19 Preprint at https://doi.org/10.1007/s11882-019-0853-7 (2019).

12. Maniakas, A. *et al.* Staphylococcus aureus on Sinus culture is associated with recurrence of chronic rhinosinusitis after endoscopic sinus surgery. *Front Cell Infect Microbiol* **8**, (2018).

13. Ou, J. *et al.* Staphylococcus aureus superantigens are associated with chronic rhinosinusitis with nasal polyps: a meta-analysis. *Eur Arch Otorhinolaryngol* **271**, 2729–2736 (2014).

14. Foreman, A. *et al.* Adaptive immune responses in Staphylococcus aureus biofilm-associated chronic rhinosinusitis. *Allergy: European Journal of Allergy and Clinical Immunology* **66**, 1449–1456 (2011).

15. Georas, S. N. & Rezaee, F. Epithelial barrier function: At the front line of asthma immunology and allergic airway inflammation. *Journal of Allergy and Clinical Immunology* **134**, 509–520 (2014).

16. Steelant, B. *et al.* Restoring airway epithelial barrier dysfunction: a new therapeutic challenge in allergic airway disease. *Rhinology journal* **54**, 195–205 (2016).

17. Chegini, Z. *et al.* The role of Staphylococcus aureus enterotoxin B in chronic rhinosinusitis with nasal polyposis. *Cell Communication and Signaling* **20**, 29 (2022).

18. Marcus, S., Roland, L. T., DelGaudio, J. M. & Wise, S. K. The relationship between allergy and chronic rhinosinusitis. *Laryngoscope Investig Otolaryngol* **4**, 13–17 (2019).

19. Wilson, K. F., McMains, K. C. & Orlandi, R. R. The association between allergy and chronic rhinosinusitis with and without nasal polyps: an evidence-based review with recommendations. *Int Forum Allergy Rhinol* **4**, 93–103 (2014).

20. Woodrow, J. S., Sheats, M. K., Cooper, B. & Bayless, R. Asthma: The Use of Animal Models and Their Translational Utility. *Cells* **12**, 1091 (2023).

21. Takeda, K. & Gelfand, E. W. Mouse models of allergic diseases. *Curr Opin Immunol* **21**, 660–665 (2009).

22. Chamanza, R. & Wright, J. A. A Review of the Comparative Anatomy, Histology, Physiology and Pathology of the Nasal Cavity of Rats, Mice, Dogs and Non-human Primates. Relevance to Inhalation Toxicology and Human Health Risk Assessment. *J Comp Pathol* **153**, 287–314 (2015).

23. Kim, D. W. *et al.* Staphylococcus aureus enterotoxin B contributes to induction of nasal polypoid lesions in an allergic rhinosinusitis murine model. *Am J Rhinol Allergy* **25**, (2011).

24. Leite-Santos, F., Tamashiro, E., de Andrade Batista Murashima, A., Anselmo-Lima, W. T. & Valera, F. C. P. Which are the best murine models to study Eosinophilic Chronic Rhinosinusitis? A contemporary review. *Braz J Otorhinolaryngol* **89**, 101328 (2023).

25. Marée, R. *et al.* Collaborative analysis of multi-gigapixel imaging data using Cytomine. *Bioinformatics* **32**, 1395–1401 (2016).

26. Bankhead, P. *et al.* QuPath: Open source software for digital pathology image analysis. *Sci Rep* **7**, (2017).

27. Courtoy, G. E. *et al.* Digital Image Analysis of Picrosirius Red Staining: A Robust Method for Multi-Organ Fibrosis Quantification and Characterization. *Biomolecules* **10**, 1585 (2020).

28. Gevaert, P., Wong, K., Millette, L. A. & Carr, T. F. The Role of IgE in Upper and Lower Airway Disease: More Than Just Allergy! *Clin Rev Allergy Immunol* **62**, 200–215 (2022).

29. Delemarre, T. *et al.* Type 2 inflammation in chronic rhinosinusitis without nasal polyps: Another relevant endotype. *Journal of Allergy and Clinical Immunology* **146**, 337-343.e6 (2020).

30. Shin, H. Animal Models in CRS and Pathophysiologic Insights Gained: A Systematic Review. *Laryngoscope Investig Otolaryngol* **1**, 116–123 (2016).

31. Al-Sayed, A. A., Agu, R. U. & Massoud, E. Models for the study of nasal and sinus physiology in health and disease: A review of the literature. *Laryngoscope Investig Otolaryngol* **2**, 398–409 (2017).

32. Norlander, T., Fukami, M., Westrin, K. M., Stierna, P. & Carlsöö, B. Formation of Mucosal Polyps in the Nasal and Maxillary Sinus Cavities by Infection. *Otolaryngology–Head and Neck Surgery* **109**, 522–529 (1993).

33. Soyka, M. B. *et al.* Defective epithelial barrier in chronic rhinosinusitis: The regulation of tight junctions by IFN-γ and IL-4. *Journal of Allergy and Clinical Immunology* **130**, 1087-1096.e10 (2012).

34. Huvenne, W. *et al.* Staphylococcus aureus enterotoxin B facilitates allergic sensitization in experimental asthma. *Clinical & Experimental Allergy* **40**, 1079–1090 (2010).

35. Finkelman, F. D. & Wills-Karp, M. Usefulness and optimization of mouse models of allergic airway disease. *Journal of Allergy and Clinical Immunology* **121**, 603–606 (2008).

36. Sahu, N., Morales, J. L., Fowell, D. & August, A. Modeling Susceptibility versus Resistance in Allergic Airway Disease Reveals Regulation by Tec Kinase Itk. *PLoS One* **5**, e11348 (2010).

37. Atochina, E. N. *et al.* Attenuated allergic airway hyperresponsiveness in C57BL/6 mice is associated with enhanced surfactant protein (SP)-D production following allergic sensitization. *Respir Res* **4**, 15 (2003).

38. Baroody, F. M., Mucha, S. M., deTineo, M. & Naclerio, R. M. Nasal challenge with allergen leads to maxillary sinus inflammation. *Journal of Allergy and Clinical Immunology* **121**, 1126-1132.e7 (2008).

39. Helman, S. N. *et al.* The Role of Allergic Rhinitis in Chronic Rhinosinusitis. *Immunol Allergy Clin North Am* **40**, 201–214 (2020).

40. Hamizan, A. W. *et al.* Allergic phenotype of chronic rhinosinusitis based on radiologic pattern of disease. *Laryngoscope* **128**, 2015–2021 (2018).

41. Ryu, G. *et al.* Role of IL-17A in Chronic Rhinosinusitis With Nasal Polyp. *Allergy Asthma Immunol Res* **12**, 507–522 (2020).

42. Lee, M. *et al.* Sinonasal Delivery of Resveratrol via Mucoadhesive Nanostructured Microparticles in a Nasal Polyp Mouse Model. *Sci Rep* **7**, 40249 (2017).

43. Kim, D.-Y. *et al.* A Recently Established Murine Model of Nasal Polyps Demonstrates Activation of B Cells, as Occurs in Human Nasal Polyps. *Am J Respir Cell Mol Biol* **55**, 170–5 (2016).

44. Jin, J., Rha, K.-S., Kim, D. W. & Kim, Y. M. IL-17C expression in nasal epithelial cells of chronic rhinosinusitis with nasal polyposis. *Eur Arch Otorhinolaryngol* **271**, 1097–105 (2014).

45. Choi, M. R. *et al.* Chloroquine Treatment Suppresses Mucosal Inflammation in a Mouse Model of Eosinophilic Chronic Rhinosinusitis. *Allergy Asthma Immunol Res* **12**, 994–1011 (2020).

46. Wee, J. H. *et al.* Effect of lipopolysaccharide and polyinosinic:polycytidylic acid in a murine model of nasal polyp. *Sci Rep* **11**, 1021 (2021).

47. Wu, L. *et al.* Quantitative comparison of three widely-used pulmonary administration methods in vivo with radiolabeled inhalable nanoparticles. *European Journal of Pharmaceutics and Biopharmaceutics* **152**, 108–115 (2020).

48. Southam, D. S., Dolovich, M., O'Byrne, P. M. & Inman, M. D. Distribution of intranasal instillations in mice: effects of volume, time, body position, and anesthesia. *American Journal of Physiology-Lung Cellular and Molecular Physiology* **282**, L833–L839 (2002).

49. Yii, A. C. A. *et al.* Precision medicine in united airways disease: A "treatable traits" approach. *Allergy* **73**, 1964–1978 (2018).

Chapter III – Development of a mouse model of *Staphylococcus aureus*- and *Pseudomonas aeruginosa*-induced neutrophilic chronic rhinosinusitis

Adapted from

Sánchez-Montalvo A[1,2], Ziani-Zeryouh A[1], Lecocq M[1], Steelant B[2], Gohy S[1,3,4], Hellings P[2,5], Bullens D[2,6], Pilette C[1,3], Hox V[1,7]. Mouse model of Staphylococcus aureus- and Pseudomonas aeruginosa-induced neutrophilic chronic rhinosinusitis. Rhinology. 2025 Apr 11. doi: 10.4193/Rhin24.545.

[1] Pole of Pneumology, ORL (airways) and Dermatology (skin) (LUNS), Institute of Experimental and Clinical Research (IREC), Université Catholique de Louvain (UCLouvain), Brussels, Belgium
[2] Department of Microbiology, Allergy and Clinical Immunology Research Group, Immunology and Transplantation, KU Leuven, Leuven, Belgium
[3] Department of Pneumology, Cliniques Universitaires Saint-Luc, 1200 Brussels, Belgium
[4] Cystic Fibrosis Reference Centre, Cliniques Universitaires Saint-Luc, 1200 Brussels, Belgium
[5] Clinical Department of Otorhinolaryngology, Head and Neck Surgery, UZ Leuven, Leuven, Belgium
[6] Clinical Division of Paediatrics, UZ Leuven, Leuven, Belgium.
[7] Department of Otorhinolaryngology, Cliniques Universitaires Saint-Luc, Brussels, Belgium.

Preface

In Chapter II, we successfully established and characterized a murine model of eosinophilic CRS, reproducing key features of T2 inflammation, in line with established protocols available in the literature.

However, while several models exist to study T2 sinonasal inflammation, there is currently no validated or standardized murine model for studying non-T2 CRS, mainly characterized by neutrophilic inflammation.

Therefore, in Chapter III, we aimed to address this gap by developing and characterizing a mouse model of neutrophilic CRS, providing a complementary tool to broaden the study of CRS pathogenesis beyond T2 immune responses.

1. Abstract

Background: Chronic rhinosinusitis is a highly prevalent upper airway disease. Its pathogenesis remains poorly understood, especially for the non-eosinophilic endotype, characterized by neutrophilic inflammation of the paranasal sinuses. Currently, no validated mouse model exists to study disease mechanisms, indicating an important research gap.

Objective: To establish a reproducible mouse model of chronic neutrophilic rhinosinusitis, comparing relevant respiratory pathogens, to allow further research on non-eosinophilic chronic rhinosinusitis pathophysiology.

Methods: a nasal tampon was surgically inserted in the nasal cavity of mice and inoculated with relevant bacteria for sinus disease: *Staphylococcus aureus*, *Streptococcus pneumoniae* and *Pseudomonas aeruginosa*. Inflammatory features in sinus mucosa were evaluated after 4, 8 and 12 weeks on decalcified skulls by histology and immunohistochemistry and by cytospins and enzyme-linked immunoassay on nasal lavage.

Results: Mice inoculated with *S. aureus* showed better survival than those inoculated with *S. pneumoniae* and *P. aeruginosa*. *S. aureus* and, to lesser extent, *P. aeruginosa* were still detectable in the nasal lavage up to 12 weeks. Mice with *S. aureus* and *P. aeruginosa*-induced chronic rhinosinusitis showed significantly hypertrophia of the epithelium, neutrophilic infiltration and fibrosis in the sinus mucosa, with increased Th1 cytokines in the nasal lavage.

Conclusion: *S. aureus* and *P. aeruginosa* are more potent inducers of neutrophilic inflammation than *S pneumoniae* in mice. This model allows us to further study non-eosinophilic chronic rhinosinusitis pathophysiology *in vivo*.

2. Introduction

After establishing a model for eosinophilic CRS in Chapter II, it became important to create a complementary model representing non-T2 CRS. This chapter describes the development and optimization of a bacterial-induced mouse model of neutrophilic inflammation in the sinonasal mucosa and its comparison with the eosinophilic model to better understand immune heterogeneity in CRS.

CRS is defined as an inflammation of the nasal and paranasal sinus mucosa leading to two or more symptoms, one of which should be either nasal blockage/obstruction/nasal secretions, including headaches/facial pressure or pain and loss of smell. These symptoms last for over twelve weeks and are confirmed by endoscopy and/or imaging [1]. Affecting around 11% of the European population [2], it is known to have a severe impact on the quality of life of patients [3] leading to significant loss of work productivity and health-care costs [4].

In the most recent guidelines, CRS is classified according to its inflammatory profile [1]. Generally, in the Western world, patients with a T2 inflammatory profile often present with NP formation with mainly activated eosinophils and Th2 response, with increased levels of IgE, IL-4, IL-5 and IL-13 in the sinus tissue [5]. In patients with a non-T2 inflammatory profile, Th1 and/or Th17 responses are observed, with mainly neutrophilic infiltration and increased levels of IFN-γ in the nose [6,7]. In Western countries, NP are less likely to occur in this endotype [8].

Environmental factors, genetic predisposition, anatomical differences, and comorbid diseases are considered risk factors for CRS [9]. Moreover, defects at the level of the sinonasal epithelium seem to play a key role in driving a chronic inflammation of the sinuses [10]. Also, the presence of certain pathogens such as *Staphylococcus aureus*, have been linked consistently to disease development or modification [11].

While most of the research dedicated to CRS has focused on T2 CRS or eosinophilic CRS (eCRS), very few studies have attempted to study non-T2 or neutrophilic CRS (nCRS). Notwithstanding, non-T2 CRS is believed to be the most frequent endotype [12] and very little is known about its pathophysiology.

Because of the disadvantages linked to clinical research, such as differences in genetic background and exposome, there has been a long-standing interest in developing animal models as a tool to study this complex disease. The crucial role of mouse models in understanding physiological and pathological processes should not be underestimated in the constantly evolving field of biomedical research. Although differences exist between human and murine airways, mouse models have proven to be a very useful tool to investigate immunological and respiratory disease mechanisms [13–15]. For eosinophilic T2 CRS, a mouse model that is based on the induction of an experimental allergy, in combination with SEB exposure, is frequently used and has been accepted within upper airway research groups [16,17]. However, for non-eosinophilic or nCRS, no such mouse model is currently available. Up till now, very few reports on nCRS mouse models have been published.

In this chapter, we optimized and validated a mouse model that was reported by Jacob and colleagues in 2001 and that is based on the combination of the surgical introduction of a bacterial source with an anatomical occlusion of the outflow tract of the paranasal sinuses [18]. In this work, we reproduced, adapted and validated this surgical technique to develop a bacterial-induced neutrophilic inflammation in the nasal mucosa in a way that reliable and reproducible results can be obtained. We provide a step-by-step protocol for this challenging but very useful and promising technique to develop a mouse model of nCRS. We tested three bacterial strains that are relevant for sinonasal disease such as *Staphylococcus aureus*, *Streptococcus pneumoniae* and *Pseudomonas aeruginosa,* and mice were evaluated at three different time points. By doing so, we were able to develop an adequate, reliable and reproducible mouse model of non-eosinophilic CRS that can help us in the future to gain a better insight into this disease entity.

3. Methodology

3.1. Experimental procedure to induce an experimental nCRS in mice

3.1.1. Ethics statement

All animal experiments were performed in compliance with the Ethical Committee guidelines (2021/UCL/MD/017), following 'Bruxelles Environnement – IBGE' guidelines, and approved under the reference code 2000/13429.8.

3.1.2. Animals

7-8 weeks old C57BL/6NRJ male mice (weighting 25-30g) were purchased from Janvier Labs and maintained in an Animal Biosafety Level 2 (ABSL-2) facility with agreement reference LA1230292. Mice were randomly divided into four different groups: control (saline) group (n=33), *S. aureus* inoculation (n=43), *S. pneumoniae* inoculation (n=41) and *P. aeruginosa* inoculation (n=49). Mice from each group were consecutively sacrificed four, eight and twelve weeks after surgery (Figure 11 A).

3.1.3. Bacteria

The different bacterial strains used for this experiment were *S. aureus* Lenticules™ (Sigma-Aldrich, CRM06571M, isolated in Oxford, UK (1940), from a subculture in a clinical/laboratory setting); *P. aeruginosa* VitroidsTM (Sigma-Aldrich, VT000256, exact isolation source not publicly specified; commonly derived from clinical samples) and *S. pneumoniae* (ATCC®, 49619TM, isolated from the sputum of a 75-year-old male patient in Phoenix, Arizona, USA). Bacteria were cultured on sheep blood agar plates (Thermo Scientific™, PB5012A) and kept overnight at 37°C in the case of *S. aureus* and *P. aeruginosa*, and plus 5% CO_2 for *S. pneumoniae*.

Then, bacteria were resuspended in saline and serial dilutions were performed from 1:1 to a $1:10^9$ dilution. Ten microliters of each dilution were seeded on Petri dishes and incubated at 37°C (plus 5% CO_2 for *S. pneumoniae*) for 24 h. The resulting number of colonies was correlated to an OD600nm to have a solution with around $1x10^9$ CFU/ml according to optical density [152].

3.1.4. Surgical procedure

The protocol described in this section is published on protocols.io, (dx.doi.org/10.17504/protocols.io.rm7vzxwzxgx1/v2). Briefly, on Day 0, mice were anesthetized, with a mix of Xylazin (maximum 15 mg/kg) and Ketamin (maximum 80 mg/kg) intraperitoneally (i.p.), and received analgesia, Temgésic (maximum 0,05 mg/kg) subcutaneously according to safety recommendations [20,21]. Mice underwent micro-surgery (Figure 17 B) using a stereomicroscope. An 8-mm midline incision was performed by using a 15-mm scalpel blade over the nasal dorsum to the snout and skin flaps were raised laterally to expose the nasal bone. A 1.5-mm microdrill (Medtronic, MI, USA) was used to drill the nasal bone over the nasal fossa and the upper part of the septum was removed. A pre-cut (4 mm x 1 mm x 1 mm) and sterilized nasal tampon (Medtronic, MI, USA) was soaked with 10 microliters of a 10^9 CFU/ml solution of the corresponding bacteria, or saline for controls. This tampon was then carefully placed in both nasal cavities blocking the sinus outflow tracts but leaving sufficient space to breathe through the inferior meatus (Figure 11 C). The skin flaps were then sutured over the tampon with 5.0 non-resorbable polypropylene sutures (Monosoft™, Coviden) and mice were placed in a cage that was heated by an IR lamp (IR100 Infrared lamp, MEDISANA®) for recovery. To overcome any postoperative pain, mice received analgesia every 12 hours for 24 hours after the procedure.

3.1.5. Humane endpoints

Once awake and active after surgery, the mice were returned to the ABSL-2 facility. Animal health and behavior were closely watched and monitored every day for one week and then four times a week until completion of the experiment to ensure the well-being of the animals. If mice reached a score of non-well-being, mainly observed with respiratory distress, or lost more than 20% of their body weight, they were euthanized according to humane endpoints.

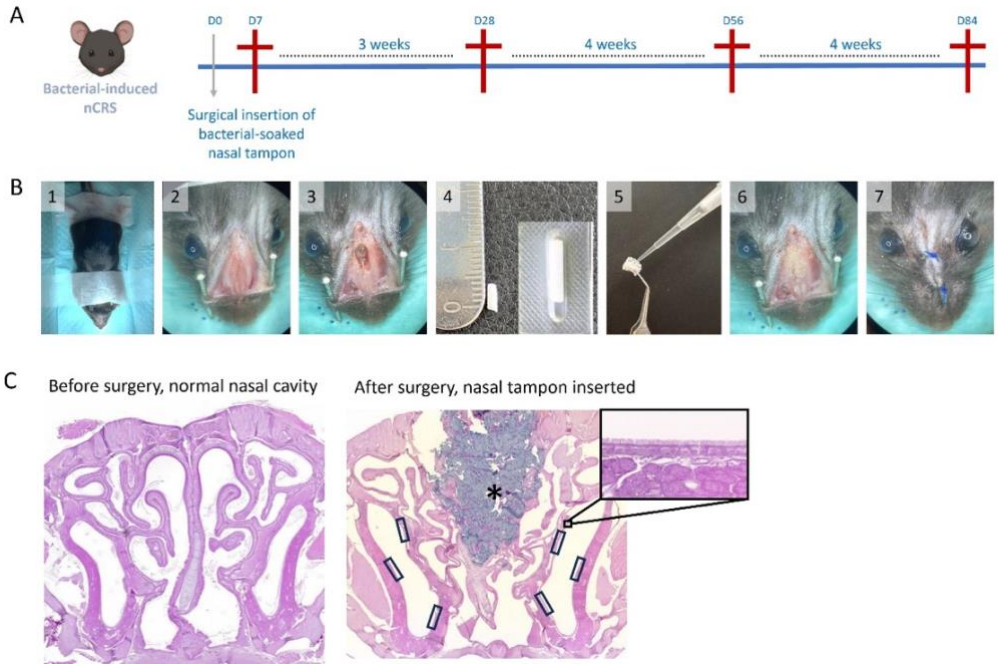

Figure 11. Experimental set up of the bacterial-induced nCRS mouse model and murine sinus anatomy.
(A) Experimental design. (B) Overview of the surgical procedure. 1- The mouse is fixed in the surgical area. 2- Skin flaps are opened and 3- the nasal bones are drilled to expose the nasal mucosa. 4- A pre-cut to size sterile nasal tampon is 5- inoculated with a saline or bacterial solution and 6- inserted into the nasal cavity of the mice. Last, 7- skin is sutured with non-resorbable sutures. (C) Murine sinus anatomy, coronal sections. Left, normal nasal cavity of a mouse without any treatment. Right, nasal cavity of a mouse with an inserted nasal

tampon inoculated with saline at four weeks post-surgery, H&E staining. Rectangles indicate the regions of the maxillary sinuses that were selected in each mouse to evaluate different histological features in a systematic way. Nasal tampon partially blocking the nasal cavity is indicated with an asterisk (*). Zoom in shows the general state at the sinus epithelial layer, without noticeable signs of inflammation due to the presence of the nasal tampon inoculated with saline.

3.2. Sacrifice and sampling

Four, eight or twelve weeks after surgery, mice were euthanized by administering an i.p. injection of pentobarbital (200mg/kg). First, blood was drawn from the inferior cava vein and serum was collected by centrifugation for 10 minutes at 650g and room temperature and stored at -20ºC. Then, a tracheotomy was performed to carry out the NL via inserting a 22G cannula (Versatus^{TM} I.V Catheter) towards the choanae. 1 ml of saline (NaCl 0.9%) was softly flushed, recovering and washing every 200 µl in the syringe, through the catheter and recovered at the nostrils. After using ten microliters for bacterial culture, the remaining NL fluid was centrifuged for 5 minutes at 450g and 4ºC to collect the cell pellets, used for performing cytospins. The supernatant was stored at -20ºC for further processing. Skulls were harvested by decapitation and skin, soft tissues and the inferior mandibula were removed. They were fixed in formaldehyde 4% and decalcified in Osteoral^{TM} (RAL Diagnostics) for 5 days. After decalcification, snout and brain were removed to keep the region containing the paranasal sinuses. The decalcified skulls were dehydrated and treated according to standard paraffin-embedding procedures. Paraffinized skulls and lungs were cut into 4-µm sections with a semi-automated microtome (ThermoFisher Scientific).

3.3. Bacterial culture

Ten microliters from NL were seeded on a sheep blood agar plate with a sterile L-shaped spreader. The agar plate was incubated at 37°C in the case of *S. aureus* and *P. aeruginosa* and plus 5% CO2 for *S. pneumoniae.* After 24 hours, bacterial colonies were identified and counted.

3.4. Cytospins from NL and inflammatory cell count

NL was collected as described above and centrifuged for 5 minutes at 450g and 4ºC to separate the cell pellet. Cells were resuspended in 100 microliters PBS and loaded into a Thermo Shandon Cytospin Centrifuge (Thermo Shandon) following the manufacturer's instructions and centrifuged at 500 revolutions per minute (rpm) for 5 minutes. Cytospins were stained by using the Kwik-Diff™ kit (Thermo Fisher Scientific). The stained slides were coverslipped and scanned by using a Pannoramic scan II (3DHistech). Total inflammatory cells and total neutrophils were manually counted in cytospins by using Qupath [22]. Results are presented as median ± IQR.

3.5. Cytokine and chemokine measurements in NL

A custom mouse pro-inflammatory panel was used to detect multiple cytokines and chemokines in the NL fluid using the MSD™ V-PLEX technology (MSD, Rockville, MD) according to the manufacturer's instructions: IFNγ, (lower limit of detection (LLD)= 0.07 pg/ml); IL-1β (LLD=0.081 pg/ml); IL-2 (LLD= 0.24 pg/ml); KC/GRO (LLD= 0.18 pg/ml); IP-10 (LLD= 0.328 pg/ml); IL-12p70 (LLD= 6.22 pg/ml); TNFα (LLD= 0.08 pg/ml); IL-33 (LLD= 0.28 pg/ml); IL-17A/F (LLD= 0.1 pg/ml); MIP-2 (LLD= 0.049 pg/ml). Results are presented as median ± IQR.

3.6. Histologic and immunohistochemical analysis of the paranasal sinuses

Four µm-thick paraffin sections were cut from tissue blocks. Stained slides were scanned using a Pannoramic Scan II (3DHistech). To analyze the below-mentioned parameters among the different mice groups, three areas of both the right and the left maxillary sinus (two areas on the lateral side and one area on the medial side) were taken to evaluate histological features (Figure 11 C). For the evaluation of the epithelium, hematoxylin and eosin (H&E) staining was performed. Epithelial thickness was evaluated by measuring the epithelial layer, from basolateral to apical pole by using Cytomine [23]. Results are presented as median of 24 measurements per mouse ± interquartile range (IQR). For the evaluation of subepithelial fibrosis, collagen deposition was evaluated by Sirius red (SR) staining with ImageJ based on the method described by Courtoy [24], in which an image analysis tool was applied to detect and segment collagen fibers in histological sections, followed by the calculation of the collagen proportionate area (CPA) to quantitatively assess the extent of fibrosis. Results are presented as median of 6 measurements per mouse ± IQR. Tissue neutrophilic infiltration was evaluated via specific immunohistochemistry (IHC) performed for the lymphocyte antigen 6 family member G (Ly6G) biomarker. As primary antibody for murine neutrophils, rat anti-mouse Ly6G (BD Bioscience, 551459) was used and incubated at room temperature for 1 hour. Quantification of murine neutrophils was performed by using QuPath [22] and expressed as a percentage of positive area. Results are presented as median of 6 measurements per mouse ± IQR. For the evaluation of bacteria presence in tissue, specific IHC was performed for *S. aureus* and *P. aeruginosa*. As primary antibodies, PA17246 from Thermo Scientific and ab68538 from Abcam were used, respectively, and incubated at RT for 1 hour.

3.7. Statistics

A Kaplan-Meier estimation curve was plotted for the post-operative survival of mice with GraphPad Prism version 8.0.0 (GraphPad Software, San Diego, CA, USA). Statistical analysis on the different outcome parameters observed was also performed by using GraphPad Prism version 8.0.0. Results are presented as median from each group ± interquartile range (IQR). Statistical differences between experimental groups, comparing disease group to the control group of the same time point, were evaluated using the Kruskal-Wallis test, with Dunn's post-hoc control test for comparing multiple groups. A value of $p<0.05$ was considered significant. For the cytokines/chemokines measurements, due to the high number of samples not reaching the lower limit of detection, because of a known important dilution factor in NL, and resulting in a low N per group, we used the Mann-Whitney U test between each inoculated group and controls within the same time point in addition to the Kruskal-Wallis test, to confirm observed trends. These are indicated in different colors in the respective graph.

4. Results

4.1. Mice inoculated with *S. aureus* have a higher survival rate than *S. pneumoniae* and *P. aeruginosa*

None of the mice inoculated with any of the bacteria showed signs of local infection at the level of the incision, nostrils, or eyes at any of the evaluated time points. A significantly lower survival rate post-surgery was observed in mice inoculated with *S. pneumoniae*-induced CRS and with *P. aeruginosa*-induced CRS, with the deaths occurring mainly within two weeks after surgery (Figure 12). In the group of mice inoculated with *S. pneumoniae*, 32 out 41 mice survived (78% of the mice). In the group of mice inoculated with *P. aeruginosa,* 37 out of 49 mice survived (75.5% of the mice). The survival rate was higher in mice inoculated with *S. aureus*, where 42 out of 43 mice survived (97.7% of the mice). Sacrifices to respect animal well-being were mainly performed within the first week following the surgery. None of the mice inoculated with saline reached a high discomfort score and 33 out of 33 mice survived (100% of the mice).

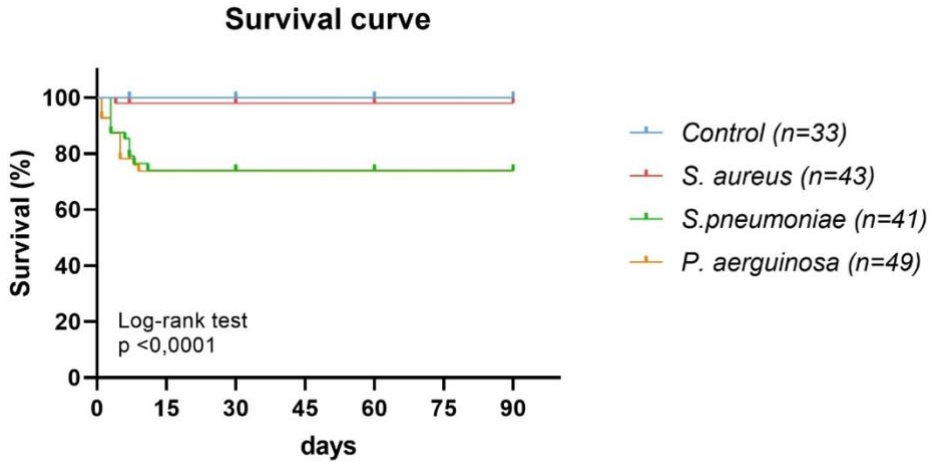

Figure 12. Survival of operated mice.
Kaplan-Meier survival curves of mice with bacterial-induced neutrophilic CRS. The survival of mice (from the date of surgery until the end of the protocol) is compared by a standard log rank to test differences between controls with a saline-inoculated nasal tampon and the different bacterial-inoculated nasal tampon groups in the probability of a death.

4.2. *S. aureus* and *P. aeruginosa* remain detectable in nasal secretions up to 12 weeks post-operatively

Bacterial persistence in the nasal cavity was assessed 24 hours after seeding the NL in agar culture. *S. aureus* could be detected in 1 out of 7 mice (14.3%) at one week after surgery; in 8 out of 13 mice (62% of the mice) at four weeks after surgery; in 7 out of 11 mice (64% of the mice) at eight weeks after surgery and in 5 out of 11 mice (45% of the mice) twelve weeks after surgery (Figure 13 A, B). *S. pneumoniae* could be detected in 4 out of 4 mice (100% of the mice) at one week after surgery; in 3 out of 9 mice (33% of the mice) at four weeks after surgery; in 4 out of 9 mice (44% of the mice) at eight weeks after surgery and in 4 out of 10 mice (40% of the mice) at twelve weeks after surgery (Figure 13 A, B). *P. aeruginosa* could be detected in 4 out of 4 mice (100% of the mice) at one week after surgery; in 6 out of 12 mice (50% of the mice) at four weeks after surgery; in 5 out of 11 mice (45% of the mice) at eight weeks after surgery and in 3 out of 10 mice (30% of the mice) at twelve weeks after surgery (Figure 13 A, B). Cultures from mice inoculated with saline only exhibited classical nasal commensals (Figure 13 B).

S. aureus and *P. aeruginosa* could also be detected in the nasal tampon of the inoculated mice by IHC up to twelve weeks after surgery (Figure 19 B). These bacteria could also be shown in the maxillary sinuses but much less abundant in the mucosa and not later than four weeks (Figure 13 C). The histological presence of *S. pneumoniae* could not be assessed. No cross-contamination was found among the three bacterial groups.

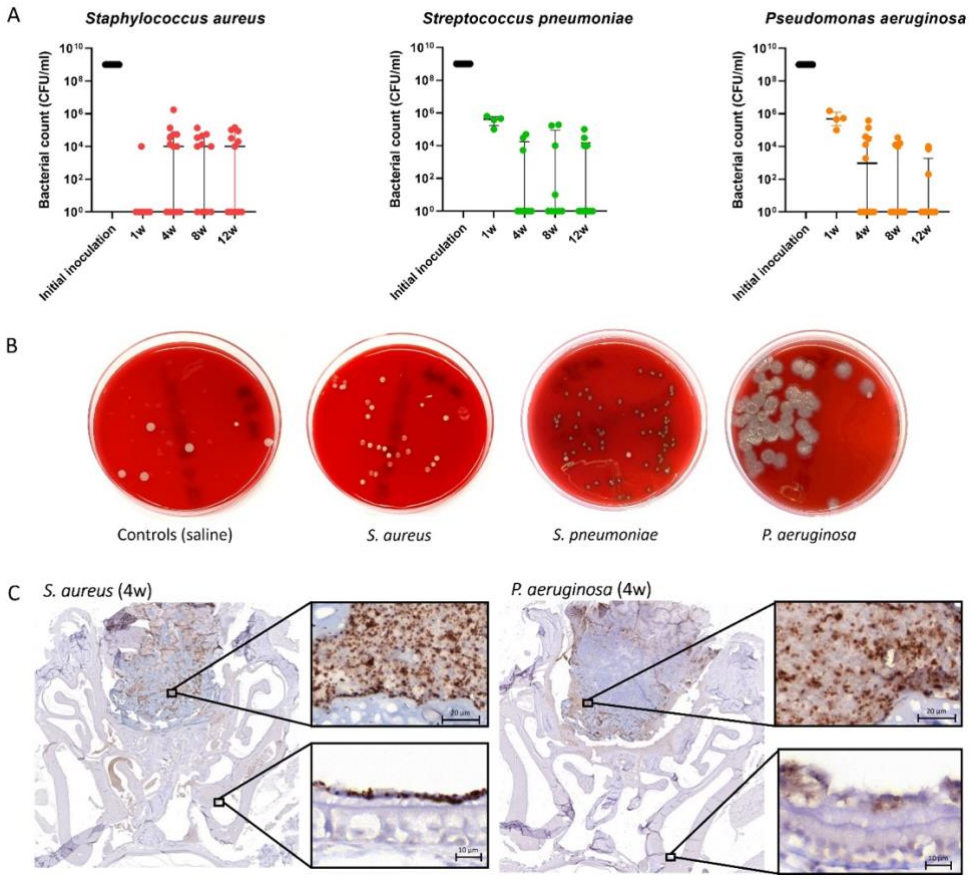

Figure 13. Bacterial cultures from NL at four, eight and twelve weeks after surgical inoculation.

Bacterial count is expressed as CFU/ml. The initial inoculation refers to the bacterial solution with which the nasal tampon was inoculated during the surgical procedure. (A) *S. aureus* count (left), *S. pneumoniae* count (middle) and *P. aeruginosa* count (right). (B) Representative pictures of the bacterial cultures obtained 24 hours after euthanasia and sampling. (C) Representative pictures of the specific staining for *S. aureus* and *P. aeruginosa* four weeks after surgery. Graphs depict median ± Interquartile range (IQR). n= 4-13 mice/group.

4.3. *S. aureus* and *P. aeruginosa* induce a more robust neutrophilic sinus inflammation than *S. pneumoniae*

The sinus epithelium of mice with experimental *S. aureus*-induced CRS was significantly hyperplastic at one week (median of 16.75 µm vs control mice with median of 13.25 µm, $p<0.05$), four weeks (median of 15.92 µm vs control mice with median of 11.96 µm, $p<0.0001$), eight weeks (median of 15.50 µm vs control mice with median of 13.17 µm, $p<0.01$) and twelve weeks (median of 14.33 µm vs control mice with median of 12.13 µm, $p<0.01$) after surgery as measured by epithelial thickness (Figure 14 A, C). For mice with *P. aeruginosa*-induced CRS, the sinus epithelium was significantly hyperplastic compared to controls at one week (median of 19.13 µm, $p<0.01$), four weeks (median of 14.83 µm, $p<0.01$), eight weeks (median of 15.75 µm, $p<0.001$) and twelve weeks (median of 14.71 µm, $p<0.001$) after surgery (Figure 14 A, C). The sinus epithelium of mice with experimental *S. pneumoniae*-induced CRS was significantly thicker at four weeks (median of 13.5 µm, $p<0.01$) and twelve weeks (median of 14.54 µm, $p<0.01$) after surgery (Figure 14 A, C).

Additionally, subepithelial fibrosis, as measured by collagen deposition, was significantly higher in mice inoculated with *S. aureus* and *P. aeruginosa* at twelve weeks post-surgery (median of 9.55% CPA, $p<0.05$, for *S. aureus* and 8.50% CPA, $p<0.05$, for *P. aeruginosa* compared to control mice, with median 2.60% CPA) with a trend already visible after four weeks in the *P. aeruginosa* group (median of 5.83, $p= 0.06$, compared to control mice with median of 2.85% CPA; Figure 14 B, D).

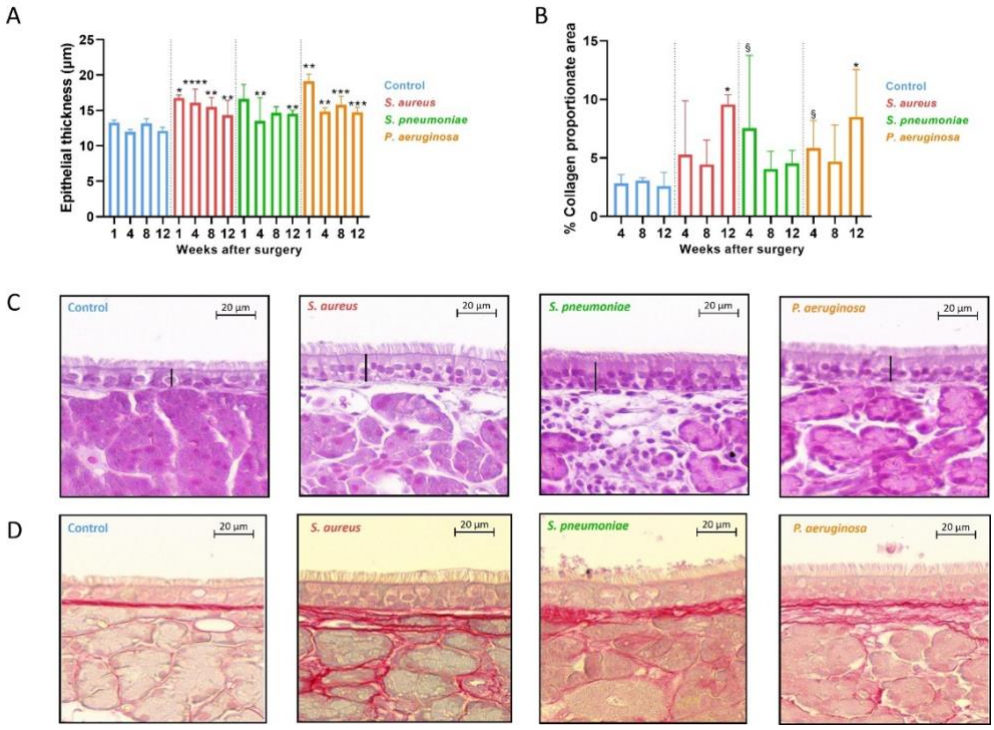

Figure 14. Histological changes in a mouse model of bacterial-induced nCRS.
(A) Epithelial thickness measurements on H&E staining. Graph depicts median (±IQR) of 24 measurements per mouse performed by using Cytomine [156]. (B) Graph depicts median (±IQR) of 6 measurements per mouse performed by using Qupath [155]. (C) Subepithelial collagen deposition, Sirius Red staining. Graph depicts median (±IQR) of 6 measurements per mouse performed by using ImageJ [(24)]. Kruskal-Wallis with Dunn's post-hoc control test for comparing multiple groups: §p<0.1; *p<0.05; **p<0.01; ***p<0.001; ****p<0.0001 compared to the control group of the same time point. n= 4-13 mice/group for epithelial thickness; 3-5 mice/group for fibrosis quantification. Scale bar= 20 µm.

Total inflammatory cells in cytospins of the NL of mice inoculated with *S. aureus* were increased at four weeks (median of 8937 cells/ml compared to control mice with median of 3211 cells/ml, p=0.06) and especially at twelve weeks (median of 14452 cells/ml compared to saline treated mice with median of 1161 cells/ml, p<0.01) after surgery (Figure 15 A). The number of neutrophils in NL was increased at four weeks (median of 11675 neutrophils/ml, compared to control mice with

median of 1170 neutrophils/ml, p<0,01) and twelve weeks (median of 12212 neutrophils/ml, compared to control mice with median of 592 neutrophils/ml, p<0.001) after surgery (Figure 15 B). The number of eosinophils (Figure 15 C), macrophages (Figure 15 D) and lymphocytes (Figure 15 E) did not differ among groups at any of the studied time points.

In mice inoculated with *P. aeruginosa,* total inflammatory cells were significantly higher at twelve weeks (median of 9059 cells/ml, compared to control mice with median of 1161 cells/ml p<0.001) after surgery (Figure 15 A). The number of neutrophils in NL was significantly increased at four weeks (median of 8002 neutrophils/ml, p<0.05) and at twelve weeks (median of 8498 neutrophils/ml, p<0.001) after surgery (Figure 15 B). The number of eosinophils (Figure 15 C) and macrophages (Figure 15 D) did not differ among groups at any of the studied time points. The number of lymphocytes was significantly higher at one week (median of 500.7 lymphocytes/ml, compared to control mice with median of 16 lymphocytes/ml p<0.01) after surgery and at eight weeks (median of 115.8 lymphocytes/ml, compared to control mice with median of 28.95 lymphocytes/ml p<0.05) after surgery (Figure 15 E).

S. pneumoniae also induced a significant increase in total inflammatory cells at twelve weeks (median of 3431 cells/ml, compared to control mice with median of 1161 cells/ml, p<0.05) after surgery (Figure 15 A), with most of them being neutrophils (median of 2714 neutrophils/ml, compared to control mice with median of 592 neutrophils/ml, p<0.05 Figure 15 B, C). The number of eosinophils (Figure 15 C), macrophages (Figure 15 D) and lymphocytes (Figure 15 E) did not differ among groups at any of the studied time points.

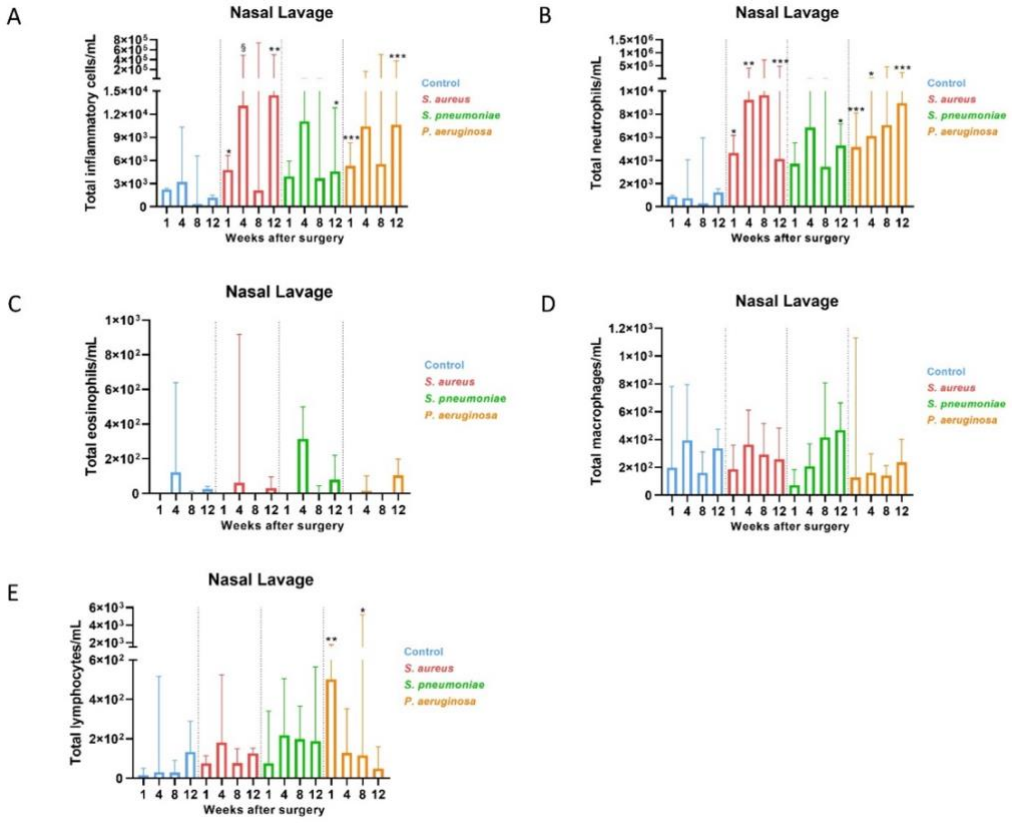

Figure 15. Inflammatory cell count in NL cytospins of a mouse model of bacterial-induced nCRS.

(A) Total inflammatory cells/ml. (B) Neutrophils/ml. (C) Eosinophils/ml. (D) Macrophages/ml. (E) Lymphocytes/ml. Graphs depict median (±IQR). Countings were performed by using Cytomine [156]. Kruskal-Wallis with Dunn's post-hoc control test for comparing multiple groups: §p<0.1; *p<0.05; **p<0.01; ***p<0.0001 compared to the control group of the same time point. n= 4-13 mice/group.

An overview of representative images of the cytospins of the NL per group can be found in Figure 16 A.

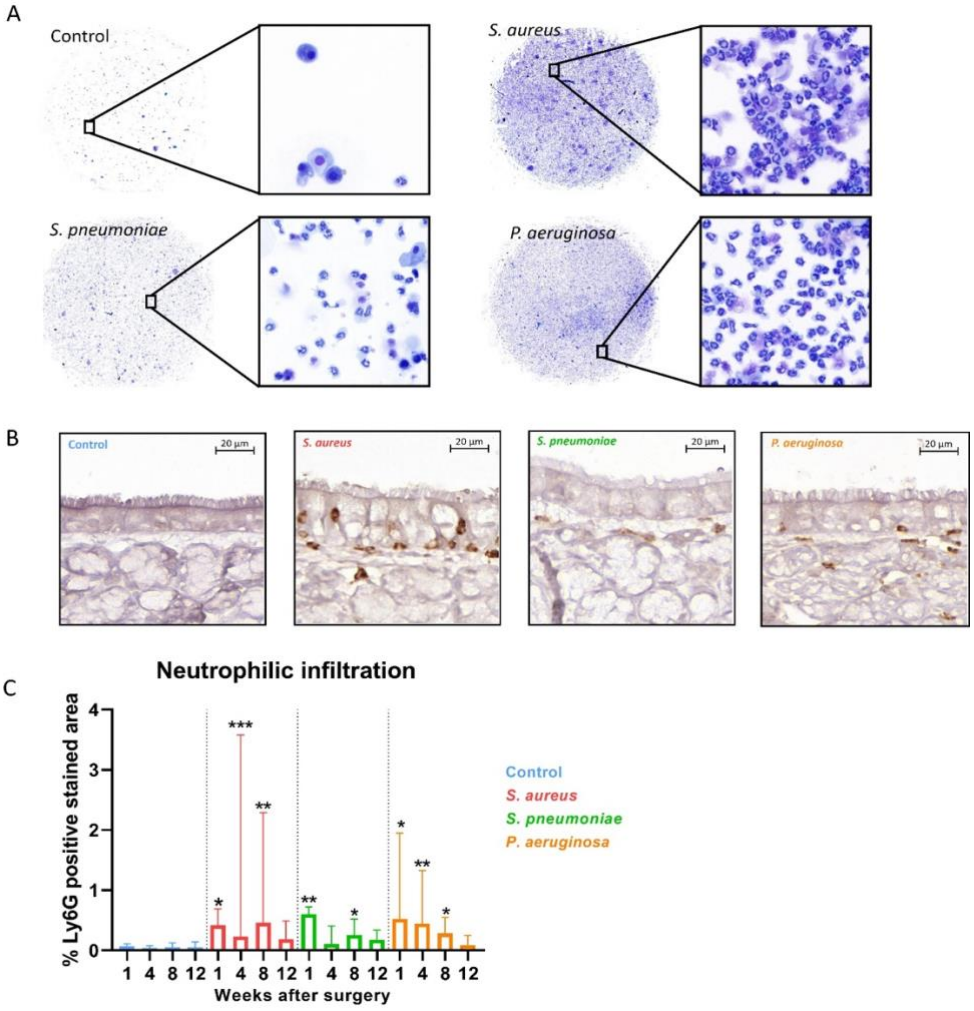

Figure 16. Neutrophils in cytospins and infiltration at the maxillary sinuses of a mouse model of bacterial-induced nCRS.

(A) Overview of the cytospins per group. (B) Histological sub- and intra-epithelial neutrophilic infiltration, Ly6G staining. (C) Ly6G staining quantification in tissue. Graph depicts median (±IQR) of 6 measurements per mouse performed by using Qupath [155]. Kruskal -Wallis with Dunn's post-hoc control test for comparing multiple groups: *p<0.05; **p<0.01; ***p<0.0001 compared to the control group of the same time point. n= 4-13 mice/group.

At the tissue level of the maxillary sinuses, this neutrophilic inflammation was confirmed by a significant epithelial neutrophilic influx in mice inoculated with *S. aureus* at one week (median of 0.42% Ly6G positive stained area, compared to control mice with median of 0.07% Ly6G positive stained area, $p<0.05$), four weeks (median of 0.26% Ly6G positive stained area, compared to control mice with median of 0.024% Ly6G positive stained area, $p<0.001$) and eight weeks (median of and 0.34% Ly6G positive stained area, compared to control mice with median of 0.052% Ly6G positive stained area, $p<0.01$) after surgery (Figure 16 D, E). The same was true for mice inoculated with *P. aeruginosa* with an epithelial neutrophilic influx at one week (median of 0.52% Ly6G positive stained area, $p<0.01$), four weeks (median of 0.35% Ly6G positive stained area, $p<0.01$) and eight weeks (median of 0.27% Ly6G positive stained area, $p<0.05$) after surgery (Figure 16 D, E). Neutrophilic tissue influx reduced slightly at the twelve weeks endpoint for both bacterial strains. In mice inoculated with *S. pneumoniae*, we found a significant neutrophilic infiltration at one week (median of 0.6% Ly6G positive stained area, $p<0.01$) and at eight weeks (median of 0.25% Ly6G positive stained area, $p<0.05$) after surgery (Figure 16 D, E).

4.4. Inoculation with *S. aureus* and *P. aeruginosa* leads to increased nasal pro-inflammatory cytokine production

To explain the neutrophilic influx, several canonical non-T2 related cytokines were measured in the NL and evaluated with the Mann-Whitney test (Figure 17, blue stars) in addition to Kruskal-Wallis statistical test (Figure 17, black stars).

The Th1 pro-inflammatory cytokine IL-1β was significantly increased in mice inoculated with *S. aureus* at four weeks (median of 15.76 pg/ml, compared to control mice with median of 2.963 pg/ml, $p<0.05$) after surgery. Also, a trend to persistent

increase at twelve weeks (median of 15.36 pg/ml, compared to control mice with median of 7.879 pg/ml, p= 0.052) after surgery was observed (Figure 17 A).
IL-1β was also significantly increased in mice inoculated with *P. aeruginosa* at four weeks (median of 15.44 pg/ml, $p<0.05$), eight weeks (median of 12.67 pg/ml, compared to control mice with median of 3.484 pg/ml, $p<0.05$), and twelve weeks (median of 21.49 pg/ml, $p<0.05$) after surgery (Figure 17 A).

We found significantly increased IL-1β production in the group of mice inoculated with *S. pneumoniae* with the Mann-Whitney statistical test, at four weeks (median of 9.788 pg/ml, $p<0.05$) after surgery (Figure 17 A).
The pro-inflammatory cytokine tumor necrosis factor alpha (TNF-α), was significantly increased in mice inoculated with *S. aureus* at four weeks (median of 7.648 pg/ml, compared to control mice with median of 2.051 pg/ml, $p<0.05$) after surgery (Figure 17 B).

Although we could not detect the canonical Th1-related cytokine IFN-γ in our samples because of high dilution in NL, we did detect changes in IP-10 (CXCL10), a chemokine secreted in response to IFN-γ. Significantly increased IP-10 production by mice inoculated with *S. aureus* was found at twelve weeks (median of 2.31 pg/ml, compared to control mice with median of 0.33 pg/ml, $p<0.05$) after surgery (Figure 17 C). A trend to increased IP-10 production in these mice could be observed at eight weeks (median of 12.17 pg/ml, compared to control mice with median of 1.19 pg/ml, $p=0.06$) after surgery (Figure 17 C).
A significant increased production of IP-10 was found in mice inoculated with *P. aeruginosa* at eight weeks (median of 8.32 pg/ml, compared to control mice with median of 1.19 pg/ml, $p<0.05$) after surgery (Figure 17 C).

MIP-2, an activator of neutrophils, was significantly increased in mice inoculated with *S. aureus* at four weeks (median of 67.96 pg/ml, compared to control mice

with median of 29.18 pg/ml, $p<0.05$), and twelve weeks (median of 119.9 pg/ml, compared to control mice with median of 45.05 pg/ml, $p<0.05$) after surgery (Figure 17 D). A trend to increased MIP-2 was observed in these mice at eight weeks (median of 43.38 pg/ml, compared to control mice with median of 21.02 pg/ml, $p=0.09$) after surgery (Figure 17 D).

When focusing on other neutrophilic chemokines, we found a trend towards IL-17A/F increase in mice inoculated with *S. aureus* at eight weeks (median of 0.3 pg/ml, compared to control mice with median 0 pg/ml, $p= 0.06$) and twelve weeks (median of 0.48 pg/ml, compared to control mice with median of 0 pg/ml, $p=0.01$) after surgery (Figure 17 E).
Mice inoculated with *S. pneumoniae* also showed a trend to increased IL-17A/F production at eight weeks (median of 0.32 pg/ml, compared to control mice with median of 0 pg/ml, $p=0.09$) after surgery (Figure 17 E).

We did not find significant variations in the levels of KC/GRO (CXCL1) in any of the experimental groups at any of the time points studied (Figure 17 F).

Other cytokines that were tested, such as IFN-γ, IL-12p70, IL-33 or IL-2, were not consistently upregulated upon bacterial inoculation, as their levels were mostly below the LLD in our NL samples (data not shown).

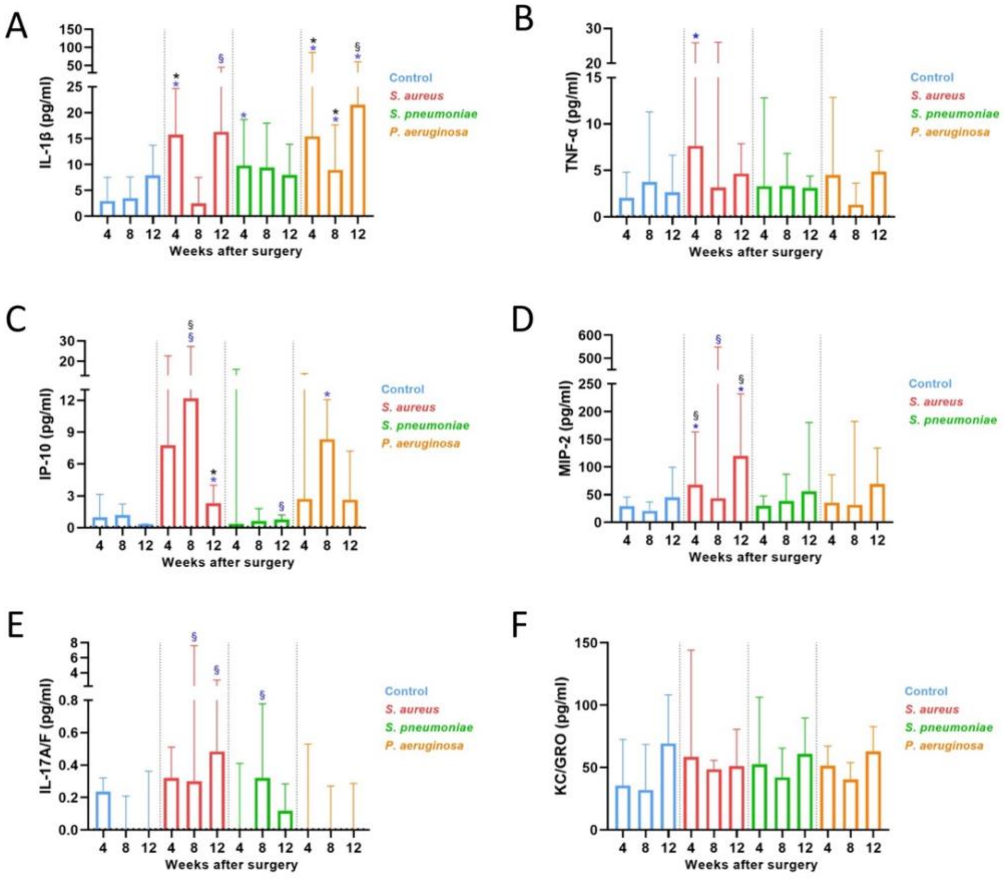

Figure 17. Cytokines and chemokines measurement by using MSDTM V-PLEX technology in the NL of a mouse model of bacterial-induced nCRS.

(A) IL-1β, LLD= 0.081 pg/ml. (B) TNF-α, LLD= 0.08 pg/ml. (C) IP-10, LLD= 0.1 pg/ml. (D) MIP-2, LLD= 0.06 pg/ml. (E) IL-17A/F, LLD= 0.1 pg/ml. (F) KC/GRO, LLD= 0.18 pg/ml. Graphs depict median (±IQR). Kruskall Wallis with Dunn's post-hoc control test for comparing multiple groups, in black *p<0.05; compared to the control group of the same time point. Because of low numbers of samples reaching the detection limit, Mann-Whitney U test was used, in blue, for comparing the inoculated mice and control mice at the corresponding time points: §p<0.1; *p<0.05. n= 3-13 mice/group.

5. Discussion

The current chapter describes the optimization and validation of a robust mouse model of bacterial-induced neutrophilic CRS that allows us to further study disease mechanisms (in an acute and a chronic form). This model is based on the combination of the introduction of a bacterial source in the nasal cavity with the obstruction of the sinus outflow tract. We were able to consistently induce general inflammatory features as well as a sinonasal neutrophilic influx, that remained present up to 12 weeks after inoculation. *S. aureus* and *P. aeruginosa* have proven to be more potent inducers of persistent local neutrophilic inflammation than *S. pneumoniae*. This model might serve as a tool to study disease mechanisms of non-eosinophilic CRS, which remains currently a major research gap.

CRS is a frequent chronic airway disease with a high disease burden and socio-economic impact. Despite non-eosinophilic CRS being the more frequent endotype, especially in Asia, very little research has been dedicated to this subtype and targeted treatments are currently unfortunately lacking. Mechanical obstruction caused by anatomical abnormalities or mucosal oedema and bacterial infection/colonization in biofilms have been postulated as potential drivers of the disease [25,26], but studies confirming these hypotheses are still lacking. A validated mouse model that mimics the human situation would be helpful in studying the disease but is currently not available.

In the past decades, researchers have experimented with animal models involving bacterial inoculation to find a reproducible model for neutrophilic CRS. In 2001, Jacob published a method previously tested in rabbits, in which a nasal tampon was surgically introduced in the nasal cavity of mice, soaked with *Bacteroides fragilis*. Authors observed a neutrophilic inflammation of the nasal septum and lateral wall of the nasal fossa four weeks after the introduction of the infected tampon [18]. A few

years later, another group used this model to compare it to eosinophilic CRS in mice. They prolonged the model to twelve weeks and used *S. pneumoniae* as a bacterial source [27]. Although these two previous publications showed very promising findings, they lacked essential information on methodological issues and outcomes, and no further publications followed using this model. Because of our interest in neutrophilic CRS pathophysiology, we decided to optimize this surgical protocol and test different bacteria and time points.

Human neutrophilic CRS is histologically characterized by epithelial hyperplasia, fibrosis, and mucosal influx of neutrophils [28]. In our mice inoculated with *S. aureus* and *P. aeruginosa*., we were able to detect these features. The predominant neutrophilic infiltration and tissue remodeling (thickened epithelium and fibrosis) found in these mice resemble the neutrophil-driven inflammation and fibrosis seen in non-eosinophilic CRS in humans [12], where this inflammation is linked to general pro-inflammatory cytokines as well as canonical Type 1 and/or Type 3 mediators [28,29]. In our mouse model, we could find a clear increase in levels of IL-1β, with trends towards increases in TNF-α, neutrophil activator MIP-2, Type 1 chemokine IP-10, which is secreted in response to IFN-γ [30], and type 3 cytokine IL-17A/F, mostly in mice inoculated with *S. aureus*. The fact that these trends often did not reach significance using ANOVA tests can be explained by the fact that we used a final volume of 1ml of saline for our NL, which led to an important dilution of nasal mediators that were often below detection limit (such as the typical Th1 cytokine IFN-γ). We therefore recommend using smaller NL volumes in case of specific study of local cytokines.

During our pilot experiments, we determined the ideal location of the nasal tampon to avoid respiratory distress but induce sinus inflammation. The nasal tampon should be very precisely located at the beginning of the opening of the maxillary sinuses, otherwise, as a very localized infiltration, neutrophils would not reach these sinuses.

The previous papers using this technique did not reported on this matter, which was, in our hands, crucial for the neutrophilic influx to reach the targeted maxillary sinuses. They also mention the inoculation of 50 µl of the bacterial solution, although, in our hands, no more than 12 µl could be used for inoculation of the nasal tampon without causing severe bronchial inhalation and overflowing of the eyes and snout by the infectious solution. Although the initial study from Jacob and company shows several pictures of the epithelial inflammation, they included the mucosa of the nasal septum and superior turbinelle, which are just adjacent to the inserted tampon.

The strength of this paper lies in the fact that we provide guidance for a reproducible mouse model of neutrophilic CRS. The surgical method has been described in depth and published in protocols.io, dx.doi.org/10.17504/protocols.io.rm7vzxwzxgx1/v2, and can be found as supplementary file within this article. In our hands, one of the most challenging parts of the protocol was to find the ideal positioning of the nasal tampon within the nasal cavity to induce local inflammation with the lowest mortality. This was obtained by removing the upper part of the septum and positioning the tampon in the upper and middle meatus of both nasal cavities, leaving enough space for nasal breathing. In this paper we also use a standardized way to evaluate sinus inflammation, focusing on 3 fixed regions of the maxillary sinuses. We chose maxillary sinuses, because they are located at a significant distance of the nasal tampon compared to the ethmoidal sinuses, to avoid neutrophil influx due to the presence of a foreign object. Thirdly, to our knowledge, we are the first to describe the use of cytospins derived from NL, which proved to be a valuable tool to quantify sinonasal (neutrophilic) inflammation. Finally, we compared the effects of three different bacteria that are relevant in upper airway disease, at three different time points to come up with the most appropriate model.

We chose *S. aureus* because, despite its well-known production of superantigens eliciting a T2 IgE mediated inflammatory response, its presence has also been linked to the enhancement of non-T2 pathways involving type 1 and 3 mediators [11]. *S. pneumoniae* was chosen because of its frequent link with acute rhinosinusitis [31]. *P. aeruginosa* is a bacterium with a high pathogenic potential, which can be detected in the microbiome of certain severe CRS patients and more frequently in those suffering from Cystic Fibrosis (CF), characterized by a non-T2 sinonasal inflammation [32]. We found that both *S. aureus* and *P. aeruginosa* were the most potent inducers of local inflammation in comparison to *S. pneumoniae*. This might be linked to the fact that *S. pneumoniae* was more easily cleared from the nasal cavities by mice. Another explanation might be that *S. aureus* and *P. aeruginosa* have both biofilm-forming capacities [33,34] which are more structurally complex, more resistant to immune responses, as well as more adaptable to various environments compared to those from *S. pneumoniae* [33–36]. Our findings, therefore, suggest that this persistent sinonasal presence of bacteria with pathogenic capacity can be the driver for a long-lasting neutrophilic inflammation. We believe that this bacterial presence is more important than the mechanical obstruction of the sinus outflow tracts, since we also detected inflammatory changes in the sinuses that were not fully blocked and for which drainage pathway was still functional (data not shown). Of note, mice that were inoculated with *P. aeruginosa* showed a prolonged and more complicated postoperative healing process, with bony overgrowth at the level of the drilling. This was also reflected in a higher mortality rate, as was the case for *S. pneumoniae* as well, compared to *S. aureus*. So, although *P. aeruginosa* could be used to study more severe exacerbations of the disease and wound healing processes, we suggest using *S. aureus* as the preferred pathogen in this mouse model.

Our findings suggest that this mouse model mimics human non-eosinophilic CRS and can be used to study the mechanisms driving inflammation and tissue damage observed in human neutrophilic CRS. New insights in the pathophysiology of non-eosinophilic CRS may allow the identification of biomarkers and even new therapeutic targets. In a second step this model could then be used to test the efficacy of existing and novel treatments for this condition. Finally, the model can serve to study the various effects of different bacterial species on the sinus mucosa. We believe that it can lead to a further and deeper understanding of this currently underexplored disease, allowing us to find novel treatment strategies for these patients that are now often left in the cold.

6. References

1. Fokkens WJ, Lund VJ, Hopkins C, Hellings PW, Kern R, Reitsma S, et al. European Position Paper on Rhinosinusitis and Nasal Polyps 2020. Rhinology journal. 2020 Feb 1;0(0):1–464.
2. Momtazmanesh S, Moghaddam SS, Ghamari SH, Rad EM, Rezaei N, Shobeiri P, et al. Global burden of chronic respiratory diseases and risk factors, 1990–2019: an update from the Global Burden of Disease Study 2019. EClinicalMedicine. 2023 May;59:101936.
3. Khan A, Huynh TMT, Vandeplas G, Joish VN, Mannent LP, Tomassen P, et al. The GALEN rhinosinusitis cohort: chronic rhinosinusitis with nasal polyps affects health-related quality of life. Rhinology journal. 2019 Jan 1;0(0):0–0.
4. Rudmik L. Economics of Chronic Rhinosinusitis. Vol. 17, Current Allergy and Asthma Reports. Current Medicine Group LLC 1; 2017.
5. Stevens WW, Peters AT, Tan BK, Klingler AI, Poposki JA, Hulse KE, et al. Associations Between Inflammatory Endotypes and Clinical Presentations in Chronic Rhinosinusitis. J Allergy Clin Immunol Pract. 2019 Nov;7(8):2812-2820.e3.
6. Cao PP, Li H Bin, Wang BF, Wang S Bin, You XJ, Cui YH, et al. Distinct immunopathologic characteristics of various types of chronic rhinosinusitis in adult Chinese. Journal of Allergy and Clinical Immunology. 2009;124(3).
7. Zhang N, Van Zele T, Perez-Novo C, Van Bruaene N, Holtappels G, DeRuyck N, et al. Different types of T-effector cells orchestrate mucosal inflammation in chronic sinus disease. Journal of Allergy and Clinical Immunology. 2008 Nov;122(5):961–8.
8. Tomassen P, Vandeplas G, Van Zele T, Cardell LO, Arebro J, Olze H, et al. Inflammatory endotypes of chronic rhinosinusitis based on cluster analysis of biomarkers. Journal of Allergy and Clinical Immunology. 2016 May 1;137(5):1449-1456.e4.
9. Min JY, Tan BK. Risk factors for chronic rhinosinusitis. Curr Opin Allergy Clin Immunol. 2015 Feb;15(1):1–13.
10. Gohy S, Hupin C, Ladjemi MZ, Hox V, Pilette C. Key role of the epithelium in chronic upper airways diseases. Vol. 50, Clinical and Experimental Allergy. Blackwell Publishing Ltd; 2020. p. 135–46.
11. Delemarre T, De Ruyck N, Holtappels G, Bachert C, Gevaert E. Unravelling the expression of interleukin-9 in chronic rhinosinusitis: A possible role for Staphylococcus aureus. Clin Transl Allergy. 2020 Dec 29;10(1):41.
12. Benjamin MR, Stevens WW, Li N, Bose S, Grammer LC, Kern RC, et al. Clinical Characteristics of Patients with Chronic Rhinosinusitis without Nasal Polyps in an Academic Setting. Journal of Allergy and Clinical Immunology: In Practice. 2019 Mar 1;7(3):1010–6.
13. Al-Sayed AA, Agu RU, Massoud E. Models for the study of nasal and sinus physiology in health and disease: A review of the literature. Laryngoscope Investig Otolaryngol. 2017 Dec;2(6):398–409.
14. Chamanza R, Wright JA. A Review of the Comparative Anatomy, Histology, Physiology and Pathology of the Nasal Cavity of Rats, Mice, Dogs and Non-human Primates. Relevance to Inhalation Toxicology and Human Health Risk Assessment. Vol. 153, Journal of Comparative Pathology. W.B. Saunders Ltd; 2015. p. 287–314.
15. Leite-Santos F, Tamashiro E, de Andrade Batista Murashima A, Anselmo-Lima WT, Valera FCP. Which are the best murine models to study Eosinophilic Chronic Rhinosinusitis? A contemporary review. Braz J Otorhinolaryngol. 2023 Sep 15;89(6):101328.
16. Kim DW, Khalmuratova R, Hur DG, Jeon SY, Kim SW, Shin HW, et al. Staphylococcus aureus enterotoxin B contributes to induction of nasal polypoid lesions in an allergic rhinosinusitis murine model. Am J Rhinol Allergy. 2011 Nov;25(6).

17. Sánchez-Montalvo A, Lecocq M, Bouillet E, Steelant B, Gohy S, Froidure A, et al. Validation and shortcomings of the most common mouse model of chronic rhinosinusitis with nasal polyps. Rhinology Journal. 2024 Mar 1;0(0):0–0.
18. Jacob A, Faddis BT, Chole RA. Chronic bacterial rhinosinusitis: description of a mouse model. Arch Otolaryngol Head Neck Surg. 2001 Jun;127(6):657–64.
19. Hung CS, Dodson KW, Hultgren SJ. A murine model of urinary tract infection. Nat Protoc. 2009;4(8):1230–43.
20. Gargiulo S, Greco A, Gramanzini M, Esposito S, Affuso A, Brunetti A, et al. Mice Anesthesia, Analgesia, and Care, Part I: Anesthetic Considerations in Preclinical Research. ILAR J. 2012 Mar 1;53(1):E55–69.
21. Buitrago S, Martin TE, Tetens-Woodring J, Belicha-Villanueva A, Wilding GE. Safety and efficacy of various combinations of injectable anesthetics in BALB/c mice. J Am Assoc Lab Anim Sci. 2008 Jan;47(1):11–7.
22. Bankhead P, Loughrey MB, Fernández JA, Dombrowski Y, McArt DG, Dunne PD, et al. QuPath: Open source software for digital pathology image analysis. Sci Rep. 2017 Dec 1;7(1).
23. Marée R, Rollus L, Stévens B, Hoyoux R, Louppe G, Vandaele R, et al. Collaborative analysis of multi-gigapixel imaging data using Cytomine. Bioinformatics. 2016 May 1;32(9):1395–401.
24. Courtoy GE, Leclercq I, Froidure A, Schiano G, Morelle J, Devuyst O, et al. Digital Image Analysis of Picrosirius Red Staining: A Robust Method for Multi-Organ Fibrosis Quantification and Characterization. Biomolecules. 2020 Nov 22;10(11):1585.
25. Hekiert AM, Kofonow JM, Doghramji L, Kennedy DW, Chiu AG, Palmer JN, et al. Biofilms correlate with TH1 inflammation in the sinonasal tissue of patients with chronic rhinosinusitis. Otolaryngol Head Neck Surg. 2009 Oct;141(4):448–53.
26. Wu J, Jain R, Douglas R. Effect of paranasal anatomical variants on outcomes in patients with limited and diffuse chronic rhinosinusitis. Auris Nasus Larynx. 2017 Aug;44(4):417–21.
27. Wang H, Lu X, Cao PP, Chu Y, Long XB, Zhang XH, et al. Histological and Immunological Observations of Bacterial and Allergic Chronic Rhinosinusitis in the Mouse. Am J Rhinol. 2008 Jul 1;22(4):343–8.
28. Cho SH, Kim DW, Gevaert P. Chronic Rhinosinusitis without Nasal Polyps. J Allergy Clin Immunol Pract. 2016 Jul;4(4):575–82.
29. Boraschi D. What Is IL-1 for? The Functions of Interleukin-1 Across Evolution. Front Immunol. 2022 Apr 6;13.
30. Coperchini F, Chiovato L, Rotondi M. Interleukin-6, CXCL10 and Infiltrating Macrophages in COVID-19-Related Cytokine Storm: Not One for All But All for One! Front Immunol. 2021 Apr 26;12.
31. Brook I. Microbiology of chronic rhinosinusitis. European Journal of Clinical Microbiology & Infectious Diseases. 2016 Jul 16;35(7):1059–68.
32. Tuli JF, Ramezanpour M, Cooksley C, Psaltis AJ, Wormald P, Vreugde S. Association between mucosal barrier disruption by Pseudomonas aeruginosa exoproteins and asthma in patients with chronic rhinosinusitis. Allergy. 2021 Nov 9;76(11):3459–69.
33. Peng Q, Tang X, Dong W, Sun N, Yuan W. A Review of Biofilm Formation of Staphylococcus aureus and Its Regulation Mechanism. Antibiotics. 2022 Dec 22;12(1):12.
34. Tuon FF, Dantas LR, Suss PH, Tasca Ribeiro VS. Pathogenesis of the Pseudomonas aeruginosa Biofilm: A Review. Pathogens. 2022 Feb 27;11(3):300.
35. Domenech M, García E, Moscoso M. Biofilm formation in Streptococcus pneumoniae. Microb Biotechnol. 2012 Jul 9;5(4):455–65.
36. Palmer J. Bacterial Biofilms in Chronic Rhinosinusitis. Annals of Otology, Rhinology & Laryngology. 2006 Sep 4;115(9_suppl):35–9.

Chapter IV – The role of secretory IgA in CRS and its potential role in shaping the nasal microbiome

Manuscript in preparation

Alba Sánchez Montalvo[1,2], Marylène Lecocq[1], Tim Van Rillaer[3], Ilke De Boeck[3], Sarah Lebeer[3], Katleen Martens[2], Sophie Gohy[1,4,5], Brecht Steelant[2], Dominique Bullens[2,6], Charles Pilette[1,4], Valérie Hox[1,8]. The role of secretory IgA in CRS and its potential role in shaping the nasal microbiome.

[1] Pole of Pneumology, ENT and Dermatology, Institute of Experimental and Clinical Research, Université Catholique de Louvain (UCLouvain), Brussels, Belgium
[2] Allergy and Clinical Immunology Research Group, Department of Microbiology, Immunology and Transplantation, KU Leuven, Leuven, Belgium
[3] University of Antwerp, Department of Bioscience Engineering, Groenenborgerlaan 171, 2020 Antwerp, Belgium
[4] Department of Pneumology, Cliniques Universitaires Saint-Luc, 1200 Brussels, Belgium
[5] Cystic Fibrosis Reference Centre, Cliniques Universitaires Saint-Luc, 1200 Brussels, Belgium.
[6] Clinical Division of Paediatrics, UZ Leuven, 3000 Leuven, Belgium.
[8] Department of Otorhinolaryngology, Cliniques Universitaires Saint-Luc, Brussels, Belgium

Preface

Building on the experimental murine models developed in Chapter II and Chapter III, Chapter IV aims to bridge preclinical research with clinical reality by incorporating human biopsy samples and patient-derived bacterial isolates.

To further investigate the role of s-IgA in CRS, we applied our established models to genetically modified mice lacking s-IgA, enabling direct assessment of its impact on the development of T2 and non-T2 sinonasal inflammation.

This chapter also introduces the application of IgA-SEQ technology to the study of CRS, being the first time this technique has been employed in the context of upper airway disease, allowing the identification of bacterial populations selectively coated by mucosal IgA. Although innovative, this approach also presented specific limitations related to the low biomass of sinonasal samples, which are discussed alongside the findings.

Altogether, Chapter IV provides a comprehensive and translational analysis of how s-IgA may shape host-microbiota interactions and inflammation in CRS.

1. Abstract

Background: Chronic rhinosinusitis (CRS) is a highly prevalent chronic inflammatory disease leading to a significant global health burden. Most of the studies investigating the role of humoral immune responses in CRS have focused on IgE, however, very little is known about the role of IgA, the most abundant antibody in nasal secretions.

Objective: Since IgA deficiencies are frequently seen in patients with CRS and evidence suggests deficits in IgA biology in CRS, we aimed to study the role and impact of this antibody in CRS.

Methods: Sinus biopsies and nasal secretions were collected from patients with CRS and healthy controls for histological analysis and ELISA. To assess the impact of secretory IgA (s-IgA) in the development of CRS *in vivo*, we used pIgR-deficient mice, inherently lacking s-IgA, in mouse models of T2 and non-T2 CRS. Inflammatory features were determined in nasal lavage (NL) fluid and in the maxillary sinus tissue. To study the interaction of human IgA with the sinonasal microbiome, nasal bacteria were harvested from patients with CRS and healthy controls, and sorted based on their IgA-coating. The DANN from the IgA-coated and -uncoated microbial fractions was extracted and the differente microbial communities were analyzed by MiSeq Illumina amplicon sequencing of the V4 region of the 16S rRNA gene (IgA-SEQ).

Results: Reduced pIgR and IgA expression was observed in tissue and was translated into decreased levels of total s-IgA1 in secretions, but not total s-IgA. *In vivo*, the absence of s-IgA attenuates inflammation in mice with experimental T2 CRS and increases the severity of inflammation in mice with bacterial-induced non-T2 CRS. IgA-SEQ technology revealed differences in microbial diversity among the IgA-coated baceria between patients with CRS and controls. It also showed several taxa being differently coated in patients with CRS than in controls.

Conclusions: Our findings suggests that not only quantitative levels of IgA, but also qualitative functional aspects of s-IgA might contribute to CRS pathophysiology, especially in non-T2 CRS.

2. Introduction

CRS is among the most frequent respiratory diseases in the world, with a prevalence of around 11% [1]. CRS is characterized by a persistent mucosal inflammation of the nasal and paranasal sinuses, leading to the typical symptoms of nasal discharge/congestion, facial pressure, impaired smell, headache, fatigue or cough. It can severely impact the quality of life of patients and is linked to an important cost for society [2], resulting in an important global health burden [3]. In the most recent guidelines, CRS is mainly classified by two main inflammatory profiles: T1 and non-T2 [4]. In western countries, patients with a T2 inflammatory profile often present with NP formation with activated eosinophils and increased levels of IgE, IL-4, IL-5 and IL-13 and are addressed as CRSwNP. In patients with a non-T2 inflammatory profile, associated with Th1/Th17/Th22 responses [4–6], increased levels of IFNg and activated neutrophils are found and often no NP are visualized in the nasal cavities. This is addressed as CRSsNP [4,7].

The nasal mucosa, along with its immune system, serves as the body's first line of defense in the airways against inhaled particles and agents. A key mechanism for mucosal tissues defense is the humoral mucosal immunity, including the production of s-IgA 8. IgA is the most abundant antibody in human secretions and its main known functions are exerted at the mucosal level under the form of s-IgA 8. Briefly, plasma cells from the lamina propria secrete IgA in the form of two subtypes: IgA1 and IgA2. Dimeric IgA can bind to the pIgR at the basolateral site of the nasal epithelium that transcytoses IgA towards the mucosal lumen. In the apical site of the epithelium IgA is then released bound to the extracellular component of the pIgR, SC, which is then addressed as s-IgA 9. The main functions exerted by s-IgA are immune exclusion; entrapment and neutralization of different pathogens 10;

regulation of immune responses 10–12; minimization of inflammatory responses by avoiding complement activation 13 and interaction with the nasal microbiome, promoting the retention of beneficial microbes and reducing colonization by harmful bacteria 13–15. Although IgA is the most abundant antibody in nasal secretions, very little attention has gone to its role in the development of CRS. Most of the knowledge about the role of s-IgA in the nasal mucosa comes from individuals with SIgAD presenting with more recurrent allergy, respiratory infections and CRS 14–17.

Several studies have examined the production of IgA in patients with CRS [18]. While serum IgA levels show no significant differences between patients with CRS and controls [19,20], Lal et al. reported increased specific IgA responses to microbial proteins, particularly against *Staphylococcus aureus*, human metapneumovirus, and herpesviruses 4 and 5 [21]. Locally, patients with CRS exhibit higher IgA levels in sinus tissue [22–26] with increased IgA+ plasma cells in CRSwNP [22–24]. Two studies report an overexpression of BAFF [24,27], a key IgA class-switching factor, which may further support enhanced local IgA production in T2 inflamed polyp tissue [28]. Another study suggests potential conversion of bacterial antigen-specific IgA to IgE in a Th2 environment [29,] though further research is needed to confirm its relevance. Findings on s-IgA levels in nasal secretions are inconsistent. Most of the studies investigating IgA levels in CRS did not characterize the specificity of IgA in these patients. One study found elevated mucosal levels of autoreactive IgA to nuclear antigens, including double stranded DNA and basement membrane components that might contribute to the disease mechanism [30]. Tsybikov et al. reported increased s-IgA in CRSwNP patients [31], while Hupin et al. found no significant differences, attributing this to IgA accumulation in subepithelial tissue rather than secretion [25]. This may be due to reduced pIgR expression, limiting IgA transport across the epithelium. Although overall s-IgA levels were unchanged, antigen-specific IgA against SEB, a key Th2 inflammation driver, was reduced [25]. The role of *S. aureus* in the development of CRS is quite well studied, but the impact of the rest of the

nasal microbiome remains quite illusive. Several studies have shown that patients with CRS exhibit nasal microbiome dysbiosis, characterized by altered bacterial diversity [32] and overrepresentation of certain pathogenic bacteria, including *Staphylococcus aureus* and *Pseudomonas aeruginosa*. Concurrently, beneficial bacteria such as *Corynebacterium accolens* and *Dolosigranulum*, which may support immune tolerance, are often depleted in these individuals [33]. This microbiome dysbiosis is thought to disrupt the epithelial barrier, allowing allergens and pathogens to provoke an excessive immune response [34–36]. Apart from that, only two studies have specifically studied the tissue expression level of pIgR in patients with CRswNP, which are reduced compared to healthy controls [25,26].

The role of s-IgA in shaping the microbiome has mostly been studied in the intestinal mucosa [37–41]. S-IgA plays a crucial role in gut homeostasis by preventing pathogen adhesion, neutralizing toxins, and shaping the microbiota. It promotes the retention of beneficial bacteria while preventing dysbiosis, partially through its polyreactivity and ability to modulate bacterial gene expression. SIgAD has been linked to microbiota alterations in the gut, highlighting its role in maintaining a balanced microbial ecosystem [40,42]. However, hardly anything is known about the role s-IgA plays on the respiratory microbiome.

In this chapter, we aimed at investigating the role of the pIgR/IgA system in CRS by combining both human biopsies and nasal secretions and the established mouse models of CRS described in Chapter II and Chapter III. We also studied the s-IgA coating levels of the different members of the nasal microbiome to find functional differences in s-IgA between patients with CRS and controls. In the context of CRS, understanding the role of the IgA system, necessary for mucosal defense, is crucial in elucidating the mechanisms of both immune and microbiome dysregulation and determining potential therapeutic targets for this frequent disease.

3. Methodology

3.1. Human analysis

3.1.1. Subjects and sampling

Tissue from the ethmoidal sinuses as well as nasal secretions were obtained from 61 patients with CRS (28 CRSsNP and 33 CRSwNP), with CRS following EPOS criteria [4], undergoing functional endoscopic sinus surgery for their disease. Ethmoidal tissue was also obtained from 21 healthy subjects undergoing surgery for lacrimal duct, skull base lesions or sphenopalatine clipping. Exclusion criteria were patients younger than 18 years old; use of systemic steroids for four weeks prior to surgery; any concomitant neoplastic process; patients suffering from systemic disease such as sarcoid, vasculitis or SLE; patients suffering from ciliary disease such as primary ciliary dyskinesia or cystic fibrosis; patients with unilateral disease; patients with incapacity to fill out forms in French/Dutch/English. Patients' characteristics are shown in Table 4 A. Tissue was washed, fixed in formol and paraffinized according to standard procedures. Nasal secretions were collected following a standardized method [43,44]; briefly, a pre-weighed nasal tampon was placed in each nostril prior to surgery for 5 minutes. Then, after weighing the nasal tampon, it was washed with 3ml of saline and centrifuged at 450g for 10 minutes at 4ºC. Supernatants were stored at -20ºC for further processing.

For the IgA-SEQ experiments, 4 microbial E-Swabs (Copan Diagnostics) were taken from both the anterior nares and middle meatus from 41 patients with CRS (21 CRSsNP and 20 CRSwNP) and 29 healthy controls from the recruited patients mentioned above, with the additional exclusion criteria of use of oral antibiotics 4 weeks prior to sample harvesting. Patients' characteristics are shown in Table 4 B. Three swabs were placed in saline solution for further processing and one swab was directly placed in the lysis solution from the DNA extraction kit (QIAamp PowerFecal Pro DNA Kit, Qiagen). The three swabs were stirred in saline solution

and filtered through 70 µm and 40 µm filters to remove big particles. A centrifugation was performed at 300g for 5 minutes at 4ºC to separate human cells and the supernatant with the bacteria was again centrifuged at 8000g for 10 minutes at 4ºC. The supernatant was collected for further processing.

All patients provided signed informed consent for the study protocol, which was approved by the local clinical Ethical committee with reference 2018/01OCT/361 with an approved amendment for nasal swabbing in 2021.

3.1.2. Sinus tissue immunohistochemistry for pIgR and IgA

4-µm paraffin sections were deparaffinized in toluene and rehydrated through graded series from methanol to distilled water and sections underwent antigen retrieval. Endogenous peroxidase, biotin, and streptavidin sites were inactivated by hydrogen peroxide, biotin, and avidin solutions or Bloxall (Vector Laboratories, Inc., USA), as appropriate. Non-specific protein binding sites were blocked with 5% bovine serum albumin in tris-buffered saline (TBS) for 1h. As human primary antibodies, mouse anti-human IgA (ThermoFisher Scientific), or mouse anti-human SC (Santa Cruz) were incubated overnight at 4°C. After washing in TBS 0.1% Tween 20, sections were incubated with rabbit anti-mouse IgG (Sigma Aldrich) for one hour. Revelation was performed by using 3,3'-Diaminobenzidine (Sigma-Aldrich). Sections were counterstained with Hematoxylin (Sigma-Aldrich) and coverslipped. Slides were scanned using a Pannoramic scan II (3DHistech). Quantification was performed by using QuPath [50] and expressed as percentage of positive area.

3.2. Mouse models of eosinophilic and neutrophilic CRS

3.2.1. Mouse model of eCRS

The model was performed as previously described in Chapter II [45] and an overview of the experimental design is shown in Figure 22 A. Briefly, 7-8 week old male pIgR$^{-/-}$ mice were bred at the host lab (N= 5) based on the publication by Johansen et al. [46]. Also, 7-8 week old C57BL/6NRJ wild-type (WT) mice (N= 5) purchased from JanvierLabs were sensitized with an intraperitoneal (i.p.) injection of 25 µg of OVA in 2mg of aluminium on days 0 and 7, followed by one week of daily intranasal (i.n.) challenges with 6% OVA. These i.n. challenges were continued three times a week for one week and then, in addition to i.n. OVA-challenges, a second i.n. challenge with SEB was co-administered for eight weeks. Mice were sacrificed after twelve weeks to evaluate inflammatory features.

3.2.2. Mouse model of nCRS

The model was performed as described in Chapter III. An overview of the experimental design is shown in Figure 23 A. Briefly, 7-8 week old pIgR$^{-/-}$ mice bred at the host lab based on the publication by Johansen et al. [46], and 7-8 week old C57BL/6NRJ WT mice purchased from JanvierLabs underwent micro-surgery to introduce a tampon in the nasal cavity. Then the tampon was inoculated with either *S. aureus* (Lenticules^{TM} Sigma-Aldrich, CRM06571M); pIgR$^{-/-}$ mice, N= 12; WT mice, N= 7) or *P. aeruginosa* (Sigma-Aldrich, VT000256, pIgR$^{-/-}$ mice, N= 13; WT mice, N= 8). The skin flaps were then sutured and the mice were left to recover. To overcome any postoperative pain, mice received analgesia every 12 hours for 24 hours after the procedure. Mice were sacrificed after four weeks to evaluate inflammatory features.

All animal experiments were performed in compliance with the ethical committee guidelines and approved under reference code 2018/UCL/MD/42 (eosinophilic model) and 2021/UCL/MD/017 (neutrophilic model). If mice reached a score of non-well-being, mainly observed with respiratory distress, or lost more than 20% of their body weight, they were euthanized according to humane endpoints.

3.2.3. Sacrifice and sampling

After completion of the models, mice were euthanized by i.p. injection of pentobarbital (200mg/kg). Blood was drawn for the inferior cava vein and serum was collected by centrifugation for 10 minutes at 650g and stored at -20ºC. Then, a tracheotomy was performed to carry out the NL via inserting a 22G cannula (Versatus^{TM} I.V Catheter) towards the choanae. 1 ml of saline solution (NaCl 0.9%) was softly flushed, recovering and washing every 200 µl in the syringe, through the catheter and recovered at the nostrils. Skulls were harvested by decapitation and skin, soft tissues and the inferior mandibula were removed. They were fixed in formaldehyde 4% and decalcified in OsteoralTM (RAL Diagnostics) for 5 days. After decalcification, the snout and brain were removed to keep the region of interest containing the paranasal sinuses. The decalcified skulls were dehydrated and treated according to standard paraffin-embedding procedures. Paraffinized skulls and lungs were cut into 4-µm sections with a semi-automated microtome (ThermoFisher Scientific).

3.2.4. Cytospins of murine NL

In the case of the nCRS model, the NL was centrifuged for 5 minutes at 450g and 4ºC to separate the cell pellet. Cells were resuspended in 100 microliters PBS and loaded into a Thermo Shandon Cytospin Centrifuge following manufacturer's instructions and centrifuged at 500 revolutions per minute (rpm) for 5 minutes.

Cytospins were stained by using the Kwik-Diff™ kit (Thermo Fisher Scientific). Total inflammatory cells and total neutrophils were manually counted in cytospins by using Qupath [47].

3.3. Histopathologic analysis of murine skulls

4-µm paraffin sections were deparaffinized in toluene and rehydrated through graded series from methanol to distilled water and sections underwent antigen retrieval. Histological features were consistently analyzed in three regions of each maxillary sinus as previously described in Chapters II and III [45]. Giemsa staining was performed to assess eosinophilic infiltration and quantification was performed by using Cytomine [48]. Results are presented as median of 6 measurements/mouse ± interquartile range (IQR). Epithelial thickness was measured from basolateral to apical poles using Cytomine [48]. Results are presented as the median of 24 measurements/mouse ± IQR.

3.4. Immunohistochemistry for and neutrophils

4-µm paraffin sections of murine skulls were treated and stained as the human samples described above. Neutrophilic infiltration was assessed through Ly6G-specific immunohistochemistry (IHC) using rat anti-mouse Ly6G (BD Bioscience, 551459) incubated for one hour at room temperature. Revelation was performed by using 3,3'-Diaminobenzidine (Sigma-Aldrich). Sections were counterstained with Hematoxylin (Sigma-Aldrich) and coverslipped. Slides were scanned using a Pannoramic scan II (3DHistech). Quantification was performed by using QuPath [155] and expressed as percentage of positive area.

3.5. ELISA for murine total IgA in nasal secretions and serum

Murine total IgA levels in NL were determined by ELISA. Goat anti-mouse IgA (ThermoFisher, 62-6700) was used as capture antibody, Purified Mouse IgAκ Isotype Control was used to create standards (Sigma-Aldrich, M1421) and Biotinylated rat anti-mouse IgA (SYnAbs, LO-MA-07) was used for detection. Detection limits were 1.5 ng/ml for serum and 4 ng/ml for NL). Serum samples were diluted 1:5 in PBS-BSA 1% and NL samples were used undiluted.

3.6. IgA-sequencing

3.6.1. Preparations of bacterial samples for IgA-SEQ

The bacterial pellets were resuspended in 1 ml of staining solution (Tryptic Soy Broth (BD 211825) 5% diluted in saline solution) and incubated with human anti-IgA (AF647, SanBio) for 20 minutes at 4ºC. Stained bacteria were washed with 15 ml of staining solution by centrifuging at 8000g for 10 minutes at 4ºC and resuspended in 500 µl of the same solution to be incubated with 0.5 µl SYTO BC (Invitrogen, B7277) for 10 minutes. After that, bacteria were stained with a fluorescent anti-human IgA, to label pre-deposited s-IgA on them. Then, bacteria were then sorted by fluorescence-activated cell sorting (FACS) based on their fluorescent signal into cytometry into IgA-positive (IgA+) and IgA-negative (IgA–) fractions. The gating strategy for the sorting based on IgA-coating is shown in Figure 18. During The DNA from the IgA+ and IgA– bacterial fractions, together with the DNA from the unsorted swab placed directly in lysis buffer, was extracted with the QIAamp PowerFecal Pro DNA Kit (Qiagen) following manufacturer's instructions.

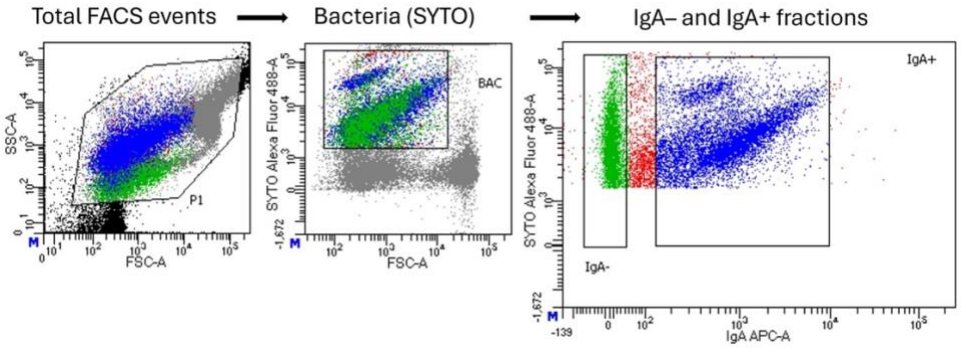

Figure 18. IgA-SEQ gating strategy for bacterial sorting based on IgA-coating. Nasal bacteria stained with mouse anti-human IgA (AF). Gating on a population based on FSC and SSC characteristics, followed by discrimination of SYTO+ bacteria from autofluorescence debris. IgA+ and IgA– bacteria were sorted from SYTO+ events.

3.6.2. Illumina 16S rRNA amplicon IgA-SEQ

The extracted DNA was used for amplification of the V4 region of the 16S rRNA gene, using barcoded forward (515F) and reverse (806R) primers. The primers used followed the dual-index paired-end sequencing strategy described in Kozich et al. [49]. PCR products obtained were visualized on 1.2% agarose gel and purified using the Agencouret AMPure XP Magnetic BeadCapture Kit (Beckman Coulter). The concentration of the samples was measured using the Qubit 3.0 Fluorometer (Life Technologies). Next, a library was prepared by pooling all PCR samples in equimolar concentrations. This library was then loaded onto a 0.8M agarose gel and purified using the NucleoSpin Gel and PCR clean-up (Macherey-Nagel). The library concentration was then measured with the Qubit 3.0 Fluorometer and denatured with 0.2N NaOH (Illumina), diluted to 6pM and spiked with 10% PhiX control DNA (Illumina). Finally, dual-index paired-end sequencing was performed using a MiSeq Desktop sequencer (Illumina). All DNA samples, as well as negative controls of both PCR (PCR grade water) and the DNA extraction, were included on the sequencing run.

3.6.3. Processing and quality control of amplicon sequencing data

Quality control and processing of the amplicon reads was performed using the nf-core/ampliseq pipeline [50] using the default settings with truncLen=c(140,140). A custom taxonomy database based on the Genome Taxonomy Database (GTDB; [51]) supplemented with mitochondrial and chloroplast 16S RNA sequences from the Silva database [52] was used for the classification steps. All downstream data handling and visualization was performed using version 1.0.6 of the tidytacos package [53] in R version 4.4.1 in coordination with the tidy verse collection of packages. Non-bacterial ASVs (eg. mitochondria) were discarded and ASVs that had a length diverging from the expected 254bp with 6 bp more or less were removed. Then the decontam package [54] was used to flag ASVs as contaminants using the frequency based and prevalence-based method considering the sample concentrations and negative controls respectively, contaminants were then removed from the data. Samples with fewer than 1000 reads were dropped from the dataset.

To monitor potential contamination, especially given the low biomass of our samples, we included controls such as saline, staining solution (used for FACS) and reagents for DNA extraction and sequencing. These were processed in parallel with biological samples. Contaminants were identified using the decontam package, which applies both frequency-based (inverse correlation with DNA concentration) and prevalence-based (higher abundance in controls) filtering. ASVs flagged by either method were removed. Samples with fewer than 1,000 high-quality reads after quality control and decontamination were also excluded to ensure reliable bacterial profiles.

3.6.4. Bioinformatic analysis

Microbiome profiles, alpha diversity and beta diversity were computed and visualized using the aforementioned tidytacos package in R. To assess the degree of IgA-binding to specific bacterial taxa, we calculated the IgA Index, also referred to as the Kau Score, as previously described [55]. This index quantifies the relative enrichment of a bacterial taxon in the IgA-bound fraction compared to the IgA-unbound fraction, providing a standardized measure of IgA targeting within the gut microbiota. Positive Kau score values indicate preferential IgA recognition, while negative or near-zero values suggest minimal or no IgA binding. Kau scores were calculated using version 0.1.2 of the IgAScores R package [55].

3.7. Statistical analysis

Analyses were performed with GraphPad Prism version 8.0.0 (GraphPad Software, San Diego). Statistical differences between multiple experimental groups, comparing disease groups to the corresponding control group, were evaluated using Kruskal-Wallis test with Dunn's post-hoc control test for comparing multiple groups. For comparing two groups, Mann-Whitney test was used. A value of $p<0.05$ was considered significant. For human analysis, results are presented as mean/group ± standard deviation (SD). For murine analysis, results are presented as median/group ± interquartile range (IQR). Microbiome and associated statistical analyses were performed in R (version 4.4.1) using the tidytacos package. Alpha diversities were represented with observed species and the Shannon index. Beta diversities were calculated using the Aitchison distance. Beta dissimilarity matrices were partitioned among covariates using the PERMANOVA implementation in the adonis2 function from the vegan package (v2.6.8). Non-parametric statistical tests were used to compare among the unbalanced groups when assessing alpha diversity or Kau scores. All P-values were corrected using the BH method and are reported as adjusted P in the case of testing multiple features or when performing a multiple pairwise comparison.

4. Results

4.1. Patients' characteristics

Table 4 summarizes the demographic and clinical characteristics of the study participants, including healthy controls, patients with CRSwNP and patients with CRSsNP, across two experimental cohorts: (A) biopsies and nasal secretions and (B) IgA-SEQ samples.

In cohort A, 33 patients with CRSwNP and 28 with CRSsNP were included, along with 21 healthy controls. The mean age ranged from 19 to 83 years, with comparable sex distribution across groups. SNOT-22 scores indicated a greater symptom burden in CRSwNP patients (mean ± SD = 52 ± 20.38) compared to CRSsNP patients (43.70 ± 21.55). Systemic eosinophil counts were elevated in both CRS groups as compared to healthy controls. Histological analysis revealed tissue eosinophilia in 19 out of 33 (58%) patients with CRSwNP and in 25 out of 28 (89%) patients with CRSsNP. In contrast, only 2 of 21 healthy controls showed eosinophilic infiltration in their tissue. Notably, tissue eosinophilia was more prevalent among patients than in controls.

In cohort B, similar trends were observed in the subset used for IgA-SEQ analysis. Among the sorted samples, tissue eosinophils were detected in 15 of 16 CRSwNP patients (94%) and in 11 of 14 CRSsNP patients (79%). Only 1 of 19 healthy controls exhibited tissue eosinophilia.

Asthma was comorbid in a subset of patients, with overall 14 CRSwNP and 10 CRSsNP individuals reporting a clinical diagnosis of asthma, compared to 3 healthy controls.

Table 4. Patients' characteristics.

A	Tissue samples and nasal secretions	Healthy controls	Patients with CRSwNP	Patients with CRSsNP
	Subjects, n	21	33	28
	Sex, F/M	15/6	15/18	14/14
	Age, years (range)	19-83	25-71	19-74
	SNOT-22 score, mean ± SD	NA	52 (±20,38)	43,70 (±21,55)
	Systemic eosinophils (/µl), mean ± SD	176,25 (±126,91)	371,26 (±276,81)	264,32 (±390,40)
	Tissue eosinophils, n positive/negative	2/19	19/14	25/3
	Asthma, n	1	12	7
B	**IgA-SEQ samples**	**Healthy controls**	**Patients with CRSwNP**	**Patients with CRSsNP**
	Non sorted samples, n	19	16	14
	Sorted samples, n	16	9	5
	Sex, F/M	15/11	10/6	3/11
	Age, years (range)	18-71	25-76	19-74
	SNOT-22 score, mean ± SD	NA	52 (±20,38)	43,70 (±21,55)
	Systemic eosinophils (/µl), mean ± SD	93,75 (±53,65)	274,38 (±233,60)	371,26 (±489,20)
	Tissue eosinophils, n positive/negative	1/18	15/1	11/3
	Asthma, n	2	2	3

Abbreviations: n, sample size; F, female; M, male; SD, standard deviation; SNOT, sino-nasal outcome test.

4.2. Patients with CRS show reduced epithelial expression of pIgR and IgA with reduced secretion of s-IgA1

pIgR expression was significantly decreased in the epithelial layer of the sinus tissue from patients with CRSsNP ($p<0.05$) and patients with CRSwNP ($p<0.05$) compared to healthy controls (Figure 19 A, C). On the other hand, no significant variations in pIgR expression were observed in submucosal glands among groups (Figure 19 B, C). Also, IgA expression was significantly reduced in the epithelial layer of sinus biopsies from patients with CRSwNP ($p<0,05$) (Figure 19 D, J) compared to healthy subjects. Submucosal IgA accumulation was not different among groups (Figure 19 E, J). In nasal secretions, the levels of s-IgA (Figure 19 F) did not differ among patients and controls. However, when measuring the levels of the different s-IgA

subtypes, a significant reduction in the levels of s-IgA1 was found in CRSwNP patients compared to healthy subjects ($p<0.001$) (Figure 19 G), which was not the case for s-IgA2 (Figure 19 H).

4.3. Patients with CRS show reduced epithelial expression of pIgR and IgA with reduced secretion of s-IgA1

pIgR expression was significantly decreased in the epithelial layer of the sinus tissue from patients with CRSsNP ($p<0.05$) and patients with CRSwNP ($p<0.05$) compared to healthy controls (Figure 19 A, C). On the other hand, no significant variations in pIgR expression were observed in submucosal glands among groups (Figure 19 B, C). Also, IgA expression was significantly reduced in the epithelial layer of sinus biopsies from patients with CRSwNP ($p<0,05$) (Figure 19 D, J) compared to healthy subjects. Submucosal IgA accumulation was not different among groups (Figure 19 E, J). In nasal secretions, the levels of s-IgA (Figure 19 F) did not differ among patients and controls. However, when measuring the levels of the different s-IgA subtypes, a significant reduction in the levels of s-IgA1 was found in CRSwNP patients compared to healthy subjects ($p<0.001$) (Figure 19 G), which was not the case for s-IgA2 (Figure 19 H).

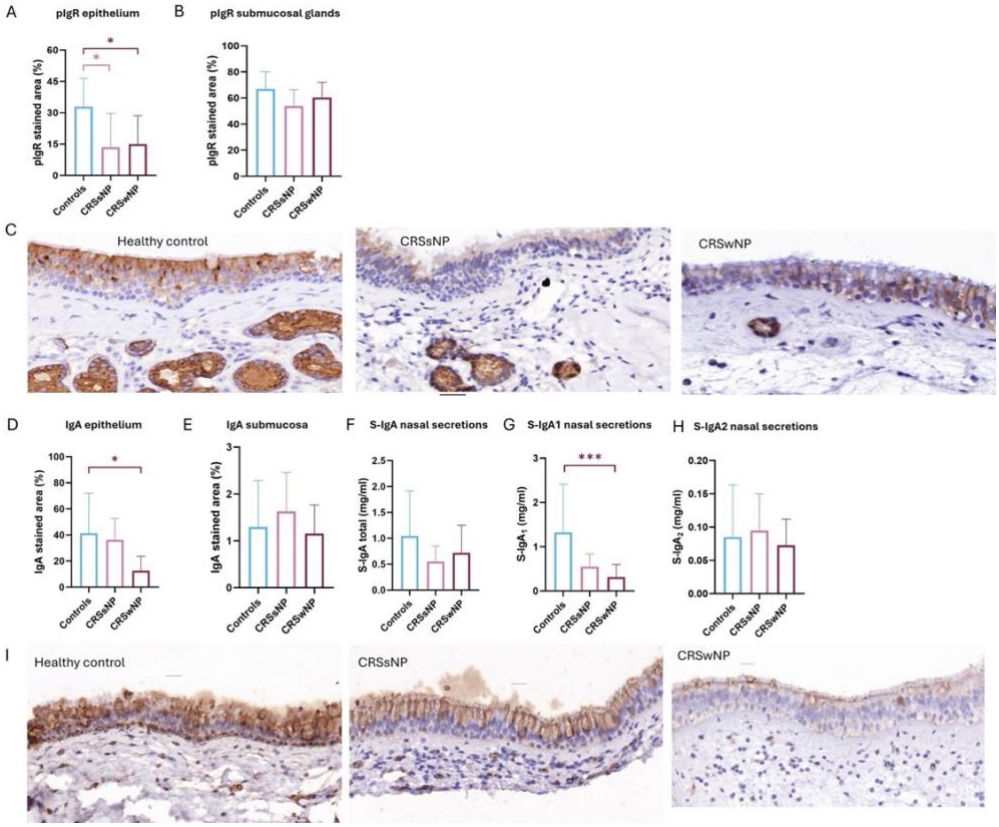

Figure 19. Evaluation of the pIgR/IgA system in patients with CRS and healthy subjects.

pIgR expression in the epithelial layer (A) and submucosal glands (B) in biopsies. Quantification was performed by using Qupath [47]. Graphs depict mean of four measurements per patient ± SD. (C) Representative pictures of pIgR expression in biopsies for each studied group. (D) Measurements of SC in nasal secretions, DL= 1,31 ng/ml. IgA expression in the epithelial layer (E) and submucosa (F) in biopsies. Quantification was performed by using Qupath [47]. Graphs depict mean (± SD) of four measurements per patient. (G) Representative pictures of IgA expression in biopsies for each studied group. Measurement in NS of (H) total IgA levels (DL= 1,83 ng/ml), (I) total s-IgA levels (DL= 2,32 ng/ml), (J) s-IgA1 levels (DL= 9,3 ng/ml), and (K) s-IgA2 levels (DL= 8,96 ng/ml). Mann-Whitney test, *p<0.05; ***p<0.0001.

4.4. s-IgA is upregulated in nasal secretions in a mouse model of type 2 CRS

To address the role of IgA in *in vivo* systems, we determined the levels of total IgA in serum and in the NL of mice suffering from CRS and compared to controls (the same WT mice with T2 eCRS and with non-T2 nCRS described in Chapter II and Chapter III).

WT mice with experimental T2 eCRS, especially mice challenged with OVA+SEB, exhibited higher levels of total IgA both in serum and in NL compared to control groups (Figure 20 A). Conversely, when determining the levels of total IgA in WT mice with experimental non-T2 nCRS, no significant changes were found in serum or NL at any of the study timepoints (Figure 20 B).

4.5. The absence of s-IgA attenuates inflammation in a mouse model of type 2 CRS but aggravates inflammation in a mouse model of non-type 2 CRS

pIgR$^{-/-}$ mice with experimental T2 CRS showed less pronounced epithelial inflammatory features in the maxillary sinus compared to WT mice. They showed less epithelial hypertrophy ($p<0.05$) (Figure 21 B, D) as well as a lower number of mucosal eosinophils as compared to WT mice with T2 CRS ($p<0.05$) (Figure 21 C, D). Only for serum IgE levels, pIgR$^{-/-}$ mice showed significantly higher levels compared to their WT peers ($p<0.01$) (Figure 21 E).

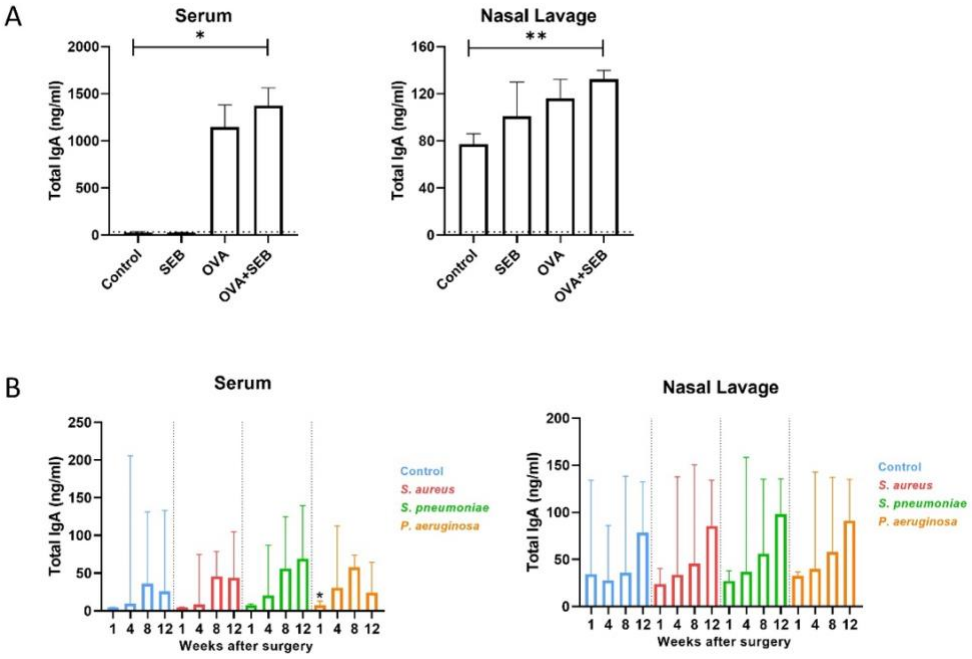

Figure 20. Levels of total IgA in serum and in NL in mouse models of experimental T2 eCRS and non-T2 nCRS.

(A) Total IgA levels in serum (left) and in NL (right) in a mouse model of experimental T2 eCRS. (B) Total IgA levels in serum (left) and in NL (right) in a mouse model of experimental non-T2 nCRS. Graphs depict median (±IQR). ELISA detection limits were 1.5 ng/ml for serum and 4 ng/ml for NL. Kruskall Wallis with Dunn's post-hoc control test for comparing multiple groups test: *$p<0.05$; **$p<0.01$.

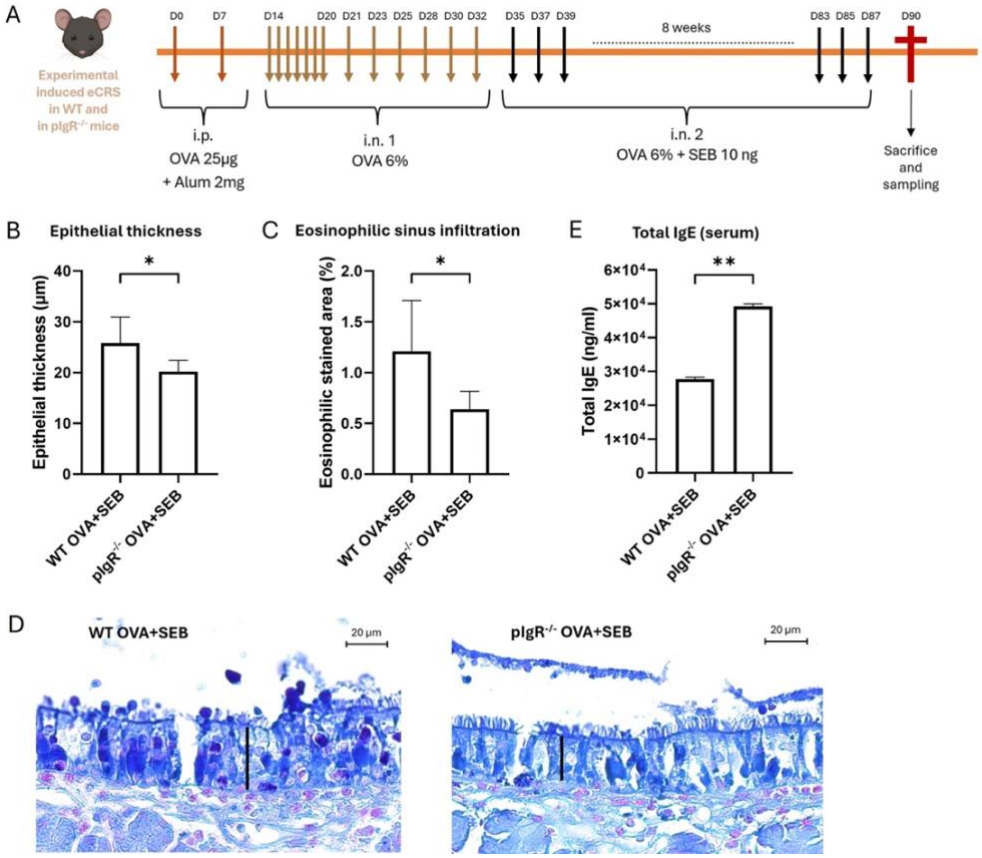

Figure 21. Experimental design and inflammatory changes in the maxillary sinuses of pIgR-/- mice with experimental allergen-induced eCRS.
(A) Experimental design to establish an allergen-induced eCRS in WT and in pIgR$^{-/-}$ mice. (B) Epithelial thickness measurements, graph depicts median (±IQR) of 24 measurements/mouse, performed by using Cytomine [48]. (B) Quantification of sub- and intra-epithelial eosinophilic infiltration in the maxillary sinus, graph depicts median (± IQR) of 6 measurements/mouse. Quantification was performed by using Qupath [47]. (C) Representative pictures of the maxillary sinus epithelial layer, Giemsa staining. Black bar indicates how the epithelial thickness measurements were performed, from the base to the apical pole of the epithelial cells. (D) Total IgE levels in serum. Scale bar = 20 µm. Mann-Whitney test, *p<0.05; **p<0.01.

When testing a mouse model of bacterial-induced non-T2 CRS in mice lacking s-IgA, we found a significantly higher mortality rate in pIgR$^{-/-}$ mice inoculated with *P. aeruginosa* compared to WT mice treated with this bacteria (69.2% vs. 13.5%; p<0,001) (Figure 22 B). This difference was not seen in mice inoculated with *S. aureus* from which 100% of both WT and pIgR$^{-/-}$ mice survived (Figure 22 B). Although we did not detect a difference in epithelial hypertrophy between WT and pIgR$^{-/-}$ mice with experimental bacterial non-T2 CRS (Figure 22 C, G), we did find a more pronounced inflammation in mice lacking s-IgA compared to WT mice. This was shown by cytospins of the NL that showed significantly higher numbers of total inflammatory cells ($p<0.01$) and neutrophils ($p<0.01$) in pIgR$^{-/-}$ mice (Figure 22 D, E). It was also confirmed at tissue level, where the mucosal neutrophilic influx was significantly higher in infected pIgR$^{-/-}$ mice compared to infected WT mice ($p<0.05$) (Figure 22 F, G).

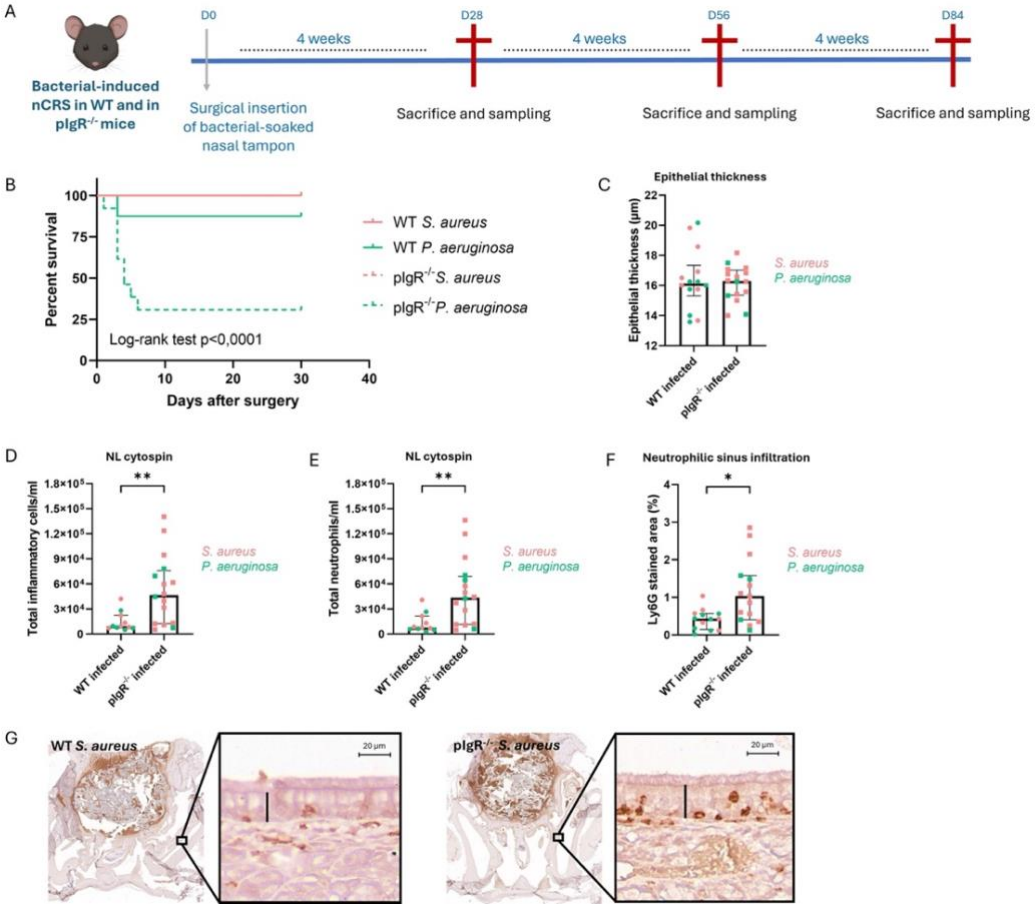

Figure 22. Experimental design, survival curve and inflammatory changes in the maxillary sinuses of pIgR $^{-/-}$ mice with experimental bacterial-induced nCRS.

(A) Experimental design to establish a bacterial-induced nCRS in WT and in pIgR$^{-/-}$ mice. (B) Kaplan-Meier survival curve of mice with bacterial-induced neutrophilic CRS. (B) Epithelial thickness measurements, graph depicts median (±IQR) of 24 measurements/mouse, performed by using Cytomine [48]. (C) Total inflammatory cells/ml in the NL. Counting was performed by using Cytomine [48]. (D) Total neutrophils/ml in the NL. Counting was performed by using Cytomine [48]. (E) Quantification of sub- and intra-epithelial neutrophilic infiltration in the maxillary sinus, graph depicts median (± IQR) of 6 measurements/mouse. Quantification was performed by using Qupath [47]. (F) Representative pictures of the maxillary sinus epithelial layer, Ly6G staining. Black bar indicates how the epithelial thickness measurements were performed, from the base to the apical pole of the epithelial cells. Graphs depict median (±IQR). Mann-Whitney test, *p<0.05; **p<0.01.

4.6. Microbiome characteristics in CRS and healthy controls

Prior to the analysis about sIgA-binding capacities of sinonasal bacteria, we determined the overall nasal microbiome composition in the non-sorted microbial samples (Figure 23). Bacterial density was similar between healthy controls and patients with CRS as measured by total FACS event counts per swab (Figure 23 A), as well as by number of copies of the 16S gene per swab (Figure 23 B). When comparing the microbial diversity across our study groups, no significant differences were seen between healthy controls and patients when using the observed index (evaluating richness) nor the Shannon index that accounts for both species' richness and evenness (Figure 23 C). The beta diversity was calculated using Aïtchison distances and compared among the study groups, groups. Although the majority of the samples seemed to cluster together, some differences could be observed, and mainly the healthy control group seemed to have a bit more diversity in the samples ($p<0,05$) (Figure 23 D).

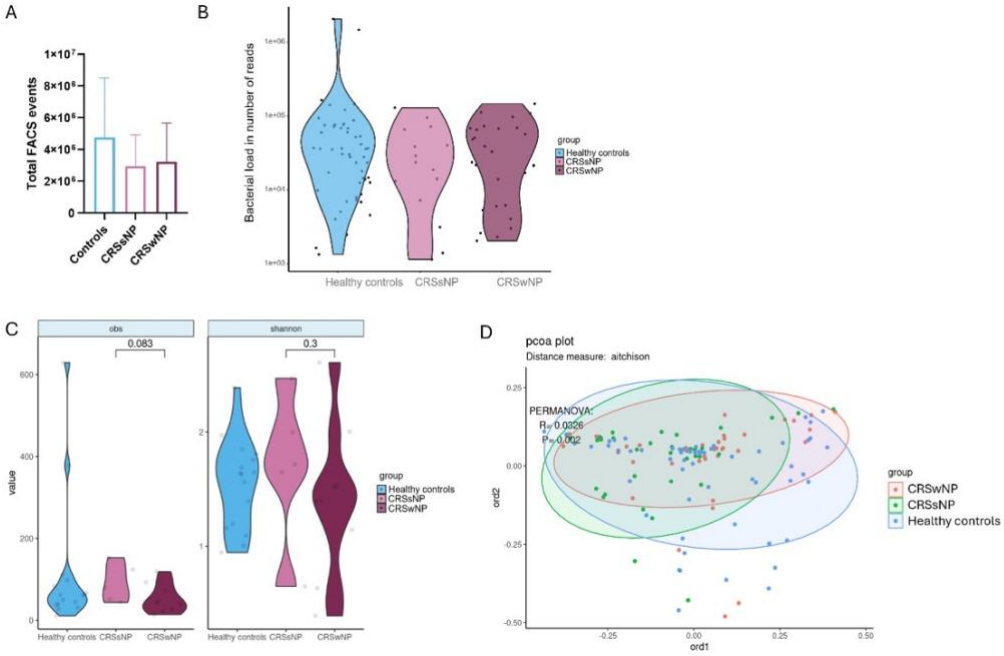

Figure 23. Comparative analysis of microbial diversity in healthy subjects and patients with CRS in the non-sorted samples.
(A) Total bacterial count quantified by number of FACS events. Graph depicts mean ± SD. (B) Bacterial load distribution measured as the number of reads across healthy controls in blue, CRSwNP in pink, CRSsNP in purple. (C) Alpha diversity metrics: observed richness (obs) Shannon diversity index (shannon) across the study groups. (D) Beta diversity analysis visualized using a principal coordinates analysis (PCoA) plot based on Aitchison distance.

When looking at the individual profiles in the non-sorted samples, patients with CRS sometimes seemed to have a dominance of potential pathogenic airway bacteria, such as *Moraxella* or *Staphylococcus*, although our alpha-diversity measures before showed no differences in diversity (Fig 23C). Overall in all study groups, *Corynebacterium* and *Dolosigranulum* were often detected. Figure 24 gives an overview of the most abundant taxa that were sequenced in the non-sorted samples of all subject groups.

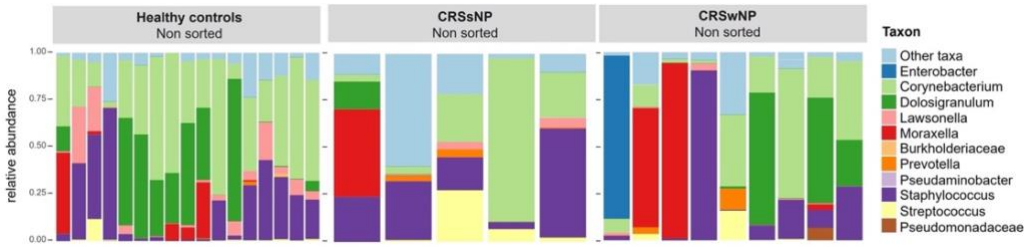

Figure 24. Relative abundance of bacterial taxa across study groups in non-sorted samples.
Each vertical bar represents one individual sample.

4.7. Bacterial s-IgA coating patterns might be different between patients with CRS and healthy controls

Our next step was to study the samples that were sorted into the IgA+ and the IgA– fractions. Regarding bacterial IgA coating, no significant correlations were seen between the percentage of bacteria coated by s-IgA (percentage of IgA^+ FACS events) and nasal s-IgA concentration (data not shown). Only a negative correlation between the total FACS events and the percentage of bacteria coated by s-IgA (percentage of IgA+ FACS events) was found (Figure 25). No significant correlations between the percentage of bacteria coated by s-IgA or nasal s-IgA concentrations and clinical data such as systemic levels of eosinophils or SNOT score (data not shown).

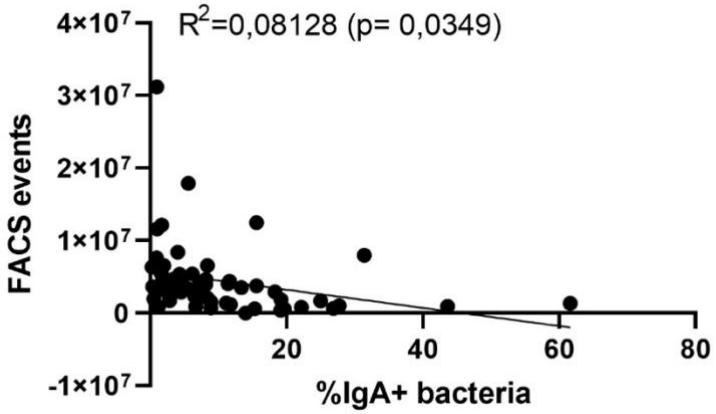

Figure 25. Correlation between total FACS events and the percentage of IgA+ bacteria in the study pooled groups.
Pearson correlation of total FACS events and percentage of bacteria in the IgA+ fraction in pooled groups.

To analyze whether nasal s-IgA targets all nasal bacteria equally in patients and controls, the microbial composition of the s-IgA$^+$ and s-IgA$^-$ samples were determined. Due to low biomass and sample processing, we were only able to sequence both fractions in 17 out of 19 healthy subjects (89%), 9 out of 16 CRSwNP (56%) and 5 out of 14 CRSsNP (36%).

During the IgA-based FACS sorting, we did not observe differences in events within both fractions, although patients with CRS showed a trend towards a higher bacterial density within the IgA+ fraction as measured by the ratio of events in the IgA+ fraction over the events in the IgA– fraction (Figure 26 A).

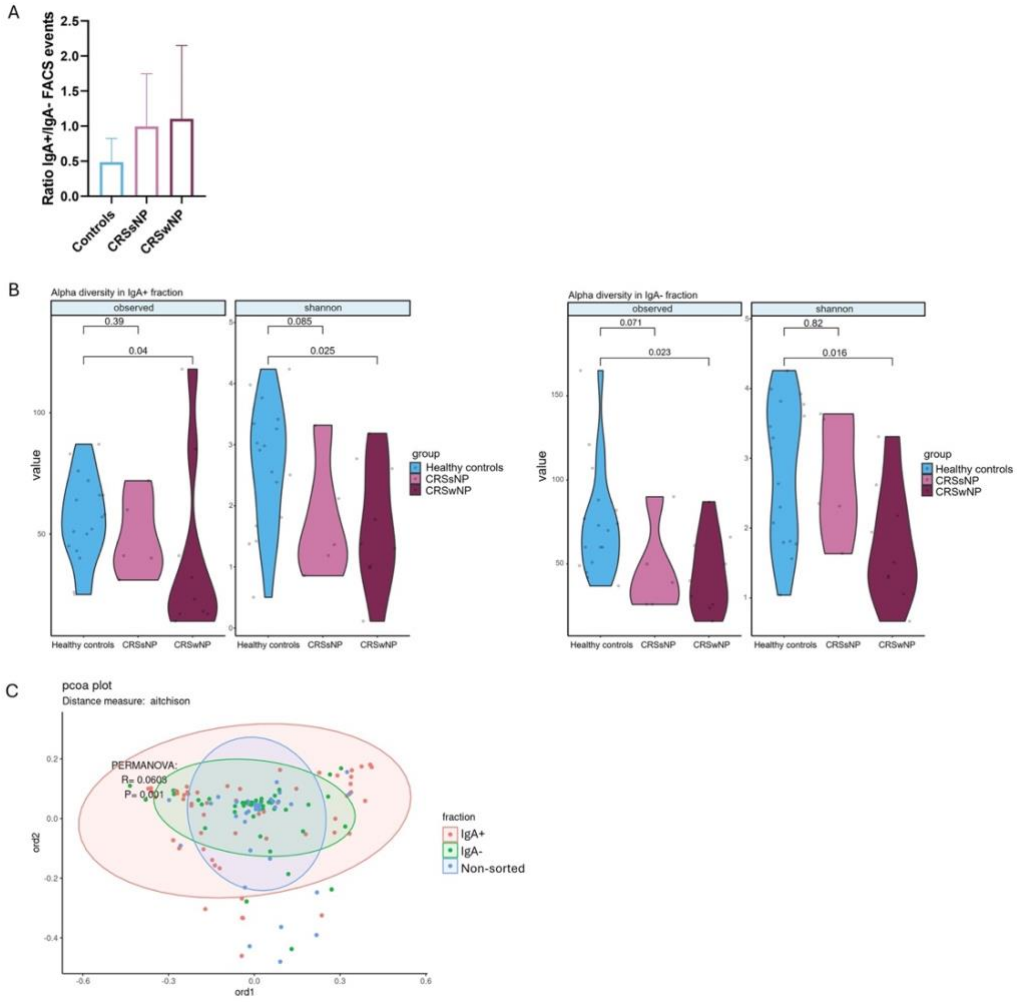

Figure 26. Analysis of bacterial targeting by IgA, alpha and beta diversity in the study groups.

(A) Ratio of IgA+/IgA− FACS events across groups. (B) Alpha diversity metrics: observed richness (obs) Shannon diversity index (shannon) across groups stratified by IgA fractions; left, IgA+ fraction; right, IgA− fraction). (C) Beta diversity visualized using a PCoA plot based on Aitchison distance, stratified by IgA fractions.

The alpha diversity across IgA-fractions was also evaluated. For species richness (observed species index), healthy controls exhibited higher diversity in both IgA+ as well as IgA– fractions compared to patients with CRSwNP (both $p<0,05$) (Figure 26 B). The Shannon diversity index followed the same trend (Figure 26 B). The study of beta diversity across IgA-fractions revealed significant differences in microbial community composition between IgA+ and IgA– fractions and non-sorted samples ($p<0,01$) (Figure 26 C). The IgA+ fraction showed the highest variability and broadest spectrum, while the tighter clustering of the IgA^- fraction and non-sorted samples indicates a more uniform composition (Figure 26 C).

Last, we analyzed and classified the distribution of the bacterial taxa of our sorted samples according to their IgA-binding capacities as expressed by the Kau score. This score is an index to classify the bacterial taxa according to their IgA-coating, being positive when the taxon is targeted by IgA, and negative when the taxon is less or not targeted by IgA (Figure 27). Unfortunately, as mentioned above, the low N per group only allowed us for making some observations and larger sample sizes are needed to draw statistically relevant conclusions.

Overall, in healthy controls, the microbiota displayed a generally wide distribution. Notably, *Moraxella, Veillonella* and *Porphyromonas* were more present in the IgA+ fraction, while *Finegoldia*, *Neisseria*, *Conservatibacter, Rhodobacteraceae* and *Alloprevotella* species looked more present in the IgA– fraction (Figure 27). In patients with CRSsNP, we could observe that taxa like *Alloprevotella*, *Micrococcus*, *Lawsonella* and *Lactobacillus* seemed enriched in the IgA+ fraction, whereas *Finegoldia, Pseudaminobacter, Streptococcus, Anaerococcus*, *Corynebacterium* and *Kocuria* seemed more abundant in the IgA– fraction (Figure 27). In patients with CRSwNP, several taxa such as *Finegoldia, Micrococcus*, *Anaerococcus, Dolosigranulum, Enterobacter, Corynebacterium* and *Lawsonella* appeared more enriched in the IgA+ fraction. However, taxa like *Neisseria*, *Conservatibacter*, *Rhodobacteraceae, Alloprevotella*, *Stenotrophomonas*, *Peptoniphilus_A, Kocuria*, *Gemella* and *Fusobacterium* were most likely found in the IgA– fraction (Figure 27).

We next evaluated the kau scores of both groups of CRS compared to healthy controls. When we zoomed deeper into the IgA-coating of these specific bacterial taxa, we found that certain taxa seem to exhibit different IgA-coating levels between patients with CRS (both groups) and controls. Overall, figure 27 shows a tendency towards higher IgA coating of several taxa that can contain species or strains with pathogenic features (e.g. *Moraxella_A*, *Porphyromonas* and *Neisseriaceae* species) in patients with CRS, especially in CRSwNP, compared to controls. Some taxa like *Neisseriaceae, Micrococcus, Lactobacillus*, *Dolosigranulum* and *Enterobacter*, seem to be more targeted by s-IgA in both groups of patients with CRS compared to healthy subjects. This suggests these bacteria are more frequently recognized and bound by IgA in CRS, implying a shift toward immune activation or loss of tolerance. On the other hand, some pathogens, like *Moraxella_A* and *Leuconostoc,* seem to be less coated by s-IgA in both groups of patients with CRS compared to healthy subjects. This may suggest a tolerogenic or non-reactive immune state.


Mean Kau-Score
<0
>=0
IgA–
Healthy controls
IgA+
IgA–
CRSsNP
IgA+
IgA–
CRSwNP
IgA+
Taxon
Finegoldia
Neisseria
Conservatibacter
Rhodobacteraceae
Neisseriaceae
Alloprevotella
Enterobacteriaceae
Stenotrophomonas
Alcaligenes
Pseudaminobacter
Microbacteriaceae
Streptococcus
Peptoniphilus_A
Mycobacteriaceae
Pseudomonadaceae
Micrococcus
Lactobacillus
Kocuria
Anaerococcus
Dolosigranulum
Gemella
Enterobacter
Blautia_A
Corynebacterium
Fusobacterium
Lawsonella
Staphylococcus
Moraxella_A
Acinetobacter
Veillonella
Prevotella
Leuconostoc
Porphyromonas
Moraxella
-0.5
0.0
0.5
1.0
Kau score

Figure 27. Differential IgA-binding of bacterial taxa across groups based on Kau score.
Boxplots show the distribution of Kau scores for various bacterial taxa in Healthy controls, CRSsNP and CRSwNP. The colors indicate whether the mean score is greater than 0 (TRUE in blue) or not (FALSE in pink). Each boxplot represents the interquartile range (IQR), with the central line denoting the median. Outliers are shown as individual points. Statistical comparisons across study groups by using the non-parametric pairwise Wilcoxon test.

5. Discussion

IgA has been largely neglected when studying the role of the humoral response in CRS, despite its key role in mucosal immunity. The present chapter investigates the role of the pIgR/IgA system in the context of CRS, focusing on its involvement in inflammation in both T2 and non-T2 inflammatory profiles in *in vivo* systems (described in Chapter II and Chapter III) and on the exploration of the interaction between s-IgA and the nasal microbiome in the pathophysiology of CRS. Our results demonstrate a significant reduction in the epithelial pIgR expression in sinus biopsies from patients with CRSwNP and CRSsNP resulting in a significantly reduced epithelial expression of IgA and s-IgA1 levels in nasal secretions in CRSwNP patients. A key role of s-IgA was confirmed by murine models. In WT mice, mice developing eCRS exhibited elevated levels of IgA in NL and serum upon exposure to OVA+SEB, which was not observed in mice with nCRS, where IgA levels remained comparable to controls, irrespective of the bacterial inoculation received. These findings suggest a differential regulation of IgA production depending on the type of inflammatory response. However, the role of s-IgA seems to be different in T2 and non-T2 inflammatory disease, since in genetically modified mice lacking s-IgA, we found that absence of s-IgA had opposing effects, attenuating eosinophilic infiltration in a T2 CRS model, but increasing neutrophilic inflammation in a non-T2 CRS model. The complexity of the IgA function was further confirmed by our observational IgA sequencing experiments, where different microbial IgA-coating patterns seemed to differ between patients with CRS and healthy subjects.

While the role of IgA is well studied in the gut [37-41], very little research has focused on its role in the airways. In our human observational study, we demonstrate a significant reduction in the epithelial pIgR expression in sinus biopsies from patients with CRSwNP and CRSsNP compared to healthy subjects. This is in line with the findings reported by Hupin et al. [25]. Only one other study by a group from Whuhan

investigated pIgR in 36 NP biopsies and found significantly decreased expression levels in CRSwNP compared to healthy controls [26].

The reduced epithelial pIgR expression indicates a defect in the epithelial barrier's ability to transport IgA to the mucosal surface. Consequently, we found lower tissue IgA expression at the epithelial level, in CRS patients. Even though a few publications report on a subsequent increase of IgA and/or IgA-producing B cells accumulation in the submucosa due to a reduced transepithelial transport [20,22–25,28,30] in our hands, IgA accumulation in the submucosa was not different among groups.

At the level of nasal secretions, we did not demonstrate any differences in total s-IgA which is in line with the findings from Hupin and colleagues [25]. Tsybikov et al., however, did find increased levels of s-IgA in both groups of CRS patients compared to controls [31]. The fact that in our samples pIgR expression in submucosal glands was maintained in CRS patients may suggest that glandular IgA secretions might be enough to compensate levels of s-IgA in nasal secretions, as it has been reported to happen in saliva [56]. Also, the phenomenon of leakage could explain the paradox of low pIgR but normal s-IgA levels in CRS groups. Patients with CRS have a dysfunctional epithelial barrier [57], which may allow leakage of immunoglobulins, including s-IgA, from the submucosa into the nasal lumen, potentially normalizing s-IgA levels in secretions despite reduced epithelial transport.

We did detect, however, a reduced presence of the subtype s-IgA1 in the secretions of patients with CRSwNP. This corresponds to the findings by Hupin et al. who reported on a similar trend, although not significant [25]. This might be explained by the fact that glandular IgA that fails to be transported lacks SC, making it less stable and even more vulnerable to degradation in the mucosal environment [9,58,59]. This may explain the finding of a selective reduction in s-IgA1 levels in patients with CRSwNP, since s-IgA1 is *per se* less resistant to enzymatic degradation than s-IgA2 [60] and also, it is the main subtype present in airway secretions [61]. Moreover, it is known that in CRSwNP, an increased protease activity, both from inflammatory cells

and from pathogenic bacteria, exists [62], which may directly contribute to epithelial barrier dysfunction and to the degradation of s-IgA1. Additionally, certain pathogens associated with CRSwNP, such as *S. aureus, N. meningitidis, N. gonorrhoeae, H. influenzae* and *S. pneumoniae*, produce proteases that can cleave the hinge region of IgA1 [63–66], leading to its inactivation and increased susceptibility to mucosal infections and bacterial colonization.

Our reported downregulation of pIgR and subsequent decrease in s-IgA1, might contribute to the inflammatory cycle in CRS, as potential inflammatory triggers may not be neutralized by s-IgA1 [25]. In the lower airways there is also evidence that s-IgA contributes to disease mechanisms or severity. In COPD, pIgR downregulation correlates with worsened airflow limitation and neutrophilic infiltration [67–71]. Opposite to what is observed in CRS, local IgA synthesis is upregulated in lung tissue [72], but in line with our findings, it does not translate into increased concentration of S-IgA in bronchial secretions. Similarly, in asthma, lower s-IgA levels are linked to poorer lung function and increased symptoms [73], with IgA deficiency being associated with allergic diseases [74,75]. Compared to CRS, where local IgA synthesis is upregulated but not translated into increased s-IgA in secretions, COPD and asthma show similar IgA dysfunctions, especially in relation to eosinophil regulation and microbial balance, highlighting IgA as a potential but unproven therapeutic target [67].

However, glandular IgA that fails to be transported will lack the SC, making it less stable and more vulnerable to degradation in the mucosal environment [9,58,59], which may explain the fact that we found a selective reduction in s-IgA1 levels in patients with CRSwNP.

Because our human experiments mainly provided us with observational data in patients with already established diseases, we decided to next study the role of IgA in the development of CRS in *in vivo* mouse models described in Chapters II and III.

Our results demonstrate that in WT mice, induction of eCRS leads to a significant increase in IgA levels in both NL and serum following OVA/SEB treatment, whereas no such variation is observed in WT mice with nCRS. This differential regulation suggests that eosinophilic inflammation may promote a local and systemic boost in IgA production, which was not the case for neutrophilic inflammation.

However, when evaluating the impact of the absence of s-IgA in genetically modified mice lacking s-IgA, things are more complex. In a first model of OVA/SEB-induced eCRS, resembling T2 inflammation in the human sinonasal mucosa, the absence of s-IgA surprisingly decreased mucosal inflammatory features at the level of the paranasal sinuses, including reduced sinus eosinophil influx. To our knowledge, only one other paper investigated OVA-induced eosinophilic airway inflammation in pIgR$^{-/-}$ mice, finding a similarly reduced influx of eosinophils in the airways [76]. This could be explained by the suggested role of s-IgA in recruiting and sustaining eosinophils within the mucosa, as described by Bartemes and colleagues [77]. This would imply that our observed reduced pIgR levels in human eosinophilic CRS tissue might rather be a result of the disease than a contributing factor. The contradictory finding of pIgR$^{-/-}$ mice producing higher serum IgE levels, could be explained by the genetic modification altering systemic IgE levels, as it has been described to happen in the gut [78]. Unfortunately, up till now the role of s-IgA in T2 inflammation in upper respiratory airways remains unexplored and further research is needed to elucidate its impact in allergic inflammation.

Secondly, we tested the role of IgA in a mouse model of pIgR$^{-/-}$ mice with bacterial-induced nCRS that mimics human non-T2 sinonasal inflammation. Interestingly, in this model we found that the absence of s-IgA aggravated neutrophilic inflammation at the level of the sinus mucosa. This finding suggests a critical role of s-IgA in controlling bacterial-induced inflammation in non-T2 CRS. The fact that we found significantly higher mortality in pIgR$^{-/-}$ mice compared to WT, highlights the importance of s-IgA in controlling respiratory infections by respiratory pathogens. Our findings are in line with several other studies that report on higher susceptibility

to bacterial respiratory infections in pIgR-deficient mice [79], or mice treated with anti-IgA [80].

These *in vivo* findings seem to imply that s-IgA plays an important role in CRS development, especially in non-T2 CRS. However, no clear-cut quantitative differences in total s-IgA were found in human CRS secretions. Therefore, we hypothesized that a functional aspect of s-IgA might play a role. One of the key roles of s-IgA that has been studied in the gut, is the control of the local microbiome [37–41]. It plays a crucial role in maintaining gut homeostasis by regulating the composition and function of the gut microbiota. It has been shown in the gut that s-IgA achieves this by binding to several antigens on the surface of bacteria, modulating their interaction with the host and promoting a balanced microbial environment [40]. However, nowadays, it is not clear how s-IgA affects the human nasal microbiome in terms of homeostasis and immunomodulation. Especially, the development of the IgA-SEQ technology has crucially contributed to our knowledge of the role of s-IgA in health and disease and in shaping the microbiome in the gut [38,40,81]. In this technique, bacteria are sorted based on their IgA-coating and then analyzed by metagenomic sequencing [55,82–84]. One recent paper studied the sinonasal bacterial-IgA interaction in healthy controls by applying the IgA-SEQ technology, revealing a highly individualized interaction between s-IgA and the nasal microbiota and suggesting that s-IgA may limit the bacterial capacity to colonize the human nose [85].

To study whether s-IgA targets the microbiome members differently in CRS than in controls, therefore influencing their maintenance and/or effects, we decided to apply the IgA-SEQ technique in our study population. Initial analysis of the microbiome composition in the unsorted samples of our study populations showed no differences in bacterial load between CRS (both CRSwNP and CRSsNP) and healthy controls as measured via observed richness and Shannon diversity. Although beta diversity measures showed that a lot of samples showed overlap, there seemed to be some significant differences in diversity between healthy controls and CRS groups. This

finding is in line with the concept of dysbiosis and corresponds to previous findings in CRS [86]. In particular, the work by De Boeck and colleagues, showed that even without major reductions in alpha diversity, patients with CRS exhibited significant alterations in bacterial community composition [87], suggesting that functional imbalances, rather than a loss of taxa, may contribute to disease pathogenesis.

Unlike what was found in the paper from Amsterdam [85], we did not find a correlation between nasal s-IgA levels and the percentage of IgA^+ bacteria. This contradicts their finding that s-IgA plays a crucial role in regulating nasal microbiota density. It needs to be noted that although significant, their correlations were weak. The reported differences might be due to technical specificities in the protocols followed. Conversely, we saw a similar high individualization of the interaction between s-IgA and nasal bacteria, with no uniform pattern across different species or individuals, especially in healthy controls. When comparing CRS patients with healthy controls, we did not detect any differences in numbers of IgA-coated bacteria, indicating that there are no quantitative implications. Interestingly we did detect a reduced alpha diversity in the IgA+ coated bacteria in CRSwNP, however this was also true for the IgA- fraction. This finding is therefore rather linked to a general dysbiosis than to differences in IgA coating. Interestingly we did detect a reduced alpha diversity in the IgA+ coated bacteria in CRSwNP, however this was also true for the IgA- fraction. This finding is therefore rather linked to a general dysbiosis than to differences in IgA coating. When evaluating the beta diversity across sorted fractions, a significant reduction was found for the non-sorted and the IgA– fraction, with IgA+ fraction being more determinant for the bacterial composition.

Regarding the IgA coating efficiency of the different microbiome members, as determined via Kau scores, we showed that certain taxa seem to be differently coated among patients and controls, although the low number of samples per group prevent us from making conclusions. Overall, CRS groups showed a tendency to have more taxa presenting with positive Kau scores (blue boxes in Figure 27) than healthy controls, indicating broader immune recognition. This might indicate a dysregulated

mucosal immune response in CRS, where commensals may become targets of mucosal immunity.

So far, the question of why some pathogenic species are coated by s-IgA and others aren't, remains unanswered. One of the theories is that it is explained by interspecies competition among bacteria since s-IgA can influence their immune evasion strategies [88]. While s-IgA typically prevents adhesion and promotes bacterial clearance, some pathogens have evolved to make use of this coating as a survival strategy. Another theory is that dysbiosis can lead to increased local IgA production and coating of possible pathogens to potentially control them as suggested in the gut [89]. Future experiments that study differences in virulence factors for bacteria that show altered IgA-coating levels could be very useful in further elucidating our findings. Also, s-IgA binding assays with the withheld bacteria can confirm our findings and provide insight into possible s-IgA defects that lie at the base of the observed data.

However, another speculation is that s-IgA response might be shaped by host-specific factors such as genetics, immune system, and environmental conditions such as inflammation, rather than by the bacterial species' immunogenicity *per se*. Therefore, it is possible that the coating capacities of s-IgA could be altered/deficient in patients with CRS. Interestingly, in patients with CRSwNP, the pathogen *Porphyromonas* seemed less IgA-targeted compared to healthy subjects. For CRSsNP, it was *Moraxella* that showed a lower Kau score than healthy controls. In the latter patient group, we saw similar trends for other pathogens, however the low number of sequenced CRSsNP samples did not allow for powerful statistics, and hence robust conclusions are therefore the main limitation of this study. This low yield is due to the well-known low microbial biomass present in the airways, that in a second step was further reduced by the FACS sorting of our samples. We tried to overcome this phenomenon by harvesting 4 microbial swabs per patient, but even with this technique we only managed to sequence both sorted groups for half of the CRSwNP group and one third of the CRSsNP one. Another limitation is the fact that

we were not able to characterize the bacteria up to the species level and therefore certain species with different pathogenic characteristics (e.g. *S. epidermidis* and *S. aureus*) could not be distinguished by this technique. We sought to address this challenge phenomenon by performing PCR on the microbial samples, but even for this biomass was too low to be detected.

Overall, our IgA-SEQ data seem to be comparable to the work performed by other researchers in the gut [84], where microbes are more abundant and more stable than in the nose [90,89]. In the gut, it is known that s-IgA can both promote and attenuate bacterial colonization, depending on mucus flow rate, disease state and differential adhesion among species [83,92–94]. Palm and colleagues described the potential of IgA-coating to target pathogenic bacteria [83]. Similarly, insights from Shapiro et al. on the role of IgA in IBD provide valuable parallels to CRS. In IBD, certain bacteria associated with inflammation exhibit high IgA-coating, suggesting a critical role in modulating disease progression [95]. However, based on the observations for gastrointestinal s-IgA, this targeting by s-IgA could imply clearance of the microbial species or the promotion of its colonization by enhanced mucus- or epithelial interactions [93]. To conclude, while the nasal microbiome differs from the gut microbiome in composition and complexity, there seems to be some evidence that the principle of IgA-mediated microbial regulation is consistent across mucosal sites.

The strength of this study is the fact that we used a translational way to study the role of IgA/pIgR biology in CRS, which greatly contributes to seeing the broader picture of our findings. While the human data showed that patients with T2 CRSwNP present with reduced levels of epithelial pIgR and subsequent reduced epithelial IgA and s-IgA1, the *in vivo* data implied that s-IgA might contribute to eosinophilic inflammation and pIgR downregulation is probably rather a consequence than a cause of the disease. For non-T2 CRS (mostly CRSsNP), which is more frequently linked to chronic infection, the *in vivo* data confirmed that s-IgA is needed to reduce the chronic inflammatory reaction upon a persistent microbial stimulus. Therefore, the observed pIgR reduction in the human samples might contribute to the disease in

this endotype. The insights provided in this study about the importance of the pIgR/IgA system in CRS pathophysiology are valuable but need further validation. While s-IgA seems to play a role in modulating the microbiota, its function in CRS remains complex, potentially varying between T2 and non-T2 inflammation. To our knowledge, we are the first to apply the IgA-SEQ technology to nasal swabs from patients with CRS and to compare them to healthy subjects, revealing decreased microbial diversity in and differential IgA coating of nasal microbes in patients with CRS compared to healthy controls. The application of IgA-SEQ to nasal microbiome samples provides novel insights into microbial targeting by s-IgA, reinforcing its relevance in CRS. Our findings emphasize the need for future research to explore therapeutic strategies aimed at restoring mucosal immunity, maybe by modulating the microbiome, and addressing the distinct immunological mechanisms underlying different CRS subtypes.

In conclusion, our study investigates the role of s-IgA in CRS, combining *in vitro* and *in vivo* research, focusing on its involvement in inflammation and microbiome interactions. It was found that patients with CRS exhibit reduced expression of the pIgR and IgA in the sinus epithelium, particularly affecting s-IgA1 secretion. Mouse models reveal that the absence of s-IgA reduces eosinophilic inflammation in T2 CRS but exacerbates neutrophilic inflammation in bacterial-induced non-T2 CRS. By applying IgA-SEQ technology, our study identifies altered microbial diversity and differential bacterial IgA-coating in patients with CRS compared to healthy individuals. These findings suggest that not just IgA quantity, but also its functional role in microbial regulation, contributes to CRS pathophysiology, particularly in non-T2 inflammation. Future research should explore therapeutic strategies aimed at restoring mucosal immunity by modulating the microbiome and addressing distinct immunological mechanisms underlying different CRS subtypes.

6. References

1. Momtazmanesh S, Moghaddam SS, Ghamari SH, Rad EM, Rezaei N, Shobeiri P, et al. Global burden of chronic respiratory diseases and risk factors, 1990–2019: an update from the Global Burden of Disease Study 2019. EClinicalMedicine. 2023 May;59:101936.
2. Lourijsen ES, Fokkens WJ, Reitsma S. Direct and indirect costs of adult patients with chronic rhinosinusitis with nasal polyps. Rhinology journal. 2020 May 1;0(0):0–0.
3. Rudmik L. Economics of Chronic Rhinosinusitis. Vol. 17, Current Allergy and Asthma Reports. Current Medicine Group LLC 1; 2017.
4. Fokkens WJ, Lund VJ, Hopkins C, Hellings PW, Kern R, Reitsma S, et al. European Position Paper on Rhinosinusitis and Nasal Polyps 2020. Rhinology journal. 2020 Feb 1;0(0):1–464.
5. Zhang N, Van Zele T, Perez-Novo C, Van Bruaene N, Holtappels G, DeRuyck N, et al. Different types of T-effector cells orchestrate mucosal inflammation in chronic sinus disease. Journal of Allergy and Clinical Immunology. 2008 Nov;122(5):961–8.
6. Cao PP, Li H Bin, Wang BF, Wang S Bin, You XJ, Cui YH, et al. Distinct immunopathologic characteristics of various types of chronic rhinosinusitis in adult Chinese. Journal of Allergy and Clinical Immunology. 2009;124(3).
7. Tomassen P, Vandeplas G, Van Zele T, Cardell LO, Arebro J, Olze H, et al. Inflammatory endotypes of chronic rhinosinusitis based on cluster analysis of biomarkers. Journal of Allergy and Clinical Immunology. 2016 May 1;137(5):1449-1456.e4.
8. Brandtzaeg P. Secretory IgA: Designed for Anti-Microbial Defense. Front Immunol. 2013;4.
9. Phalipon A, Cardona A, Kraehenbuhl JP, Edelman L, Sansonetti PJ, Corthésy B. Secretory Component. Immunity. 2002 Jul;17(1):107–15.
10. Li Y, Jin L, Chen T. The Effects of Secretory IgA in the Mucosal Immune System. Biomed Res Int. 2020 Jan 8;2020:1–6.
11. Chu PG, Arber DA. CD79: A Review. Applied Immunohistochemistry & Molecular Morphology. 2001 Jun;9(2):97–106.
12. Diana J, Moura IC, Vaugier C, Gestin A, Tissandie E, Beaudoin L, et al. Secretory IgA Induces Tolerogenic Dendritic Cells through SIGNR1 Dampening Autoimmunity in Mice. The Journal of Immunology. 2013 Sep 1;191(5):2335–43.
13. Corthésy B. Multi-Faceted Functions of Secretory IgA at Mucosal Surfaces. Front Immunol. 2013;4.
14. Jorgensen GH, Gardulf A, Sigurdsson MI, Sigurdardottir STh, Thorsteinsdottir I, Gudmundsson S, et al. Clinical Symptoms in Adults with Selective IgA Deficiency: A Case-Control Study. J Clin Immunol. 2013 May 7;33(4):742–7.
15. Fadlallah J, El Kafsi H, Sterlin D, Juste C, Parizot C, Dorgham K, et al. Microbial ecology perturbation in human IgA deficiency. Sci Transl Med. 2018 May 2;10(439).
16. Schwitzguébel AJP, Jandus P, Lacroix JS, Seebach JD, Harr T. Immunoglobulin deficiency in patients with chronic rhinosinusitis: Systematic review of the literature and meta-analysis. Journal of Allergy and Clinical Immunology. 2015 Dec;136(6):1523–31.
17. Stevens WW, Peters AT. Immunodeficiency in Chronic Sinusitis: Recognition and Treatment. Am J Rhinol Allergy. 2015 Mar 1;29(2):115–8.
18. Sánchez Montalvo A, Gohy S, Rombaux P, Pilette C, Hox V. The Role of IgA in Chronic Upper Airway Disease: Friend or Foe? Frontiers in Allergy. 2022 Mar 9;3.
19. Aazami H, Seif F, Ghalehbaghi B, Mohebbi A, Ahmadi A, Babaheidarian P, et al. Levels of total IgA and IgA subclasses in the serum of chronic rhinosinusitis patients. Med J Islam Repub Iran. 2018;32(1):1–4.

20. Van Zele T, Gevaert P, Holtappels G, Van Cauwenberge P, Bachert C. Local immunoglobulin production in nasal polyposis is modulated by superantigens. Clinical and Experimental Allergy. 2007 Dec;37(12):1840–7.
21. Lal D, Song L, Brar T, Cope EK, Keim P, Williams S, et al. Antibody responses to the host microbiome in chronic rhinosinusitis. Int Forum Allergy Rhinol. 2023 Aug 1;13(8):1503–10.
22. Aazami H, Seif F, Ghalehbaghi B, Babaheidarian P, Mohebbi A, Ahmadi A, et al. Local eosinophils are associated with increased IgA subclass levels in the sinonasal mucosa of chronic rhinosinusitis with polyp patients. Allergy, Asthma and Clinical Immunology. 2020 Apr 25;16(1).
23. Sokoya M, Ramakrishnan VR, Frank DN, Rahkola J, Getz A, Kingdom TT, et al. Expression of immunoglobulin D is increased in chronic rhinosinusitis. Annals of Allergy, Asthma and Immunology. 2017 Oct 1;119(4):317-323.e1.
24. Kato A, Peters A, Suh L, Carter R, Harris KE, Chandra R, et al. Evidence of a role for B cell-activating factor of the TNF family in the pathogenesis of chronic rhinosinusitis with nasal polyps. Journal of Allergy and Clinical Immunology. 2008;121(6).
25. Hupin C, Rombaux P, Bowen H, Gould H, Lecocq M, Pilette C. Downregulation of polymeric immunoglobulin receptor and secretory IgA antibodies in eosinophilic upper airway diseases. Allergy: European Journal of Allergy and Clinical Immunology. 2013 Dec;68(12):1589–97.
26. Zhang QP, Xiang R, Xu Y, Deng ZF, Kong YG, Chen SM, et al. [Expression and significance of polymeric immunoglobulin receptor in nasal polyps]. Lin Chung Er Bi Yan Hou Tou Jing Wai Ke Za Zhi. 2017 Jan;31(1):43–7.
27. Dilidaer, Zheng Y, Liu Z, Hu X, Zhang J, Hu L, et al. Increased BAFF expression in nasal polyps is associated with local IgE production, Th2 response and concomitant asthma. European Archives of Oto-Rhino-Laryngology. 2017 Apr 1;274(4):1883–90.
28. Sánchez-Segura A, Brieva JA, Rodríguez C. Regulation of immunoglobulin secretion by plasma cells infiltrating nasal polyps. Laryngoscope. 2000;110(7):1183–8.
29. Takeda K, Sakakibara S, Yamashita K, Motooka D, Nakamura S, El Hussien MA, et al. Allergic conversion of protective mucosal immunity against nasal bacteria in patients with chronic rhinosinusitis with nasal polyposis. Journal of Allergy and Clinical Immunology. 2019 Mar 1;143(3):1163-1175.e15.
30. Tan BK, Li QZ, Suh L, Kato A, Conley DB, Chandra RK, et al. Evidence for intranasal antinuclear autoantibodies in patients with chronic rhinosinusitis with nasal polyps. Journal of Allergy and Clinical Immunology. 2011;128(6).
31. Tsybikov NN, Egorova E V., Kuznik BI, Fefelova E V., Magen E. Anticytokine autoantibodies in chronic rhinosinusitis. Allergy Asthma Proc. 2015 Nov 1;36(6):473–80.
32. De Rudder C, Calatayud Arroyo M, Lebeer S, Van de Wiele T. Modelling upper respiratory tract diseases: getting grips on host-microbe interactions in chronic rhinosinusitis using in vitro technologies. Microbiome. 2018 Dec 24;6(1):75.
33. Gómez-García M, Moreno-Jimenez E, Morgado N, García-Sánchez A, Gil-Melcón M, Pérez-Pazos J, et al. The Role of the Gut and Airway Microbiota in Chronic Rhinosinusitis with Nasal Polyps: A Systematic Review. Int J Mol Sci. 2024 Jul 27;25(15):8223.
34. Sun N, Ogulur I, Mitamura Y, Yazici D, Pat Y, Bu X, et al. The epithelial barrier theory and its associated diseases. Allergy. 2024 Dec 7;79(12):3192–237.
35. Losol P, Sokolowska M, Hwang YK, Ogulur I, Mitamura Y, Yazici D, et al. Epithelial Barrier Theory: The Role of Exposome, Microbiome, and Barrier Function in Allergic Diseases. Allergy Asthma Immunol Res. 2023;15(6):705.
36. Peebles AB, Peebles Jr RS. Dysbiosis of the respiratory tract mucosa—how microbial imbalances lead to asthma. Ann Transl Med. 2023 Jan;11(1):1–1.
37. Pietrzak B, Tomela K, Olejnik-Schmidt A, Mackiewicz A, Schmidt M. Secretory IgA in Intestinal Mucosal Secretions as an Adaptive Barrier against Microbial Cells. Int J Mol Sci. 2020 Dec 4;21(23):9254.

38. León ED, Francino MP. Roles of Secretory Immunoglobulin A in Host-Microbiota Interactions in the Gut Ecosystem. Front Microbiol. 2022 Jun 2;13.
39. Pabst O, Slack E. IgA and the intestinal microbiota: the importance of being specific. Mucosal Immunol. 2020 Jan;13(1):12–21.
40. Pabst O, Izcue A. Secretory IgA: controlling the gut microbiota. Nat Rev Gastroenterol Hepatol. 2022 Mar 3;19(3):149–50.
41. Gupta S, Gupta SL, Singh A, Oswal N, Bal V, Rath S, et al. IgA Determines Bacterial Composition in the Gut. Crohns Colitis 360. 2023 Jul 1;5(3).
42. Takeuchi T, Ohno H. IgA in human health and diseases: Potential regulator of commensal microbiota. Front Immunol. 2022 Nov 10;13.
43. Watelet JB, Gevaert P, Holtappels G, Van Cauwenberge P, Bachert C. Collection of nasal secretions for immunological analysis. European Archives of Oto-Rhino-Laryngology. 2004 May 1;261(5):242–6.
44. Scadding G, Hellings P, Alobid I, Bachert C, Fokkens W, van Wijk RG, et al. Diagnostic tools in Rhinology EAACI position paper. Clin Transl Allergy. 2011 Jun 10;1(1):2.
45. Sánchez-Montalvo A, Lecocq M, Bouillet E, Steelant B, Gohy S, Froidure A, et al. Validation and shortcomings of the most common mouse model of chronic rhinosinusitis with nasal polyps. Rhinology Journal. 2024 Mar 1;0(0):0–0.
46. Johansen FE, Pekna M, Norderhaug IN, Haneberg B, Hietala MA, Krajci P, et al. Absence of Epithelial Immunoglobulin a Transport, with Increased Mucosal Leakiness, in Polymeric Immunoglobulin Receptor/Secretory Component–Deficient Mice. J Exp Med. 1999 Oct 4;190(7):915–22.
47. Bankhead P, Loughrey MB, Fernández JA, Dombrowski Y, McArt DG, Dunne PD, et al. QuPath: Open source software for digital pathology image analysis. Sci Rep. 2017 Dec 1;7(1).
48. Marée R, Rollus L, Stévens B, Hoyoux R, Louppe G, Vandaele R, et al. Collaborative analysis of multi-gigapixel imaging data using Cytomine. Bioinformatics. 2016 May 1;32(9):1395–401.
49. Kozich JJ, Westcott SL, Baxter NT, Highlander SK, Schloss PD. Development of a Dual-Index Sequencing Strategy and Curation Pipeline for Analyzing Amplicon Sequence Data on the MiSeq Illumina Sequencing Platform. Appl Environ Microbiol. 2013 Sep;79(17):5112–20.
50. Straub D, Blackwell N, Langarica-Fuentes A, Peltzer A, Nahnsen S, Kleindienst S. Interpretations of Environmental Microbial Community Studies Are Biased by the Selected 16S rRNA (Gene) Amplicon Sequencing Pipeline. Front Microbiol. 2020 Oct 23;11.
51. Parks DH, Chuvochina M, Rinke C, Mussig AJ, Chaumeil PA, Hugenholtz P. GTDB: an ongoing census of bacterial and archaeal diversity through a phylogenetically consistent, rank normalized and complete genome-based taxonomy. Nucleic Acids Res. 2022 Jan 7;50(D1):D785–94.
52. Quast C, Pruesse E, Yilmaz P, Gerken J, Schweer T, Yarza P, et al. The SILVA ribosomal RNA gene database project: improved data processing and web-based tools. Nucleic Acids Res. 2012 Nov 27;41(D1):D590–6.
53. Wittouck S, Rillaer T Van, Smets W, Lebeer S. Tidytacos: An R package for analyses on taxonomic composition of microbial communities. J Open Source Softw. 2025 Jan 31;10(105):6313.
54. Davis NM, Proctor DM, Holmes SP, Relman DA, Callahan BJ. Simple statistical identification and removal of contaminant sequences in marker-gene and metagenomics data. Microbiome. 2018 Dec 17;6(1):226.
55. Jackson MA, Pearson C, Ilott NE, Huus KE, Hegazy AN, Webber J, et al. Accurate identification and quantification of commensal microbiota bound by host immunoglobulins. Microbiome. 2021 Dec 30;9(1):33.
56. Engeland CG, Bosch JA, Rohleder N. Salivary biomarkers in psychoneuroimmunology. Curr Opin Behav Sci. 2019 Aug;28:58–65.

57. Huang Z, Liu J, Sun L, Ong HH, Ye J, Xu Y, et al. Updated epithelial barrier dysfunction in chronic rhinosinusitis: Targeting pathophysiology and treatment response of tight junctions. Allergy. 2024 May 19;79(5):1146–65.
58. Motegi Y, Kita H, Kato M, Morikawa A. Role of Secretory IgA, Secretory Component, and Eosinophils in Mucosal Inflammation [Internet]. Vol. 122, Int Arch Allergy Immunol. 2000. Available from: www.karger.com/journals/iaa
59. Stadtmueller BM, Huey-Tubman KE, López CJ, Yang Z, Hubbell WL, Bjorkman PJ. The structure and dynamics of secretory component and its interactions with polymeric immunoglobulins. Elife. 2016 Mar 4;5.
60. Kerr MA, Loomes LM, Bonner BC, Hutchings AB, Senior BW. Purification and Characterization of Human Serum and Secretory IgAl and lgA2 Using Jacalin. In: Lectin Methods and Protocols. New Jersey: Humana Press; p. 265–78.
61. Kirkeby L, Rasmussen TT, Reinholdt J, Kilian M. Immunoglobulins in Nasal Secretions of Healthy Humans: Structural Integrity of Secretory Immunoglobulin A1 (IgA1) and Occurrence of Neutralizing Antibodies to IgA1 Proteases of Nasal Bacteria. Clinical Diagnostic Laboratory Immunology. 2000 Jan;7(1):31–9.
62. Kato A, Schleimer RP, Bleier BS. Mechanisms and pathogenesis of chronic rhinosinusitis. Journal of Allergy and Clinical Immunology. 2022 May;149(5):1491–503.
63. Prokopenko Y, Zinchenko A, Karlinsky D, Kotelnikova O, Razgulyaeva O, Gordeeva E, et al. Protective Antimicrobial Effect of the Potential Vaccine Created on the Basis of the Structure of the IgA1 Protease from Neisseria meningitidis. Vaccines (Basel). 2024 Nov 30;12(12):1355.
64. Woof JM, Russell MW. Structure and function relationships in IgA. Mucosal Immunol. 2011 Nov;4(6):590–7.
65. Kilian M, Russell MW. Microbial Evasion of IgA Functions. In: Mucosal Immunology. Elsevier; 2005. p. 291–303.
66. Qiu J, Brackee GP, Plaut AG. Analysis of the specificity of bacterial immunoglobulin A (IgA) proteases by a comparative study of ape serum IgAs as substrates. Infect Immun. 1996 Mar;64(3):933–7.
67. Wang X, Zhang J, Wu Y, Xu Y, Zheng J. SIgA in various pulmonary diseases. Eur J Med Res. 2023 Aug 27;28(1):299.
68. PILETTE C, GODDING V, KISS R, DELOS M, VERBEKEN E, DECAESTECKER C, et al. Reduced Epithelial Expression of Secretory Component in Small Airways Correlates with Airflow Obstruction in Chronic Obstructive Pulmonary Disease. Am J Respir Crit Care Med. 2001 Jan 1;163(1):185–94.
69. Polosukhin V V., Cates JM, Lawson WE, Zaynagetdinov R, Milstone AP, Massion PP, et al. Bronchial Secretory Immunoglobulin A Deficiency Correlates With Airway Inflammation and Progression of Chronic Obstructive Pulmonary Disease. Am J Respir Crit Care Med. 2011 Aug 1;184(3):317–27.
70. Polosukhin V V., Richmond BW, Du RH, Cates JM, Wu P, Nian H, et al. Secretory IgA Deficiency in Individual Small Airways Is Associated with Persistent Inflammation and Remodeling. Am J Respir Crit Care Med. 2017 Apr 15;195(8):1010–21.
71. Blackburn JB, Schaff JA, Gutor S, Du RH, Nichols D, Sherrill T, et al. Secretory cells are the primary source of pIgR in small airways. 2021.
72. Ladjemi MZ, Lecocq M, Weynand B, Bowen H, Gould HJ, Van Snick J, et al. Increased IgA production by B-cells in COPD via lung epithelial interleukin-6 and TACI pathways. European Respiratory Journal. 2015 Apr;45(4):980–93.
73. Balzar S, Strand M, Nakano T, Wenzel SE. Subtle Immunodeficiency in Severe Asthma: IgA and IgG₂ Correlate with Lung Function and Symptoms. Int Arch Allergy Immunol. 2006;140(2):96–102.

74. Shkalim V, Monselize Y, Segal N, Zan-Bar I, Hoffer V, Garty BZ. Selective IgA Deficiency in Children in Israel. J Clin Immunol. 2010 Sep 23;30(5):761–5.
75. Abo Ali FH, Mahmoud NE, El-Sayed AYM, Abdelmaksoud MF, Shata AK, Fouad SH. Selective IgA Deficiency a Probable Risk of Recurrent Chest Infections in Asthmatics. J Asthma Allergy. 2021 Nov;Volume 14:1323–33.
76. Smits HH, Gloudemans AK, van Nimwegen M, Willart MA, Soullié T, Muskens F, et al. Cholera toxin B suppresses allergic inflammation through induction of secretory IgA. Mucosal Immunol. 2009 Jul;2(4):331–9.
77. Bartemes KR, Cooper KM, Drain KL, Kita H. Secretory IgA induces antigen-independent eosinophil survival and cytokine production without inducing effector functions. Journal of Allergy and Clinical Immunology. 2005 Oct;116(4):827–35.
78. Shimada S, Kawaguchi-Miyashita M, Kushiro A, Sato T, Nanno M, Sako T, et al. Generation of polymeric immunoglobulin receptor-deficient mouse with marked reduction of secretory IgA. J Immunol. 1999 Nov 15;163(10):5367–73.
79. Richmond BW, Du RH, Han W, Benjamin JT, van der Meer R, Gleaves L, et al. Bacterial-derived Neutrophilic Inflammation Drives Lung Remodeling in a Mouse Model of Chronic Obstructive Pulmonary Disease. Am J Respir Cell Mol Biol. 2018 Jun;58(6):736–44.
80. Renegar KB, Small PA. Immunoglobulin A mediation of murine nasal anti-influenza virus immunity. J Virol. 1991 Apr;65(4):2146–8.
81. Yang Y, Palm NW. Immunoglobulin A and the microbiome. Curr Opin Microbiol. 2020 Aug;56:89–96.
82. Kau AL, Planer JD, Liu J, Rao S, Yatsunenko T, Trehan I, et al. Functional characterization of IgA-targeted bacterial taxa from undernourished Malawian children that produce diet-dependent enteropathy. Sci Transl Med. 2015 Feb 25;7(276).
83. Palm NW, de Zoete MR, Cullen TW, Barry NA, Stefanowski J, Hao L, et al. Immunoglobulin A Coating Identifies Colitogenic Bacteria in Inflammatory Bowel Disease. Cell. 2014 Aug;158(5):1000–10.
84. DuPont HL, Jiang ZD, Alexander AS, DuPont AW, Brown EL. Intestinal IgA-Coated Bacteria in Healthy- and Altered-Microbiomes (Dysbiosis) and Predictive Value in Successful Fecal Microbiota Transplantation. Microorganisms. 2022 Dec 29;11(1):93.
85. van Dalen R, Elsherbini AMA, Harms M, Alber S, Stemmler R, Peschel A. Secretory IgA impacts the microbiota density in the human nose. Microbiome. 2023 Oct 21;11(1):233.
86. Fischer JL, Lee JT. Update on the Role of the Microbiome in Chronic Rhinosinusitis. Curr Treat Options Allergy. 2024 May 4;11(2):17–33.
87. De Boeck, I. et al. Anterior Nares Diversity and Pathobionts Represent Sinus Microbiome in Chronic Rhinosinusitis. mSphere 4, (2019).
88. Maisetta G, Batoni G. Editorial: Interspecies Interactions: Effects on Virulence and Antimicrobial Susceptibility of Bacterial and Fungal Pathogens. Front Microbiol. 2020 Aug 26;11.
89. Liu CM, Price LB, Hungate BA, Abraham AG, Larsen LA, Christensen K, et al. Staphylococcus aureus and the ecology of the nasal microbiome. Sci Adv. 2015 Jun 5;1(5).
90. Zhou X, Shen X, Johnson JS, Spakowicz DJ, Agnello M, Zhou W, et al. Longitudinal profiling of the microbiome at four body sites reveals core stability and individualized dynamics during health and disease. Cell Host Microbe. 2024 Apr;32(4):506-526.e9.
91. Tan X, Liu H, Qiu W, Li Z, Ge S, Luo Y, et al. The nasal microbiota is a potential diagnostic biomarker for sepsis in critical care units. Microbiol Spectr. 2024 Jul 2;12(7).
92. Hoces D, Arnoldini M, Diard M, Loverdo C, Slack E. Growing, evolving and sticking in a flowing environment: understanding IgA interactions with bacteria in the gut. Immunology. 2020 Jan 27;159(1):52–62.
93. McLoughlin K, Schluter J, Rakoff-Nahoum S, Smith AL, Foster KR. Host Selection of Microbiota via Differential Adhesion. Cell Host Microbe. 2016 Apr;19(4):550–9.

94. Donaldson GP, Ladinsky MS, Yu KB, Sanders JG, Yoo BB, Chou WC, et al. Gut microbiota utilize immunoglobulin A for mucosal colonization. Science (1979). 2018 May 18;360(6390):795–800.
95. Shapiro JM, de Zoete MR, Palm NW, Laenen Y, Bright R, Mallette M, et al. Immunoglobulin A Targets a Unique Subset of the Microbiota in Inflammatory Bowel Disease. Cell Host Microbe. 2021 Jan 13;29(1):83-93.e3.

Chapter V – General discussion and future research perspectives

1. General discussion

The nasal mucosa, along with its immune system, serves as the body's first line of defense in the airways against inhaled particles and agents [1]. When the epithelial barrier in the airways is triggered by environmental or microbiota-derived antigens, inflammation can arise giving rise to rhinitis or rhinosinusitis [2].

In the most recent guidelines, chronic rhinosinusitis (CRS) is classified into two main inflammatory profiles: T2 and non-T2 [3]. In western countries, T2 inflammation is frequently associated with NP (CRSwNP), characterized by eosinophil activation and elevated IgE, IL-4, IL-5, and IL-13. These patients often suffer from concomitant allergies, asthma, or aspirin-exacerbated respiratory disease (AERD). Non-T2 inflammation (commonly CRSsNP in Western countries) involves Th1/Th17/Th22 responses, increased IFNγ, and neutrophil activation increased levels of IFNγ and activated neutrophils are found and often no NP are visualized in the nasal cavities and are often linked to bacterial infections, environmental irritants and smoking [3-6].

The host must protect the airways from potential harmful inhaled agents such as pathogens, allergens and irritants and maintain the balance of the local microbiota in the nose to prevent chronic infection. Moreover, it must maintain the balance between local colonizing microbiota and the risk of chronic presence of opportunistic pathogens in the nose. Several mechanisms exist to achieve this, with the production of s-IgA [7] as a key element. While s-IgA is well studied in the gut [8-14], hardly anything is known about the role of s-IgA in the respiratory airways. Also in the lower airways, several studies have shown abnormalities in the IgA-pathways in asthma and COPD [15,16]. Apart from that, most of the knowledge about the role of s-IgA in the nasal mucosa comes from individuals with SIgAD presenting with more recurrent allergy, respiratory infections and CRS [17-20] among others.

This dissertation aimed at investigating the potential role that s-IgA might play in disease development or modulation of CRS. We presented several findings that, to our belief, contribute to a better understanding of the role of this key molecule in mucosal defense and in CRS. Yet, many questions remain unanswered, and this work has raised several new ones.

In a first step, we studied human tissue to search for observed differences in IgA biology between patients with CRS and healthy controls. Interestingly, we found decreased expression levels of the transepithelial IgA receptor pIgR in both phenotypes of CRS compared to controls. The reduced epithelial pIgR expression indicates a defect in the epithelial barrier's ability to transport IgA to the mucosal surface. In our study population this led to a decreased s-IgA1 release in nasal secretions, but not s-IgA2 nor total levels of s-IgA. Epithelial barrier dysfunction in CRS is known to lead to increased barrier permeability [21]. This compromised barrier may allow leakage of immunoglobulins, including IgA, from the submucosa into the nasal lumen, potentially normalizing IgA levels in secretions despite reduced epithelial transport. This phenomenon of leakage could explain the paradox of low pIgR expression but normal s-IgA levels in our CRS groups. Also, the fact that we did not find an accumulation of subepithelial IgA in our patients with CRS, pleads for this explanation. Submucosal IgA that fails to be transported lacks the SC, making it less stable and more vulnerable to degradation in the mucosal environment [22-24]. Additionally, the fact that a similar pIgR expression in submucosal glands is maintained across study groups may suggest that glandular IgA secretions might be enough to compensate the levels of s-IgA in nasal secretions, as it has been reported to happen in saliva [25].

The specific downregulation of s-IgA1 found might be explained by the fact that it is the immunoglobulin subtype that is the most sensitive to proteolytic breakdown. It is known that in CRSwNP there is an increased protease activity, both from inflammatory cells and from pathogenic bacteria [26], which may directly contribute to both epithelial barrier dysfunction as well as to the degradation of s-IgA1.

Additionally, certain pathogens associated with CRSwNP, such as *S. aureus, N. meningitidis, N. gonorrhoeae, H. influenzae* and *S. pneumoniae*, produce proteases that can cleave the hinge region of IgA1 [27-30]. This is particularly important, as s-IgA1 is the main subtype produced in the respiratory tract [31]. On the other hand, s-IgA2, which is more resistant to proteases, is normally more abundant in other mucosal surfaces, such as the gastrointestinal tract, where bacterial load is heavier and more complex than in the airways [30,32,33]. Therefore, according to our findings, s-IgA1 would be more prone to proteolytic breakdown in nasal secretions of patients with CRSwNP, importantly interfering with the neutralization of pathogens as the main source of s-IgA in the nasal mucosa, leaving it more vulnerable to microbial invasion and persistent inflammation.

We therefore hypothesize that the downregulation of s-IgA1 in CRSwNP may exacerbate the inflammatory cycle in CRS, as potential inflammatory triggers may not be adequately neutralized by s-IgA1 [34]. Whether these reduced levels are rather a cause or consequence of the disease development, therefore remains unanswered by these experiments.

On another note, the link between upper and lower airway diseases is well established, with overlapping inflammatory mechanisms observed in CRS and lung diseases such as asthma and chronic obstructive pulmonary disease (COPD), supporting the concept of 'united airway disease' [35].

In COPD, reduced serum IgA levels and downregulation of pIgR expression in the bronchial epithelium correlate with worse airflow limitation, neutrophilic infiltration, and increased risk of exacerbations [36,37]. Similarly, in CRSsNP, where neutrophilic inflammation dominates, s-IgA1 degradation may contribute to epithelial barrier dysfunction and persistent inflammation, mirroring COPD-associated defects in mucosal immunity [38-41]. The proteolytic degradation of SC and s-IgA1 by neutrophil-derived enzymes in COPD [41] aligns with the protease activity observed in CRSsNP. Opposite to what is observed in patients with CRS, local IgA

synthesis is upregulated in lung tissue [42], but like our findings, it does not translate into increased concentration of S-IgA in bronchial secretions. Conversely, in asthma and CRSwNP, where T2 inflammation predominates, despite increased local IgA synthesis in asthma, no such increase has been observed in CRS. Instead, s-IgA1 degradation in CRSwNP may result from increased proteolytic activity, preventing its accumulation in nasal secretions. In asthma, lower serum IgA levels correlate with worse lung function and exacerbations, while s-IgA has been linked to eosinophil activation [43]. This is like findings in CRSwNP, where eosinophilic inflammation and increased proteolytic activity may drive s-IgA1 degradation, impairing its protective function in mucosal immunity. Moreover, IgA's dual role in both immune defense and immune regulation is evident across airway diseases. While low s-IgA levels in both asthma and COPD correlate with increased susceptibility to infections, its ability to activate eosinophils and basophils in T2 inflammatory environments suggests a complex role in allergic responses [44]. Despite its protective role on infectious, allergic and autoimmune diseases, s-IgA could can also have negative effects such as perpetuating allergic reactions and exacerbations in asthma due to its known function as eosinophil and basophil activator, although it may protect versus parasitic infestations [45,46]. While s-IgA could serve as a potential target for the treatment of lung diseases, there is lack of evidence at both preclinical and clinical levels on whether s-IgA can provide benefits for patients with airway diseases.

Nowadays, investigation of the pathophysiology of CRS is limited due to high interindividual variability, low representative tissue samples, and low experimental reproducibility because of the different *ex vivo* conditions. Moreover, the variability among subjects in etiology, microbiome composition, genetics, extent of inflammation, and response to microbes make human research even more complicated. In recent years, murine models emerged as a potential tool to study immunological pathways in respiratory diseases. Although differences exist between humans and mice, their organization and immunological responses of the upper airway are comparable [47-49]. For this reason, we sought to study the role of s-IgA by

using murine models of CRS. Because of the important differences between the different CRS endotypes, we wanted to study its role in each of the endotypes and therefore we developed two different mouse models.

In the first part of this thesis, we aimed at implementing a mouse model of T2 CRS. In the past decades, a mouse model showing eosinophilic infiltration, goblet cell hyperplasia, epithelial thickness and NP-like lesions had become more and more used and accepted among upper airway research groups. It was based on an intra-peritoneal sensitization of mice with the experimental allergen OVA, followed by nasal challenges with OVA to induce an allergic inflammation in the upper airways and, at a later stage, coadministration of nasal challenges with SEB [50]. During the process of implementation and development of this model in our lab, we ran into certain inconsistencies that could lead to misinterpretation of results by other research groups. In chapter 2 of this thesis, we critically evaluated this (by now frequently used) OVA+SEB mouse model [51]. While the model successfully mimicked some features of human T2 inflammation, including eosinophilic infiltration, goblet cell hyperplasia, and subepithelial fibrosis, it did not replicate the formation of macroscopic polyps—arguably the most defining feature of the human disease. This limitation challenges the model's applicability in studying key mechanisms underlying NP development. Another limitation was the fact that no significant differences in inflammatory or structural changes were found between mice treated with OVA alone and those treated with OVA+SEB. This raises questions about the added value of SEB in this context and suggests the model may represent severe allergic rhinitis or CCAD rather than eCRSwNP. Finally, we found that the model did not show a lack of tight junction disruption that is seen in human CRSwNP. Since this epithelial barrier dysfunction is thought to play a pivotal role in disease progression and NP formation, this might be an explanation of the shortcomings of the model. Taken together, our findings highlight that while the OVA+SEB model is useful for studying T2 inflammation in general, it has its limitations as a reliable representation of human CRSwNP.

For our study of IgA in CRS, we also wanted to use a mouse model of non-eosinophilic non-T2 CRS. When looking into literature, we found only two models that were published reporting on a non-T2 CRS mouse model. We tested a first model that was once described by a Chinese group and used chronic exposure to LPS [52], however, this model was not reproducible in our hands. Then we moved to a second model of non-eosinophilic CRS that was described by Jacob and colleagues [53] and repeated by Wang et al. [54]. This model was based on the combination of the introduction of a bacterial source in the nose with a blockage of the sinus outflow tract, mimicking the presumed human situation in the majority of non-eosinophilic CRS [54]. It was based on a surgical procedure during which a pre-cut to size nasal tampon soaked with *a* bacterial solution was inserted in the nasal cavity of mice, remaining *in situ* until completion of the model. We adapted this protocol to our needs and, in chapters 3 and 4, we describe the development and validation of a reproducible mouse model of non-T2 nCRS. During our pilot experiences, we determined the ideal location of the nasal tampon to avoid respiratory distress but induce sinus inflammation. As we did in our eCRS mouse model, we tried to standardize our read-out of murine sinus inflammation and focused on the mean values of 3 fixed areas of the maxillary sinuses, which were in all cases at a distance from the inserted nasal tampon. The challenging surgical technique, involving the insertion of a bacterial-inoculated nasal tampon into the nasal cavity, effectively induced a local inflammation at the sinonasal mucosa. It led to epithelial hyperplasia, subepithelial fibrosis and neutrophilic infiltration observed in response to inoculation with *S. aureus* and *P. aeruginosa*, successfully recapitulating hallmark features of human nCRS. In contrast, *S. pneumoniae* elicited a less potent inflammatory response, possibly due to differences in biofilm formation capacities and bacterial clearance mechanisms [55-58]. Additionally, *S. pneumoniae* and *P. aeruginosa* demonstrated a high mortality rate, complicating the use of these pathogens. These findings validated the importance of specific bacterial strains in modulating immune responses, with *S. aureus* emerging as a preferred pathogen for

inducing robust inflammation with manageable postoperative outcomes. Furthermore, the introduction of innovative methodologies, such as cytospin analysis for NL fluid, provided new tools for quantifying neutrophilic inflammation. Our detailed protocol ensures reproducibility, overcoming major challenges such as positioning the nasal tampon to minimize mortality while achieving consistent inflammatory outcomes. We believe this work provides a critical advancement to the field of CRS research, where such a validated model was lacking. Addressing the remaining limitations and exploring the full potential of this model should be one of the main focuses of future research. Testing other clinically relevant bacterial strains or polymicrobial infections could enhance the model's versatility and relevance to human disease. The model's adaptability also presents opportunities to explore additional bacterial species or polymicrobial infections, shedding light on the diverse microbial contributions to non-eosinophilic CRS. Another critical avenue is leveraging the model to test the efficacy of existing and novel therapies. Antibiotics, anti-inflammatory agents, and microbiome-modulating treatments could be evaluated for their ability to mitigate inflammation and prevent tissue damage. Additionally, the model offers a platform to investigate the interplay between the sinonasal epithelium and bacterial biofilms, with potential implications for understanding barrier dysfunction in CRS. Last, this model could facilitate the development of diagnostic tools and the identification of novel biomarkers for non-eosinophilic CRS, helping in the stratification of patients and the personalization of treatment approaches. Its applicability to a broad range of research questions makes it a valuable resource for unraveling the complex pathophysiology of non-eosinophilic CRS and improving outcomes for affected patients.

In Chapter IV, we used these established mouse models to study our hypothesis that the absence of s-IgA leads to an exacerbation of sinus inflammation in CRS. Interestingly, the use of murine models lacking s-IgA, through genetic deletion of the pIgR, revealed differential roles of s-IgA in the pathophysiology of T2 and non-T2 CRS. Although $pIgR^{-/-}$ mice with T2 eCRS produced higher systemic IgE levels,

the absence of s-IgA protected the mice from epithelial hyperplasia and eosinophilic infiltration. We found that similar findings were reported by Smits and colleagues [59] in the only other publication investigating pIgR deficiency in the context of eosinophilic airway disease, also reporting lower eosinophil levels in the lungs of OVA-treated mice lacking s-IgA compared to their WT peers. These findings suggest a deleterious effect of s-IgA on T2-driven inflammation and a possible explanation for this lies in its role in eosinophil activation and immune modulation. S-IgA can enhance eosinophil survival and degranulation via FcαRI (CD89) [23,43,60,61], and therefore it could potentially sustain T2 inflammation in CRSwNP. Also, while typically essential for mucosal defense, excessive s-IgA immune complex formation in CRSwNP might impair pathogen clearance, leading to prolonged inflammation [15,62]. This could explain why pIgR-deficient mice, despite elevated systemic IgE levels, showed reduced eosinophilic infiltration and epithelial hyperplasia. Conversely, in non-T2 bacterial-induced nCRS, our hypothesis held true. Here the absence of s-IgA worsened inflammation *in vivo*, as evidenced by increased neutrophilic infiltration and epithelial thickening in response to bacterial pathogens such as *S. aureus* and *P. aeruginosa*. The pronounced impact of *P. aeruginosa* in pIgR-deficient mice leading to a significant mortality rate in knockout mice, highlighted the importance of s-IgA in mitigating acute bacterial infection. Our findings are in line with similar investigations reporting higher susceptibility of pIgR-deficient mice to respiratory infections [63-66].

Because of the finding that s-IgA seems to exert its most important role in dealing with bacterial-induced inflammation, we decided to focus on the role of s-IgA in controlling the nasal microbiome. Regarding the interaction of s-IgA with the microbiome, a lot of research has been carried out in the intestinal mucosa [8,9,13,67,68]. In the gut, s-IgA is known to have specific and non-specific properties, depending on how it is generated. Through T cell-dependent pathways, s-IgA undergoes affinity maturation and can specifically target commensal or pathogenic microbes [69,70]. However, a significant portion of s-IgA is produced via T cell-independent

mechanisms, leading to broader, polyreactive binding to conserved microbial components such as polysaccharides, lipopolysaccharides (LPS), peptidoglycan and flagellin [69,71]. In the gut, polyreactive s-IgA predominates under steady-state conditions. It helps to maintain mucosal homeostasis by preventing bacterial overgrowth and promoting immune exclusion [69,70]. At the same time, T cell-dependent responses can drive the production of highly specific, high-affinity IgA that targets particular microbial species when necessary [69,72]. Although the nasal mucosa is less extensively studied than the gut, similar dynamics are thought to exist. Both polyreactive and antigen-specific sIgA responses are suggested to coexist in the upper airways, contributing to the balance between immune tolerance to commensals and defense against pathogens [7]. In summary, s-IgA represents a dynamic spectrum between broad, low-affinity binding and targeted, high-affinity immune exclusion, depending on the nature of antigen exposure and the immunological context.

Therefore, we know that s-IgA plays a crucial role in gut homeostasis by preventing pathogen adhesion, neutralizing toxins and shaping the microbiota. It is believed to promote the retention of beneficial bacteria while preventing dysbiosis, partially through its polyreactivity and ability to modulate bacterial gene expression. Morevoer, s-IgA deficiency leads to microbiota alterations, highlighting its role in maintaining a balanced microbial ecosystem [13,73,74]. However, hardly anything is known about the role of s-IgA in the airways, probably because the nasal microbiome is lower in density, diversity and complexity compared to the gut [75].

Especially, the development of the IgA-SEQ technology, in which bacteria are sorted based on their IgA-coating and then analyzed by metagenomic sequencing [76-79], has contributed substantially to our knowledge of the role of s-IgA in shaping the microbiome in the gut [8,13,73,78]. Up till now, only one publication has applied the IgA-SEQ technology in nasal swabs from healthy volunteers, revealing differential coating of certain nasal microbial members by s-IgA [80]. It suggests that s-IgA might

play a role in regulating nasal microbiota density, with higher s-IgA levels correlating with reduced bacterial colonization. Interestingly, the interaction between s-IgA and nasal bacteria seemed highly individualized, with no uniform pattern across different species or individuals.

To our knowledge, we are the first to apply IgA-SEQ on nasal microbiome samples from patients with CRS to study the interaction of s-IgA with nasal microbes in comparison with healthy subjects. However, the main limitation is that we ended up with a low number of samples per group, preventing us from stating conclusions and only allowing us to point some observations. Our IgA-SEQ approach did not show a correlation between s-IgA and bacterial density, but we did confirm the high variability in IgA coating patterns among individuals and among taxa and altered diversity in CRS compared to healthy individuals. Analysis of IgA coating patterns of nasal bacteria indicated some differences between patients with CRS and healthy controls. Our data supports previous findings reporting that CRS is associated with dysbiosis, characterized by general reduced microbial diversity and overrepresentation of pathogenic species [80-83]. The importance of nasal microbiome composition and its interaction with the host immune system is increasingly recognized in CRS pathophysiology. Dysbiosis likely disrupts the epithelial barrier and contributes to chronic inflammation by facilitating pathogen overgrowth and altering host-microbe interactions [84,85]. The differential coating by s-IgA could indicate that certain pathogens can prevent IgA-targeting, escaping from its control and neutralizing function or that IgA from patients is defective against certain pathogens.

We wondered why s-IgA might target differently these pathogens. Van Dalen and colleagues, who applied for the first time IgA-SEQ technology to nasal swabs from healthy volunteers [80], speculated that s-IgA response might be shaped by host-specific factors such as genetics, immune system, and environmental conditions rather than by the bacterial species' immunogenicity *per se*. Additionally, s-IgA

levels might be influenced by bacterial colonization, with higher deposition observed in colonized individuals due to continuous immune stimulation in their study [80]. This further raises the question of whether therapeutic interventions in CRS could influence IgA-coating patterns, potentially altering microbial interactions and disease progression. Shapiro el al. showed in patients with IBD, that biologic and immunomodulatory treatments significantly impact IgA-coating profiles, while antibiotics and steroids exert minimal effects [86], probably due to the superficial level at which these anti-inflammatory medications attenuate the immune reaction in IBD [87]. Future research should explore whether biologic or immunomodulatory treatments could similarly alter IgA dynamics in CRS, potentially restoring microbial balance and improving disease outcomes.

Generally, while the nasal microbiome differs from the gut microbiome in composition and complexity, there seems to be some evidence that the principle of IgA-mediated microbial regulation is consistent across mucosal sites. However, our approach has some technical limitations. Our low number of samples per group, due to low biomass that can be collected from nasal swabs and sample processing, and the fact that we could not distinguish among bacterial species, led us to observe minor differences across our groups and prevented us from making robust conclusions. Future studies are needed and should focus on larger patient cohorts or higher bacterial yields to elucidate the long-term effects of s-IgA dysfunction in CRS pathophysiology.

Overall, we believe that the strength of this dissertation lies in its translational approach to study the role of IgA/pIgR biology in CRS, allowing for a comprehensive understanding of its implications. While the human data showed that patients with T2 CRSwNP present with reduced levels of epithelial pIgR and subsequent reduced epithelial IgA and s-IgA1, the *in vivo* data implied that s-IgA might contribute to eosinophilic inflammation and pIgR downregulation is probably rather a consequence than a cause of the disease. For non-T2 CRS (mostly

corresponding to patients with CRSsNP), which is more frequently linked to chronic infection, the *in vivo* data confirmed that s-IgA is needed to a reduce the chronic neutrophilic reaction upon a persistent microbial stimulus. This suggests that the observed pIgR reduction in human samples could contribute to disease progression in this endotype. These findings provide valuable insights into the importance of the pIgR/IgA system in CRS pathophysiology, although further validation is required. While s-IgA appears to influence the microbiota regulation, its role in CRS remains complex and may differ between T2 and non-T2 inflammation. The application of IgA-SEQ to nasal microbiome samples offers novel perspectives on microbial targeting by s-IgA, reinforcing its significance in CRS.

Our findings highlight the need for future research to explore therapeutic strategies aimed at restoring mucosal immunity, potentially through microbiome modulation, and addressing the distinct immunological mechanisms underlying different CRS subtypes. Additionally, interventions to counteract dysbiosis, such as probiotics, microbial transplantation or microbiome-targeted therapies, could complement existing treatments for CRS by reducing dysbiosis and promoting immune tolerance. Given the heterogeneity of CRS, stratifying patients based on their inflammatory profile (T2 vs non-T2) and microbiome composition may enable personalized treatment approaches. Longitudinal studies investigating the impact of microbiome-targeted therapies and interventions to enhance mucosal immunity are needed. Additionally, exploring the interplay between s-IgA and specific bacterial species, including their role in biofilm formation, may provide novel insights into CRS pathophysiology.

To conclude this section, we would like to highlight some of the major gaps that remain in CRS research.

One of the most challenging gaps in the field is the limited understanding of the mechanisms driving non-T2 inflammation, which remain poorly characterized and currently especially lacks targeted therapeutic options.

Additionally, a deeper understanding is needed of how acute inflammation transitions into chronic disease, particularly regarding the role of epithelial barrier dysfunction and mucosal immune responses in initiating and perpetuating inflammation.

Current patient stratification is still limited, largely due to the absence of reliable biomarkers capable of predicting treatment response or disease progression.

Finally, regional and ethnic differences, such as the higher prevalence of neutrophilic CRSwNP observed in Asian populations, further emphasize the need for more diverse, geographically adjusted research efforts to fully address the complexity and variability of CRS.

2. Future research perspectives

This dissertation paves the way to several perspectives in the field of CRS research and the study of the role of IgA. Below, we summarize the current ongoing work and the proposed approaches to advance in our understanding of CRS pathogenesis.

a) One priority may be extending research on the specific functions of s-IgA1 versus s-IgA2 in mucosal immunity and inflammation. Understanding how these subtypes interact with the sinonasal microbiome and the immune system might reveal novel therapeutic targets. These two IgA subtypes differ in their susceptibility to bacterial IgA1 proteases, with s-IgA1 being more vulnerable, particularly to cleavage by pathogens like *Haemophilus influenzae* and *Streptococcus pneumoniae*. In contrast, s-IgA2, with its protease-resistant structure, may offer more stable immune defense [32]. An altered s-IgA1/s-IgA2 ratio in CRS could reflect disruptions in immune homeostasis and microbial composition. Future research should examine how these subtypes interact with the sinonasal microbiome, influence epithelial immunity and contribute to inflammatory processes in CRS. Profiling their distribution across CRS endotypes and investigating their impact on bacterial recognition could provide insights into disease mechanisms.

b) Secondly, following our IgAseq experiments, future experiments should investigate virulence factors in bacteria with altered IgA-coating levels, as these may play a key role in immune evasion and microbial persistence. Comparative transcriptomic and proteomic analyses could identify key virulent factors that may be differentially expressed in IgA coated and non-coated bacteria. Functional assays, including phagocytosis and/or intracellular survival or immune evasion, would clarify whether IgA binding enhances immune resistance. Understanding how certain specific bacterial properties, such as

biofilm formation, protease production or immune modulation**,** influence IgA binding may provide deeper insights into host-microbe interactions in CRS. This could help to identify bacterial mechanisms driving inflammation and dysbiosis, potentially leading to targeted therapies aimed at restoring immune balance.

c) Building on previous findings, we aim to confirm the data of our IgA seq experiments by evaluating the IgA-binding capacity to various bacterial species using an‘IgA-binding assay, which is currently ongoing in the host lab. Following the deposition assay published by Van Dalen et al. [80], we aim at assessing the individual s-IgA binding capacities from our patient's nasal secretions to human nasal bacterial isolates, obtained in collaboration with the Cliniques Universitaires Saint-Luc, to complement our IgA-SEQ approach. The protocol involves culturing bacterial isolates, incubating them with patients' derived s-IgA, staining with anti-human IgA, and analyzing fluorescence intensity of the IgA deposition by flow cytometry. Preliminary results indicate that the binding assay protocol is adequate to get the corresponding bacterial-deposited-IgA signal by flow cytometry (Figure 28). This approach will allow us to study IgA deposition on bacteria cultured in both standard and nutrient-limited conditions, providing insights into how environmental factors influence IgA recognition. The analysis will include key sinonasal microbes and potential pathogens, such as *Staphylococcus aureus,* and *Moraxella spp.*, next to more beneficial commensals such as *Corynebacterium accolens* and *Dolosigranulum*. This study will refine our understanding of host-microbiome interactions and the specificity of IgA responses in the nasal environment. Overall, the s-IgA binding assays with the withheld bacteria can confirm our findings and provide insight into possible s-IgA defects that lie at the base of the observed data.

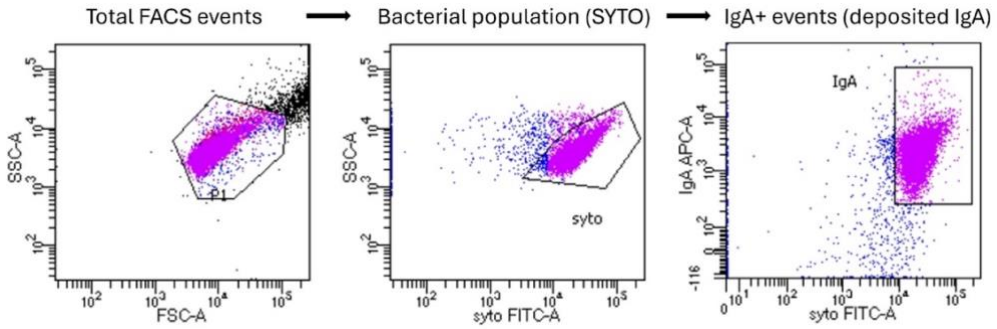

Figure 28. Gating strategy for the ongoing optimization of the 'IgA-binding assay' by flow cytometry.

Total bacterial events collected from the FACS analysis were gated based on forward scatter area (FSC-A) and side scatter area (SSC-A) to exclude debris. Bacterial population was identified using the SYTO nucleic acid stain (SYTO FITC-A), distinguishing bacteria from non-bacterial events. The IgA+ bacterial population was detected by staining with an anti-IgA antibody conjugated to APC and gated based on IgA fluorescence (IgA APC-A). Events within the IgA+ gate represent bacteria that have IgA deposited on their surface.

d) A key future direction for applying IgA-SEQ to sinonasal samples from CRS patients and healthy individuals is increasing the cohort size. This is essential to validate our findings, enhance statistical power, and improve the generalizability of results. A larger sample of sequenced fractions would enable detailed subgroup analyses, identification of IgA-coating patterns linked to specific inflammatory endotypes, and a deeper exploration of IgA-microbiome interactions. Additionally, integrating IgA-SEQ with multi-omics approaches or single-cell RNA sequencing and/or bulk RNA sequencing, will provide a more detailed understanding of the immunological and microbial landscape in CRS, potentially guiding targeted interventions to restore mucosal immunity and microbiome balance.

e) This dissertation did not address the role of IgA-producing B cells, despite evidence of B cell dysfunction in CRS, particularly in CRSwNP [15,16,33,88-96]. Local B cell activation and antibody production are crucial to CRS pathogenesis, and investigating IgA-producing B cell abundance, distribution, and differentiation could provide further insights. Key pathways, including TGF-beta, APRIL, and BAFF, should be investigated for potential abnormalities.

3. References

1. KNIGHT, D. A. & HOLGATE, S. T. The airway epithelium: Structural and functional properties in health and disease. Respirology 8, 432–446 (2003).
2. Schleimer, R. P. et al. Epithelium, Inflammation, and Immunity in the Upper Airways of Humans: Studies in Chronic Rhinosinusitis. Proc Am Thorac Soc 6, 288–294 (2009).
3. Fokkens, W. J. et al. European Position Paper on Rhinosinusitis and Nasal Polyps 2020. Rhinology journal 0, 1–464 (2020).
4. Tomassen, P. et al. Inflammatory endotypes of chronic rhinosinusitis based on cluster analysis of biomarkers. Journal of Allergy and Clinical Immunology 137, 1449-1456.e4 (2016).
5. Zhang, N. et al. Different types of T-effector cells orchestrate mucosal inflammation in chronic sinus disease. Journal of Allergy and Clinical Immunology 122, 961–968 (2008).
6. Cao, P. P. et al. Distinct immunopathologic characteristics of various types of chronic rhinosinusitis in adult Chinese. Journal of Allergy and Clinical Immunology 124, (2009).
7. Brandtzaeg, P. Secretory IgA: Designed for Anti-Microbial Defense. Front Immunol 4, (2013).
8. Pabst, O. & Izcue, A. Secretory IgA: controlling the gut microbiota. Nat Rev Gastroenterol Hepatol 19, 149–150 (2022).
9. Gupta, S. et al. IgA Determines Bacterial Composition in the Gut. Crohns Colitis 360 5, (2023).
10. Donaldson, G. P. et al. Gut microbiota utilize immunoglobulin A for mucosal colonization. Science (1979) 360, 795–800 (2018).
11. Peterson, D. A., McNulty, N. P., Guruge, J. L. & Gordon, J. I. IgA Response to Symbiotic Bacteria as a Mediator of Gut Homeostasis. Cell Host Microbe 2, 328–339 (2007).
12. Mantis, N. J., Rol, N. & Corthésy, B. Secretory IgA's complex roles in immunity and mucosal homeostasis in the gut. Mucosal Immunol 4, 603–611 (2011).
13. León, E. D. & Francino, M. P. Roles of Secretory Immunoglobulin A in Host-Microbiota Interactions in the Gut Ecosystem. Front Microbiol 13, (2022).
14. Hoces, D., Arnoldini, M., Diard, M., Loverdo, C. & Slack, E. Growing, evolving and sticking in a flowing environment: understanding IgA interactions with bacteria in the gut. Immunology 159, 52–62 (2020).
15. Sánchez Montalvo, A., Gohy, S., Rombaux, P., Pilette, C. & Hox, V. The Role of IgA in Chronic Upper Airway Disease: Friend or Foe? Frontiers in Allergy 3, (2022).
16. Bertrand, Y., Sánchez-Montalvo, A., Hox, V., Froidure, A. & Pilette, C. IgA-producing B cells in lung homeostasis and disease. Front Immunol 14, 1117749 (2023).
17. Fadlallah, J. et al. Microbial ecology perturbation in human IgA deficiency. Sci Transl Med 10, (2018).
18. Jorgensen, G. H. et al. Clinical Symptoms in Adults with Selective IgA Deficiency: A Case-Control Study. J Clin Immunol 33, 742–747 (2013).
19. Schwitzguébel, A. J.-P., Jandus, P., Lacroix, J.-S., Seebach, J. D. & Harr, T. Immunoglobulin deficiency in patients with chronic rhinosinusitis: Systematic review of the literature and meta-analysis. Journal of Allergy and Clinical Immunology 136, 1523–1531 (2015).
20. Stevens, W. W. & Peters, A. T. Immunodeficiency in Chronic Sinusitis: Recognition and Treatment. Am J Rhinol Allergy 29, 115–118 (2015).
21. Huang, Z. et al. Updated epithelial barrier dysfunction in chronic rhinosinusitis: Targeting pathophysiology and treatment response of tight junctions. Allergy 79, 1146–1165 (2024).

22. Phalipon, A. et al. Secretory Component. Immunity 17, 107–115 (2002).
23. Motegi, Y., Kita, H., Kato, M. & Morikawa, A. Role of Secretory IgA, Secretory Component, and Eosinophils in Mucosal Inflammation. Int Arch Allergy Immunol vol. 122 www.karger.com/journals/iaa (2000).
24. Stadtmueller, B. M. et al. The structure and dynamics of secretory component and its interactions with polymeric immunoglobulins. Elife 5, (2016).
25. Engeland, C. G., Bosch, J. A. & Rohleder, N. Salivary biomarkers in psychoneuroimmunology. Curr Opin Behav Sci 28, 58–65 (2019).
26. Kato, A., Schleimer, R. P. & Bleier, B. S. Mechanisms and pathogenesis of chronic rhinosinusitis. Journal of Allergy and Clinical Immunology 149, 1491–1503 (2022).
27. Prokopenko, Y. et al. Protective Antimicrobial Effect of the Potential Vaccine Created on the Basis of the Structure of the IgA1 Protease from Neisseria meningitidis. Vaccines (Basel) 12, 1355 (2024).
28. Kilian, M. & Russell, M. W. Microbial Evasion of IgA Functions. in Mucosal Immunology 291–303 (Elsevier, 2005). doi:10.1016/B978-012491543-5/50019-X.
29. Qiu, J., Brackee, G. P. & Plaut, A. G. Analysis of the specificity of bacterial immunoglobulin A (IgA) proteases by a comparative study of ape serum IgAs as substrates. Infect Immun 64, 933–937 (1996).
30. Woof, J. M. & Russell, M. W. Structure and function relationships in IgA. Mucosal Immunol 4, 590–597 (2011).
31. Kirkeby, L., Rasmussen, T. T., Reinholdt, J. & Kilian, M. Immunoglobulins in Nasal Secretions of Healthy Humans: Structural Integrity of Secretory Immunoglobulin A1 (IgA1) and Occurrence of Neutralizing Antibodies to IgA1 Proteases of Nasal Bacteria. Clinical Diagnostic Laboratory Immunology 7, 31–39 (2000).
32. Gleeson, P. J., Camara, N. O. S., Launay, P., Lehuen, A. & Monteiro, R. C. Immunoglobulin A Antibodies: From Protection to Harmful Roles. Immunol Rev 328, 171–191 (2024).
33. Lin, M., Du, L., Brandtzaeg, P. & Pan-Hammarstrom, A. IgA subclass switch recombination in human mucosal and systemic immune compartments. Mucosal Immunol 7, 511–520 (2014).
34. Hupin, C. et al. Downregulation of polymeric immunoglobulin receptor and secretory IgA antibodies in eosinophilic upper airway diseases. Allergy: European Journal of Allergy and Clinical Immunology 68, 1589–1597 (2013).
35. Bousquet, J., Van Cauwenberge, P. & Khaltaev, N. Allergic rhinitis and its impact on asthma. The Journal of allergy and clinical immunology vol. 108 Preprint at https://doi.org/10.1067/mai.2001.118891 (2001).
36. PILETTE, C. et al. Reduced Epithelial Expression of Secretory Component in Small Airways Correlates with Airflow Obstruction in Chronic Obstructive Pulmonary Disease. Am J Respir Crit Care Med 163, 185–194 (2001).
37. Putcha, N. et al. Lower serum IgA is associated with COPD exacerbation risk in SPIROMICS. PLoS One 13, e0194924 (2018).
38. Polosukhin, V. V. et al. Bronchial Secretory Immunoglobulin A Deficiency Correlates With Airway Inflammation and Progression of Chronic Obstructive Pulmonary Disease. Am J Respir Crit Care Med 184, 317–327 (2011).
39. Polosukhin, V. V. et al. Secretory IgA Deficiency in Individual Small Airways Is Associated with Persistent Inflammation and Remodeling. Am J Respir Crit Care Med 195, 1010–1021 (2017).
40. Blackburn, J. B. et al. Secretory cells are the primary source of pIgR in small airways. Preprint at https://doi.org/10.1101/2021.11.10.467794 (2021).

41. Pilette, C., Ouadrhiri, Y., Dimanche, F., Vaerman, J.-P. & Sibille, Y. Secretory Component Is Cleaved by Neutrophil Serine Proteinases but its Epithelial Production Is Increased by Neutrophils through NF-κB– and p38 Mitogen-Activated Protein Kinase–Dependent Mechanisms. Am J Respir Cell Mol Biol 28, 485–498 (2003).
42. Ladjemi, M. Z. et al. Increased IgA production by B-cells in COPD via lung epithelial interleukin-6 and TACI pathways. European Respiratory Journal 45, 980–993 (2015).
43. Bartemes, K. R., Cooper, K. M., Drain, K. L. & Kita, H. Secretory IgA induces antigen-independent eosinophil survival and cytokine production without inducing effector functions. Journal of Allergy and Clinical Immunology 116, 827–835 (2005).
44. Southworth, T. et al. The relationship between airway immunoglobulin activity and eosinophils in COPD. J Cell Mol Med 25, 2203–2212 (2021).
45. Iikura, M. et al. Secretory IgA induces degranulation of IL-3-primed basophils. J Immunol 161, 1510–5 (1998).
46. Abu-Ghazaleh, R. I., Fujisawa, T., Mestecky, J., Kyle, R. A. & Gleich, G. J. IgA-induced eosinophil degranulation. J Immunol 142, 2393–400 (1989).
47. Al-Sayed, A. A., Agu, R. U. & Massoud, E. Models for the study of nasal and sinus physiology in health and disease: A review of the literature. Laryngoscope Investig Otolaryngol 2, 398–409 (2017).
48. Chamanza, R. & Wright, J. A. A Review of the Comparative Anatomy, Histology, Physiology and Pathology of the Nasal Cavity of Rats, Mice, Dogs and Non-human Primates. Relevance to Inhalation Toxicology and Human Health Risk Assessment. Journal of Comparative Pathology vol. 153 287–314 Preprint at https://doi.org/10.1016/j.jcpa.2015.08.009 (2015).
49. Leite-Santos, F., Tamashiro, E., de Andrade Batista Murashima, A., Anselmo-Lima, W. T. & Valera, F. C. P. Which are the best murine models to study Eosinophilic Chronic Rhinosinusitis? A contemporary review. Braz J Otorhinolaryngol 89, 101328 (2023).
50. Kim, D. W. et al. Staphylococcus aureus enterotoxin B contributes to induction of nasal polypoid lesions in an allergic rhinosinusitis murine model. Am J Rhinol Allergy 25, (2011).
51. Sánchez-Montalvo, A. et al. Validation and shortcomings of the most common mouse model of chronic rhinosinusitis with nasal polyps. Rhinology Journal 0, 0–0 (2024).
52. Wang, S. et al. Establishment of a mouse model of lipopolysaccharide induced neutrophilic nasal polyps. Exp Ther Med (2017) doi:10.3892/etm.2017.5208.
53. Jacob, A., Faddis, B. T. & Chole, R. A. Chronic bacterial rhinosinusitis: description of a mouse model. Arch Otolaryngol Head Neck Surg 127, 657–64 (2001).
54. Wang, H. et al. Histological and Immunological Observations of Bacterial and Allergic Chronic Rhinosinusitis in the Mouse. Am J Rhinol 22, 343–348 (2008).
55. Palmer, J. Bacterial Biofilms in Chronic Rhinosinusitis. Annals of Otology, Rhinology & Laryngology 115, 35–39 (2006).
56. Domenech, M., García, E. & Moscoso, M. Biofilm formation in Streptococcus pneumoniae. Microb Biotechnol 5, 455–465 (2012).
57. Tuon, F. F., Dantas, L. R., Suss, P. H. & Tasca Ribeiro, V. S. Pathogenesis of the Pseudomonas aeruginosa Biofilm: A Review. Pathogens 11, 300 (2022).
58. Peng, Q., Tang, X., Dong, W., Sun, N. & Yuan, W. A Review of Biofilm Formation of Staphylococcus aureus and Its Regulation Mechanism. Antibiotics 12, 12 (2022).
59. Smits, H. H. et al. Cholera toxin B suppresses allergic inflammation through induction of secretory IgA. Mucosal Immunol 2, 331–339 (2009).

60. Shin, S.-H., Ye, M.-K., Park, J. & Geum, S.-Y. Immunopathologic Role of Eosinophils in Eosinophilic Chronic Rhinosinusitis. Int J Mol Sci 23, 13313 (2022).
61. Lamkhioued, B., Soussi Gounni, A., Gruart, V., Pierceo, A. & Capron, M. Human Eosinophils Express a Receptor for ~ Secretory Component. Role in Secretory IgA-Dependent Activation*. Eur. J. Immunol vol. 25 (1995).
62. Bakema, J. E. & van Egmond, M. The human immunoglobulin A Fc receptor FcαRI: a multifaceted regulator of mucosal immunity. Mucosal Immunol 4, 612–624 (2011).
63. Renegar, K. B. & Small, P. A. Immunoglobulin A mediation of murine nasal anti-influenza virus immunity. J Virol 65, 2146–2148 (1991).
64. Renegar, K. B. & Small, P. A. Passive transfer of local immunity to influenza virus infection by IgA antibody. J Immunol 146, 1972–8 (1991).
65. Tjärnlund, A. et al. Polymeric IgR knockout mice are more susceptible to mycobacterial infections in the respiratory tract than wild-type mice. Int Immunol 18, 807–816 (2006).
66. Richmond, B. W. et al. Bacterial-derived Neutrophilic Inflammation Drives Lung Remodeling in a Mouse Model of Chronic Obstructive Pulmonary Disease. Am J Respir Cell Mol Biol 58, 736–744 (2018).
67. Pietrzak, B., Tomela, K., Olejnik-Schmidt, A., Mackiewicz, A. & Schmidt, M. Secretory IgA in Intestinal Mucosal Secretions as an Adaptive Barrier against Microbial Cells. Int J Mol Sci 21, 9254 (2020).
68. Pabst, O. & Slack, E. IgA and the intestinal microbiota: the importance of being specific. Mucosal Immunol 13, 12–21 (2020).
69. Lycke, N. Y. & Bemark, M. The regulation of gut mucosal IgA B-cell responses: recent developments. Mucosal Immunol 10, 1361–1374 (2017).
70. Pabst, O. New concepts in the generation and functions of IgA. Nat Rev Immunol 12, 821–832 (2012).
71. Moor, K. et al. High-avidity IgA protects the intestine by enchaining growing bacteria. Nature 544, 498–502 (2017).
72. Bemark, M., Boysen, P. & Lycke, N. Y. Induction of gut IgA production through T cell-dependent and T cell-independent pathways. Ann N Y Acad Sci 1247, 97–116 (2012).
73. Jackson, M. A. et al. Accurate identification and quantification of commensal microbiota bound by host immunoglobulins. Microbiome 9, 33 (2021).
74. Kau, A. L. et al. Functional characterization of IgA-targeted bacterial taxa from undernourished Malawian children that produce diet-dependent enteropathy. Sci Transl Med 7, (2015).
75. Palm, N. W. et al. Immunoglobulin A Coating Identifies Colitogenic Bacteria in Inflammatory Bowel Disease. Cell 158, 1000–1010 (2014).
76. DuPont, H. L., Jiang, Z.-D., Alexander, A. S., DuPont, A. W. & Brown, E. L. Intestinal IgA-Coated Bacteria in Healthy- and Altered-Microbiomes (Dysbiosis) and Predictive Value in Successful Fecal Microbiota Transplantation. Microorganisms 11, 93 (2022).
77. Yang, Y. & Palm, N. W. Immunoglobulin A and the microbiome. Curr Opin Microbiol 56, 89–96 (2020).
78. Takeuchi, T. & Ohno, H. IgA in human health and diseases: Potential regulator of commensal microbiota. Front Immunol 13, (2022).
79. Escapa, I. F. et al. New Insights into Human Nostril Microbiome from the Expanded Human Oral Microbiome Database (eHOMD): a Resource for the Microbiome of the Human Aerodigestive Tract. mSystems 3, (2018).

80. van Dalen, R. et al. Secretory IgA impacts the microbiota density in the human nose. Microbiome 11, 233 (2023).
81. De Boeck, I. et al. Anterior Nares Diversity and Pathobionts Represent Sinus Microbiome in Chronic Rhinosinusitis. mSphere 4, (2019).
82. Psaltis, A. J., Mackenzie, B. W., Cope, E. K. & Ramakrishnan, V. R. Unraveling the role of the microbiome in chronic rhinosinusitis. Journal of Allergy and Clinical Immunology 149, 1513–1521 (2022).
83. Fischer, J. L. & Lee, J. T. Update on the Role of the Microbiome in Chronic Rhinosinusitis. Curr Treat Options Allergy 11, 17–33 (2024).
84. Sun, N. et al. The epithelial barrier theory and its associated diseases. Allergy 79, 3192–3237 (2024).
85. Mahdavinia, M., Keshavarzian, A., Tobin, M. C., Landay, A. L. & Schleimer, R. P. A comprehensive review of the nasal microbiome in chronic rhinosinusitis (CRS). Clinical & Experimental Allergy 46, 21–41 (2016).
86. Shapiro, J. M. et al. Immunoglobulin A Targets a Unique Subset of the Microbiota in Inflammatory Bowel Disease. Cell Host Microbe 29, 83-93.e3 (2021).
87. Cholapranee, A., Hazlewood, G. S., Kaplan, G. G., Peyrin-Biroulet, L. & Ananthakrishnan, A. N. Systematic review with meta-analysis: comparative efficacy of biologics for induction and maintenance of mucosal healing in Crohn's disease and ulcerative colitis controlled trials. Aliment Pharmacol Ther 45, 1291–1302 (2017).
88. Aazami, H. et al. Local eosinophils are associated with increased IgA subclass levels in the sinonasal mucosa of chronic rhinosinusitis with polyp patients. Allergy, Asthma and Clinical Immunology 16, (2020).
89. Tan, B. K., Peters, A. T., Schleimer, R. P. & Hulse, K. E. Pathogenic and protective roles of B cells and antibodies in patients with chronic rhinosinusitis. Journal of Allergy and Clinical Immunology vol. 141 1553–1560 Preprint at https://doi.org/10.1016/j.jaci.2018.03.002 (2018).
90. Buchheit, K. M. & Hulse, K. E. Local immunoglobulin production in nasal tissues. Annals of Allergy, Asthma & Immunology 126, 127–134 (2021).
91. Kato, A. et al. Evidence of a role for B cell-activating factor of the TNF family in the pathogenesis of chronic rhinosinusitis with nasal polyps. Journal of Allergy and Clinical Immunology 121, (2008).
92. Van Zele, T., Gevaert, P., Holtappels, G., Van Cauwenberge, P. & Bachert, C. Local immunoglobulin production in nasal polyposis is modulated by superantigens. Clinical and Experimental Allergy 37, 1840–1847 (2007).
93. Kett, K., Brandtzaeg, P., Radl, J. & Haaijman, J. J. Different subclass distribution of IgA-producing cells in human lymphoid organs and various secretory tissues. J Immunol 136, 3631–5 (1986).
94. Hoon Yoon, Y. et al. The role of B cell Activating Factor (BAFF) expression on pathogenesis of nasal polyp in chronic rhinosinusitis with nasal polyposis. Rhinology journal 52, 390–396 (2014).
95. Dilidaer et al. Increased BAFF expression in nasal polyps is associated with local IgE production, Th2 response and concomitant asthma. European Archives of Oto-Rhino-Laryngology 274, 1883–1890 (2017).
96. Bai, J. & Tan, B. K. B Lineage Cells and IgE in Allergic Rhinitis and CRSwNP and the Role of Omalizumab Treatment. Am J Rhinol Allergy 37, 182–192 (2023).

PUBLICATIONS AND CONGRESS COMMUNICATIONS

Publications

Sánchez Montalvo A, Gohy S, Rombaux P, Pilette C, Hox V. The Role of IgA in Chronic Upper Airway Disease: Friend or Foe? Front Allergy. 2022 Mar 9;3:852546. doi: 10.3389/falgy.2022.852546. PMID: 35386640; PMCID: PMC8974816.

Bertrand Y, **Sánchez-Montalvo A**, Hox V, Froidure A, Pilette C. IgA-producing B cells in lung homeostasis and disease. Front Immunol. 2023 Mar 1;14:1117749. doi: 10.3389/fimmu.2023.1117749.

Sanchez-Montalvo A, Lecocq M, Bouillet E, Steelant B, Gohy S, Froidure A, Bullens D, Pilette C, Hox V. Validation and shortcomings of the most common mouse model of chronic rhinosinusitis with nasal polyps. Rhinology. 2024 Aug 1;62(4):446-456. doi: 10.4193/Rhin23.331. PMID: 38497676.

Sánchez-Montalvo A, Ziani-Zeryouh A, Lecocq M, Steelant B, Gohy S, Hellings P, Bullens D, Pilette C, Hox V. Mouse model of Staphylococcus aureus- and Pseudomonas aeruginosa-induced neutrophilic chronic rhinosinusitis. Rhinology. 2025 Apr 11. doi: 10.4193/Rhin24.545.

Sánchez-Montalvo Alba, Ziani-Zeryouh Aaron, Lecocq Marylène, Steelant Brecht, Bullens Dominique, Pilette Charles, Hox Valérie. Surgical procedure to induce an experimental post-infectious neutrophilic rhinosinusitis in mice – *Manuscript in preparation*.

Sánchez-Montalvo Alba, Lecocq Marylène, Van Rillaer Tim, De Boeck Ilke, Lebeer Sarah, Martens Katleen, Gohy Sophie, Steelant Brecht, Bullens Dominique, Pilette Charles, Hox Valérie – *Manuscript in preparation*.

EAACI board and JMA groups (Sánchez-Montalvo Alba as JMA group 6 major contributor). Environment and Immunology in a changing world: Review by participants of the European Academy of Allergy and Clinical Immunology (EAACI) Immunology Winter School 2023 – *Manuscript in preparation*.

Posters

Sánchez-Montalvo Alba, Lecocq Marylene, Ziani Aaron, Bouzin Caroline, Pilette Charles, Hox Valérie. pIgR and IgA system in an eosinophilic mouse model of chronic rhinosinusitis. ERS Lung Science Conference 2022 (Estoril, Portugal).

Sánchez-Montalvo Alba, Lecocq Marylene, Ziani Aaron, Bouzin Caroline, Pilette Charles, Hox Valérie. pIgR and IgA system in an eosinophilic mouse model of chronic rhinosinusitis. World Immune Regulation Meeting 2022 (Davos, Switzerland).

Sánchez-Montalvo Alba, Lecocq Marylene, Ziani Aaron, Steelant Brecht, Bullens Dominique, Pilette Charles, Hox Valérie. Mouse model of non-Type 2 CRS: the superior effect of *S. aureus* compared with *S. pneumoniae* and *P. aeruginosa*. World Immune Regulation Meeting 2022 (Davos, Switzerland).

Sánchez-Montalvo Alba, Lecocq Marylene, Ziani Aaron, Steelant Brecht, Bullens Dominique, Pilette Charles, Hox Valérie. Mouse model of non-Type

2 CRS: the superior effect of *S. aureus* compared with *S. pneumoniae* and *P. aeruginosa*. European Academy of Allergy and Clinical Immunologgy (EAACI) Winter School 2023 (Davos, Switzerland).

Sánchez-Montalvo Alba, Lecocq Marylene, Martens Katleen, Van Rillaer Tim, De Boeck Ilke, Lebeer Sarah, Bullens Dominique, Pilette Charles, Hox Valérie. The impact of secretory IgA on nasal microbiome control and its link to the development of chronic rhinosinusitis. EAACI ISMA-RHINA 2024 (Helsinki, Finland).

Oral presentations

Sánchez-Montalvo Alba, Lecocq Marylene, Ziani Aaron, Steelant Brecht, Bullens Dominique, Pilette Charles, Hox Valérie. A mouse model of non-Type 2 CRS. Journées de la recherche respiratoire 2022 (Reims, France)

Sánchez-Montalvo Alba, Lecocq Marylene, Ziani Aaron, Steelant Brecht, Bullens Dominique, Pilette Charles, Hox Valérie. A mouse model of non-Type 2 CRS. ISMA-RHINA Digital 2022.

Sánchez-Montalvo Alba, Lecocq Marylene, Ziani Aaron, Steelant Brecht, Bullens Dominique, Pilette Charles, Hox Valérie. Mouse model of non-Type 2 CRS: the superior effect of *S. aureus* compared with *S. pneumoniae* and *P. aeruginosa*. EAACI Hybrid Congress 2023 (Hamburg, Germany).

Sánchez-Montalvo Alba, Lecocq Marylene, Ziani Aaron, Steelant Brecht, Bullens Dominique, Pilette Charles, Hox Valérie. Mouse model of non-Type 2 CRS: the superior effect of *S. aureus* compared with *S. pneumoniae* and *P. aeruginosa*. European Rhinologic Society 2023 (Sofia, Bulgaria).

Awards

Best poster presentation at EAACI Winter School 2023 (Davos, Switzerland).

Best Flash talk at EAACI Hybrid Congress 2023 (Hamburg, Germany).

Nomination and selection to participate in the 72nd Lindau Nobel Laureate Meeting 2023 (Lindau, Germany).